Spring 2021

Effect of Oxidative Stress on Lifespan and Cellular Survival

Benedicth Onyeka Ukhueduan

EFFECT OF OXIDATIVE STRESS ON LIFESPAN AND CELLULAR SURVIVAL

by

Benedicth Onyeka Ukhueduan

Bachelor of Science
University of Minnesota Duluth, 2016

Bachelor of Applied Science
University of Minnesota Duluth, 2016

Submitted in Partial Fulfillment of the Requirements

For the Degree of Doctor of Philosophy in

Biological Sciences

College of Arts and Sciences

University of South Carolina

2021

Accepted by:

Rekha Patel, Major Professor

David Reisman, Committee Member

Alissa Armstrong, Committee Member

Johannes Stratmann, Committee Member

Maksymillian Chruszcz, Committee Member

Tracey L. Weldon, Interim Vice Provost and Dean of the Graduate School

DEDICATION

This dissertation is dedicated to my loving mother Mrs. Felicia E Ukhueduan, a very strong, gentle but brave woman who taught me to be an independent God-fearing woman, to my late Uncle Mr. Michael I. Oduah and late Godmother (mama) Louisa Nwulia both of whom inspired the love of life-long learning in me, to Mrs. Indhira Carmel Handy my lab grandma, without whom this work would not exist my whole family, all my endearing friends, and finally, to caffeine, sugar, Spotify and C/K dramas, my companions through many a long nights of writing.

ACKNOWLEDGEMENTS

I would like to say thank you to my research advisor and mentor, Dr. Rekha Patel, first for allowing me to be my true self in the lab always, and secondly, for knowing how to push me to do my best and giving me the encouragement and support when I needed it the most. I have enjoyed the lab family environment (e.g., allowing me to host secrete Santa every year!) you have created, and while you can sometimes be very strict in mentoring us “using tough love”, it has allowed me to mature and grow into the proud black scientist I am today, and for that I will be eternally grateful.

I would also like to say a huge thank you to all the members of my graduate committee: Dr. Reisman, Dr. Armstrong, Dr. Chruszcz, and Dr. Stratmann who have been extremely supportive of me throughout my journey, for all the last-minute recommendation letter requests, for all the quick office drop-in for pep talks, for all the unexpected Alexa and coffee maker impromptu gifts, for all the extra tips and practice talks, for all the constructive feedbacks and for inspiring me to keep pushing on. Thank you for always being there to mentor me through and through.

I am also greatly indebted to my immediate family (my mom, my two fatherly-brothers and my 3 motherly-sisters) my extended family (my two-brother in-laws, my sister-in law and my nieces and nephews) my Big Aunties (Veronica Elikwu, Marina Oduah and Daina Bouyones), my cousins (Anthea, Marina, Philp

and Michael), my Godmother Mrs. Sarah Chundun Dokotri, and to my adopted family (grandma and grandpa Neatons, and the Weiland family) for all their unconditional love and support as I powered through graduate school. For all the kind thoughts and words, for all the care packages, for all the calls and funny videos, for all the support (financially and otherwise), for all the prayers, and blessing; you all have been my village of support, and I will not have made it far without all of you. I love you all dearly!

I would also like to thank my next village of support, as they have become my family and have been cheering me on from day 1: My forever roommate/sister Dr. Chigozie Azike and her family, Tancia Bradshaw, Natalie Sanchez, Geetha Clarke, Claire Hann and Eilea Knots my home girls! To Drs Evelyn Chukwurah, Samuel Burnett, and Kenneth Frederick my adopted lab siblings, Ms. Edna my hair savior, and my girlfriends back in Minnesota (Salam Girmay, Paige Strobel and her family, Valentine Irungu, Marianne Neba-Siri, Ceriah Juean and Julie Wolf).

I would like to thank My SC Columbia NIH Prep 2016-2017 Cohort members: most especially Devon Eddins for always supporting, encouraging, and sending me all sorts of career motivated things… My Grace-Jordan MacFadden professors program family members for all the continuous professional guidance and support, most especially Samantha McNeal, for being my writing/study buddy.

Finally, to all the other figures in my life that I did not mention. Thank you all.

ABSTRACT

When cells experience oxidative stress, the integrated stress response (ISR) signaling pathway is activated. One of the first outcomes of such ISR-activated response is to temporarily halt protein synthesis, which aids in cellular recovery. However, if cells cannot recover from the stress, they activate the cell death pathways which kills the affected cells, usually by apoptosis, which can then lead to either acquisition or prevention of diseases depending on the situation. In physiological aging, a compromised stress response is observed as an organism ages, which leads to disrupted homeostasis and elevated risk of disease. Thus, longevity of an organism is directly related to its ability to effectively cope with cellular stressors such as oxidative stress. Intracellular reactive oxygen species (ROS) resulting from normal metabolism cause most damage to cellular macromolecules and the mitochondria play a central role in this process as they are the principal source of ROS. Under the oxidative stress umbrella, this thesis is divided into two parts; 1) evaluating if oxidative stress contributes to aging and lifespan using a *Daphnia* as model for aging research and 2) exploring the regulatory role of PKR in determining cellular survival in response to oxidative stress in mammalian cells.

The relationship between naturally occurring variations in the mitochondrial (MT) genomes leading to differences in the rate of aging associated organismal decline remains relatively unexplored. MT complex I, a

component of electron transport chain (ETC), is a key source of ROS and the *NADH dehydrogenase subunit 5* (ND5) is a highly conserved core protein of the essential subunits that constitute the backbone of complex I. We explored if there are naturally occurring, inherited sequence variations in ND5 that may correlate with a short or long lifespan. Our results indicate that the short-lived clones have ND5 variants that correlate with reduced complex I activity, increased oxidative damage to proteins, and heightened expression of ROS scavenger enzymes.

During cellular stress, PKR is catalytically activated transiently by its protein activator PACT and TRBP inhibits PKR to bring about a timely cellular recovery. We have previously established that TRBP phosphorylated after oxidative stress binds to and inhibits PKR more efficiently promoting cell survival. In this study, we investigated if phosphorylation of TRBP enhances its interaction with PACT to bring about additional PKR inhibition. Our data establishes that phosphorylation of TRBP has no effect on PACT-TRBP interaction. TRBP's inhibitory action on PKR at late time points after oxidative stress, is mediated exclusively by its enhanced interaction with PKR. Consequently, cells lacking TRBP are more sensitive to apoptosis in response to oxidative stress and show persistent PKR activation. These results establish that PKR inhibition by stress induced TRBP phosphorylation occurs by its direct binding to PKR and is important for preventing apoptosis due to sustained PKR activation. This work has important implications on cellular survival as well as aging and can be extended to understand several age-related disease conditions.

TABLE OF CONTENTS

LIST OF FIGURES

LIST OF ABBREVIATIONS

ATP ..... Adenosine triphosphate

ALS ..... Amyotrophic lateral sclerosis

Bp .....Base Pairs

BN-PAGE.....Blue Native PAGE

CADs .....Caspase-activated DNases

CAT.....Catalase Enzyme

CN-PAGE ..... Clear Native PAGE

DAPI 4,6-Diamidino-2-Phenylindole

DMEM..... Dulbecco's Modified Eagle Medium

DNA ..... Deoxyribonucleic acid

DsRBM .....Double-stranded RNA Binding Domain

DsRNA.....Double Stranded RNA

eIF2.....Eukaryotic Initiation Factor 2

eIF2B ..... eIF2 Guanine Nucleotide Exchange Factor 2B

eIF2α..... Eukaryotic Initiation Factor 2 α subunit

EGFP .....Enhanced Green Fluorescent Protein

ER.....Endoplasmic reticulum

ERK1/2 .....Extracellular signal–Regulated Kinase

ETC..... Electron transport chain

EV ..... Empty Vector

FTLD.....Frontotemporal lobar degeneration

G3BP1 .....Ras-GTPase-activating-protein-(SH3 domain)-binding-protein-1

GCN2 ..... General Control Non-Derepressible 2

GFP ..... Green Fluorescent Protein

HIV ..... Human immunodeficiency virus

HSF ..... Heat Shock Factor

HSR ..... Heat Shock Response

IEADS .....Intrinsic enzyme antioxidant defense pathway

IFN .....Interferon

IPTG ..... Isopropyl Beta-D-1-Thiogalactopyranoside

ISR .....Integrated Stress Response

JNK .....c-Jun N-terminal Kinase

kDa .....Kilo Daltons

K296R PKR .....Dominant negative PKR mutant

KD .....Kinase Domain

KO..... Knockout

MAPK/ERK 1/2 ..... Mitogen Activated Protein Kinase

MEFs .....Mouse Embryonic Fibroblasts

mRNA .....Messenger RNA

ORFs .....Open Reading Frames

PACT ..... **P**KR **act**ivating protein

PARP1 ..... Poly-ADP Ribose Polymerase 1

PBS..... Phosphate Buffer Saline

PKR ..... Protein Kinase R

RNA .....Ribonucleic acid

ROS .....Reactive Oxygen Species

RW20 ..... Rough Wood 20

Sir2 ..... Sirtuin 2

SOD ..... Super Oxide Dismutase

TRBP ..... TAR RNA Binding Protein

TRBP DDDD ..... Phospho-mimic TRBP point mutant.

TRBP AAAA ..... Phospho-defective TRBP mutant

Wt ..... Wild type

XVI-11 ..... Lake Sixteen Clone 11

YPD media ..... Yeast extract, peptone, and dextrose

CHAPTER 1

INTRODUCTION[1]

[1] To be adapted into a comprehensive review titled: '*Daphnia* as a model for aging research'.

1.1 OXIDATIVE STRESS AND THE MITOCHONDRIAL THEORY OF AGING

Aging causes an irreversible time-dependent decrease in normal cellular functions over time, resulting in a compromised stress response that leads to homeostatic imbalance and elevated risk of disease (López-Otín et al., 2013). Even though aging is a progressively slow, degenerative and a relatively universally conserved process, the basic molecular mechanisms that fully describe this evolutionary process remain widely ambiguous (Cui et al., 2012; Liguori et al., 2018). The rise of age-associated diseases (e.g., cancer, diabetes, and neurodegenerative diseases) necessitates that we understand the underlining pathways and possible therapeutic interventions to maintain a healthy lifespan (Liguori et al., 2018; Rebelo-Marques et al., 2018). There are many facets to the aging process that have been uncovered through numerous experiments in multiple model organisms such as the nematode *Caenorhabditis elegans* (*C. elegans*) (Lapierre & Hansen, 2012; Mack et al., 2018) and fruit fly *Drosophila melanogaster* (*D. melanogaster*) (Flatt et al., 2008) in the past 3 decades (Lapierre & Hansen, 2012; Mack et al., 2018). A comprehensive review written by Lopez-Otin et al, for the first time described what are now classified as the 9 hallmarks of aging (Figure1.1) (López-Otín et al., 2013). These hallmarks are genomic instability, telomere attrition, epigenetic alterations, stem cell exhaustion, deregulated nutrient sensing, altered intracellular communication, cellular senescence, MT dysfunction and loss of proteostasis (López-Otín et al., 2013). While several hallmarks of aging have been identified, the molecular mechanisms that govern aging are still incompletely understood. Therefore,

aging can be broadly defined as a complex biological process that encompasses multiple tissues and their subsequent decline with time.

In physiological aging, a compromised stress response is observed as an organism ages, which leads to disrupted homeostasis and elevated risk of disease (Maguire & Slater, 2013; Young & Maguire, 2019). Thus, longevity of an organism is directly related to its ability to effectively cope with cellular stressors such as oxidative stress. Previous research linking oxidative damage and decreased lifespan using various invertebrate model organisms of aging including nematodes (Lapierre & Hansen, 2012; Mack et al., 2018; Uno & Nishida, 2016), fruit flies (Mitchell et al., 2015; Perez et al., 2009), budding yeast aka; *Saccharomyces cerevisiae* (*S. cerevisiae*) (Gershon & Gershon, 2000a, 2000b); and vertebrate models such as mouse aka *Mus Musculus* (*M. musculus*) (Buffenstein et al., 2008; Mitchell et al., 2015) have shown that increase in oxidative damage to DNA, lipids and proteins in cells is corelated with accelerated aging and decreased lifespan (Berlett & Stadtman, 1997; Buffenstein et al., 2008; Liguori et al., 2018; Pomatto & Davies, 2018a). Furthermore, increased lifespan is correlated with cellular ability to alleviate continuing or increased oxidative damage. An increase in endogenous ROS (reactive oxygen species) such as superoxide, hydrogen peroxide and nitric oxide also leads to genome instability and a decrease in proteostasis due to accumulation of misfolded, oxidized proteins (Birben et al., 2012; Buffenstein et al., 2008; Cui et al., 2012; Maeda & Inoguchi, 2010). Oxidative stress is thus defined as a state of imbalance between ROS production and the ability of the cell to produce

antioxidants to clear the ROS (Andersen, 2004; Birben et al., 2012; Giacco & Brownlee, 2010; Liguori et al., 2018; Sosa et al., 2013). From the various molecular characteristics of the aging process, several theories of aging have been developed (Cui et al., 2012; Pomatto & Davies, 2018b), each with ample supporting experimental evidence, but I have limited the scope of this introduction to the free radical theory of aging.

The free radical theory of aging states that free radicals produced from normal metabolism leads to the aging process in organisms (Doonan et al., 2008; Harman, 1992; Sirnonianl & Coyle, 1996). The mitochondrial (MT) theory of aging, currently known as the oxidative stress theory of aging or free radical theory of aging, first introduced by Harman in 1956 and further expanded in 1992, states that free oxygen radicals generated as by-products of several biochemical pathways are significant contributors to a decreased lifespan and acquisition of age-related diseases (Buffenstein et al., 2008; Harman, 1992; Pomatto & Davies, 2018b; Sastre, Federico V . Pallardo, Jos&, 2000). More specifically, a great deal of evidence has connected the MT electron transport chain (ETC) , which consists of multiple redox donor complexes, as a major site for the generation of damaging free oxygen radicals (Lin & Beal, 2006; Pamplona & Barja, 2006; Sastre, Federico V . Pallardo, Jos&, 2000). The current oxidative stress theory is a modification of the free radical theory and includes all ROS such as peroxides and nitric oxide that are not free radicals (Buffenstein et al., 2008; Cui et al., 2012; Kawamura & Muraoka, 2018; Sastre, Federico V . Pallardo, Jos&, 2000). This theory has been called into question on multiple

occasions by some scholars in the aging research community and has undergone multiple modifications (Betteridge, 2000; Buffenstein et al., 2008; Cui et al., 2012; Doonan et al., 2008; Perez et al., 2009; Pomatto & Davies, 2018b; Warraich et al., 2020). The current oxidative stress theory has two fundamental concepts that have remained unchanged throughout the modification processes. These two concepts are, 1) there is an increase in the accumulation of oxidatively damaged macromolecules with age due to a growing imbalance of antioxidant/oxidants and 2) accumulation of oxidatively damaged macromolecules lead to an increase of the degenerative cellular phenotypes seen as organisms age (Warraich et al., 2020). These two concepts show the interplay between how high ROS levels, some of which are free radicals, produced via the ETC during normal metabolism damage essential cellular components and macromolecules, with particular emphasis being on proteins as they have been shown to play a large part in the phenotypes of aging (Betteridge, 2000; Cui et al., 2012; S. D. Gupta, 2010; Simioni et al., 2018). It is also important to note that the free radical theory of aging, as well as several other theories of aging, are not able to fully explain the aging process, again emphasizing the numerous mechanisms that may act in a cumulative manner contributing to the universal biological decline known as aging.

Most of the free radicals and cellular ROS are generated by the mitochondria with as much as 90% of total cellular ROS being produced from the mitochondria as by product of normal cellular metabolism (Betteridge, 2000; Cui et al., 2012; Kozie et al., 2011; Lin & Beal, 2006; Pamplona & Barja, 2006;

Sastre, Federico V . Pallardo, Jos&, 2000). The detrimental effects of free radicals and ROS produced via normal metabolism are neutralized by several ROS scavenging enzymes including superoxide dismutase (SOD) and catalase (CAT) (Birben et al., 2012; Burton & Jauniaux, 2011; Enzor & Place, 2014; Kruman et al., 1997; Maeda & Inoguchi, 2010; Nikooyeh & Neyestani, 2016; Rahal et al., 2014; Warraich et al., 2020). Along with glutathione peroxidase, these enzymes make up the main intrinsic enzymatic antioxidant defense system (IEADS) (Maritim et al., 2003; Simioni et al., 2018; Warraich et al., 2020). The non-enzymatic extrinsic antioxidant defense system, which is not the focus of this work, includes dietary compounds, minerals, and vitamins to name a few (Harman, 1992; Warraich et al., 2020). Figure 2 summarizes these pathways.

In IEADS, SOD enzymatically converts the extremely toxic superoxide anion into hydrogen peroxide (which is another harmful by product) and molecular oxygen (Maritim et al., 2003; Pomatto & Davies, 2018a; Rahal et al., 2014; Simioni et al., 2018; Warraich et al., 2020). In mammals there are three SOD isoforms that utilize different metals as a cofactor and are located at different subcellular locations: SOD1, a cytoplasmic SOD using cofactors Cu and Zn, SOD2 a mitochondrial SOD using cofactor Mn, and SOD3 an extracellular SOD using cofactors Cu and Zn (Doonan et al., 2008; Enzor & Place, 2014; Pang & Wang, 2008; Quinlan et al., 2013). CAT is another scavenging enzyme that converts hydrogen peroxide into oxygen and water (Enzor & Place, 2014; Maritim et al., 2003; Shi et al., 2013). SOD and CAT have been found to complement each other such that the hydrogen peroxide, which is a harmful by

product of SOD activity on superoxide anion, is then be processed by CAT (Kruk et al., 2019; Quinlan et al., 2013; Sastre, Federico V . Pallardo, Jos&, 2000; Shi et al., 2013; X. Wang et al., 2007).

Studies have shown that ROS induces damage in various macromolecules of the cell but damage to proteins and lipids have been implicated the most in aging processes (Burton & Jauniaux, 2011; Harman, 1992; Liguori et al., 2018; Maritim et al., 2003; Pomatto & Davies, 2018b, 2018a). This is because cumulative ROS accumulation leads to oxidative damage over time and oxidized proteins lose their catalytic function (Burton & Jauniaux, 2011; Pomatto & Davies, 2018b; Warraich et al., 2020). Age-associated loss of physical function is strongly correlated to the increase in the oxidative damage to proteins which then leads to their hydrolysis (Kruk et al., 2019; Pomatto & Davies, 2018b, 2018a). Additionally, oxidative damage to a protein's active site can induce a particular loss/gain of functional abilities which can affect the biochemical pathways the protein is a member of, leading to more deleterious dysregulation of signaling and normal cellular function. One such example is the oxidative damage to proteins in the form of a loss of sulfhydryl (-SH) groups, which leads to an increase in the number and amount of misfolded proteins in cells (Berlett & Stadtman, 1997; Bu et al., 2017; Pomatto & Davies, 2018b).

Many studies have examined the relationship between levels of ROS, SOD, CAT, and longevity (David Adams & Klaidman, 2006; Doonan et al., 2008; Flatt et al., 2008; Ou et al., 2014; Pomatto & Davies, 2018b; Shi et al., 2013; Warraich et al., 2020). These studies have used several different model

organisms but most studies were done using *D. melanogaster* and *C. elegans* (Flatt et al., 2008; Lapierre & Hansen, 2012; Mack et al., 2018; Murthy & Ram, 2015). Originally published in 1994, Orr and Sohal found that when SOD2 and CAT are overexpressed in *D. melanogaster* there was an extension in lifespan (Orr & Sohal, 2003). Upon further examination, there was a bias in the study which resulted in a corrected conclusion of there being no significant change in lifespan in these transgenic flies (Flatt et al., 2008; Murthy & Ram, 2015; Orr & Sohal, 2003). Using *C. elegans*, Cabreiro *et a*l found that SOD1 overexpressing worms live longer but the life span extension is due to the activation of conserved stress response pathways, such as the heat shock response, as opposed to a decreased amount of oxidative stress (Cabreiro et al., 2011). Similar work has been performed in mice with equally conflicting results (Buffenstein et al., 2008; Mitchell et al., 2015).

Although the relationship between ROS presence and longevity is still unclear, it is established and generally well accepted that the effects of high levels of ROS are detrimental to the overall health and life span of an organism. Previous work has demonstrated that increased ROS levels leading to carbonyl formation in proteins render them nonfunctional and eventually cause protein aggregates that induce proteotoxic stress (Shi et al., 2013). The ability to respond to proteotoxic stress has been well studied in multiple organisms (Bu et al., 2017; Pomatto & Davies, 2018b; Shi et al., 2013) and numerous studies have demonstrated that the ability to successfully respond to this stress to restore cellular homeostasis declines with age (Bolton & Smith, 2018; Burton &

Jauniaux, 2011; Kourtis & Tavernarakis, 2011a; Redza-Dutordoir & Averill-Bates, 2016; Rimmelé et al., 2014). Proteotoxic stress is not exclusively caused by ROS, thus previous studies showing no extension in lifespan when ROS is reduced in organisms may indicate there is another cause of this stress leading to the age-related effects (Kourtis & Tavernarakis, 2011a; Rahal et al., 2014). Therefore, it is possible that the inability to deal with the ROS induced damage to proteins as an organism ages may be one of the several contributing factors that negatively affect lifespan.

In this dissertation, I describe the dynamic interplay between cellular stress response pathways and cellular homeostasis as well as aging processes. The work is divided in two parts, 1) using a new model for aging, an invertebrate microcrustacean, *Daphnia pulex,* I have studied if the ROS generation by mitochondria correlates with protein damage and lifespan and 2) using a mammalian cell culture model, I have studied the regulation of cellular survival in response to oxidative stress. This work has important implications on cellular survival as well as aging and can be applied to understanding several age-related disease conditions.

1.2 *DAPHNIA* AS A MODEL FOR STRESS RESPONSE AND AGING RESEARCH

Daphnia is a unique model for research on aging as it complements the more traditional models (Ebert, 2005). The *D. pulex* species complex are closely related freshwater microcrustaceans (adult length: 1-2 mm) and are present in ponds and lakes throughout North America (Ebert, 2005; Harris et al., 2012;

Schumpert et al,, 2015). (Figure 3) Ecologists have studied *Daphnia* for nearly two centuries for research on life history, physiology, nutrition, predation, parasitology, toxicology, and behavior (Colbourne et al., 2011; Harris et al., 2012; Schwartz et al., 2016; Ty, 1991; Zhu et al., 2010). The two closely related ecotypes of *Daphnia* have dramatically different lifespans. *Daphnia pulex* (*D. pulex*) is short-lived (20-25 days on average) and *Daphnia pulicaria* (*D. pulicaria*) is long-lived (60-65 days on average) (Ebert, 2005; Hu et al., 2018; Kvist et al., 2020; Van Damme et al., 2017). With both their genomes fully sequenced, these two *Daphnia* ecotypes offer a great tool for aging research because they are genetically almost identical and reproduce via parthenogenesis (isogenic clonal populations) (Colbourne et al., 2011; Ebert, 2005; Harris et al., 2012; Schumpert et al,, 2015; Van Damme et al., 2017). Furthermore, their large genome (roughly 30,000 protein coding genes), has a lot of commonalities with the human genome, making them a great arthropod model for studying complex biological process such as aging (Schumpert et al., 2015). *Daphnia* is also an established model in evolutionary genetics (Colbourne et al., 2011; Hu et al., 2018; Kvist et al., 2018, 2020; Van Damme et al., 2017) due to its cyclic parthenogenesis and a short generation time 25- 64 days. In cyclic parthenogenesis, females reproduce asexually, but when environmental conditions are poor, isogenic male offspring are produced and sexual reproduction results in dormant eggs that can remain viable for > 250 years (Colbourne et al., 2011; Ebert, 2005; Harris et al., 2012; Schumpert et al, 2015). (Figure 1.4) Since it is easy to maintain clonally reproducing lines in the lab, large numbers of genetically identical individuals can

be produced. This presents an outstanding opportunity to integrate naturally present genetic variations with aging phenotypes against an unchanging genetic background . As *Daphnia* have sexual and asexual phases, it also permits setting up crosses. As crustaceans, *Daphnia* shed their carapace every 2-3 days and maintain somatic cell proliferation throughout adulthood (Ebert, 2005). Another useful feature of *Daphnia* is that their transparent carapace body, will allow staining for senescence or ROS in whole animals or dissected organs without sectioning. Furthermore, *Daphnia* have significantly more genes than *Drosophila* or *C. elegans* raising the possibility that additional genes with relevance to human aging could be identified (Harris et al., 2012).

Over many years, model organisms have been used to gain a better understanding of the mechanistic pathways that could be evolutionarily conserved. *Daphnia* has been very well established in ecological research geared towards the study of extreme environmental conditions such as temperature, oxygen supply, toxicity of leaching chemicals and change in nutrient available in water columns around the world (Schwartz et al., 2016; Seyoum & Pradhan, 2019; Shaw et al., 2008; Zhu et al., 2010). However, in the last decade, *Daphnia* has emerged as a highly potential new model to study the role of natural genetic variations on the aging process (Harris et al., 2012; Schumpert et al., 2014; Schumpert et al., 2016; Schumpert et al, 2015; Schwartz et al., 2016; Tong et al., 2017). Of the nine hallmarks of aging, *Daphnia* have been successfully used to study six of the hallmarks making it a strong emerging model for aging research.

The most studied environmental factor that affects reproduction and lifespan is temperature as it plays a role in the determination of energy expenditure utilization and allocation in most organisms (Fulda et al., 2010; Maguire & Slater, 2013). Protein homeostasis and robust heat shock response (HSR) plays an important anti-aging role (Cabreiro et al., 2011; Kourtis & Tavernarakis, 2011a; Schumpert et al., 2014). We studied the HSR in *Daphnia* by examining Hsp70 induction in short and long-lived ecotypes at equivalent young, middle, and old ages. The HSR decline was seen at a much younger age in short-lived ecotypes compared to the long-lived ecotypes (Schumpert et al., 2014; Schumpert et al., 2016). We further showed that the loss of HSR in the short-lived clones resulted from the inactivation of the heat shock factor 1 (HSF1), a transcription factor essential for HSR (Schumpert et al., 2014). We also examined telomere length, and telomerase activity in the short- and long-lived ecotypes (Schumpert et al., 2015). Surprisingly, the short-lived ecotype maintained telomere length throughout its lifespan while the long-lived ecotype exhibited telomere erosion with age (Schumpert et al., 2015). The short-lived ecotype contained high amounts of telomerase activity throughout lifespan, but the long-lived ecotype showed a steady decline with age (Schumpert et al., 2015). Thus, telomere erosion and genomic instability is not a cause for the characteristically short lifespan in the short-lived ecotype (Schumpert et al., 2014, 2015; Schumpert et al., 2016). Our results suggest that the short-lived ecotype might have accumulated excessive oxidative damage long before their telomeres

erode. The effect of other cellular stressors such as oxidative stress on lifespan and physiological aging in *Daphnia* has remained unknown.

In addition to examining aging-related molecular pathways, our lab has established protocols for using RNAi to knock down gene expression in *Daphnia* (Schumpert et al,, 2015). We were the first to establish a feeding-based RNAi methodology for gene knock-down to genetically manipulate *Daphnia*. In this study, we knocked down the melanin synthesis pathway in *D. melanica* which have a darker pigmentation in their carapace as a defense against UV exposure (Schumpert et al., 2015). Our target gene was phenoloxidase which is essential for synthesis of melanin (Schumpert et al,, 2015). By feeding *Daphnia* bacteria expressing double-stranded RNA (dsRNA) from a region of phenoloxidase mRNA, we observed a reduction in phenoloxidase mRNA and a corresponding reduction in melanin levels indicated by a loss in carapace pigmentation (Schumpert et al,, 2015).

We also used this *Daphnia* RNAi feeding method to investigate the role of Sir2 protein in HSR (Schumpert et al., 2014; Schumpert et al,, 2016). Sir2, originally discovered in yeast, is a member of the histone deacetylase (HDACs family) of enzymes (Gershon & Gershon, 2000a; Hallows et al., 2006; Sauve et al., 2006) and plays a role in gene silencing by deacetylation of histones and non-histone proteins (e.g. HSF and p53) leading to an overall repression of transcription and other cellular functions (Hallows et al., 2006; Sauve et al., 2006; Y. Wang et al., 2011). Higher activity was shown extends lifespan by effectively

stimulating the HSR response thus protecting organisms from extreme heat shock exposure (Gershon & Gershon, 2000b, 2000a; Tanny et al., 1999).

Our lab was the first to fully clone and, characterize sequence similarity between the catalytic regions of *Daphnia* Sir2 and its human ortholog Sirt1 (Schumpert et al,, 2016). The highest conserved regions were in the domains of the protein important for its deacetylase enzyme function (i.e. the NAD+ dependent deacetylase) and substrate binding regions (Schumpert et al,, 2016). Furthermore, we showed that a) the *Daphnia* Sir2 open reading frame (ORF) encoded, *in vitro* translated protein had catalytic activity similar to the human recombinant Sirt1 protein, b) Overexpression of *Daphnia* Sir2 protected mammalian cells from cell death resulting from heat shock which we interpreted to be the result of *Daphnia* Sir2-dependent deacetylation of HSF-1, leading to a more robust cellular response to the proteotoxic stress, and c) *Daphnia pulicaria* Sir2 mRNA levels increased with age but the enzyme activity decreased with age indicating possible regulation of enzyme activity by a post-translational mechanism (Schumpert et al,, 2016). Finally, when we knocked down Sir2 expression using RNAi feeding method, we noticed that it resulted in a severely compromised HSR and significant reduction in lifespan (Schumpert et al,, 2016). These studies have laid a good foundation and shown that it is now possible to not only study biological pathways that affect aging, but *Daphnia* can also be genetically manipulated to better establish a direct causal relationship between genes and aging processes.

1.3 LIMITATIONS OF INVERTEBRATE MODELS FOR MOLECULAR MANIPULATIONS

In the last few decades, invertebrate model systems, especially the nematode and the fruit fly, have made significant contributions to our current understanding of regulation of lifespan and aging (Erdogan et al., 2016; Flatt et al., 2008; Gershon & Gershon, 2000a; Lapierre & Hansen, 2012). Their short generation times and the relative ease of culturing them make these much easier model organisms as compared to higher eukaryotes. Although we continue to make remarkable leaps in our knowledge of aging using invertebrate models, major limitations and challenges remains to be tackled. There are two major limitations to use *Daphnia* as a model system for research on aging. These two limitations are: 1) availability of technologies for culturing *Daphnia* cells and 2) the linkage of age-related phenotypes to specific molecular pathways is missing due to easy methods for gene manipulation being available. The lack of a) stable *daphnia* cell lines and inability to culture primary cells, b) commercially available antibodies specific for *Daphnia* proteins, c) universally available genetic ortholog annotation for accurate comparison of human gene homologs and d) easy methods to manipulate gene expression for a direct cause and effect relationship studies makes it nearly impossible to perform meaningful molecular studies with *Daphnia*. Thus, when studying the effect of oxidative stress on cell survival and homeostasis, I switched from the invertebrate to mammalian system.

1.4 OXIDATIVE STRESS RESPONSE PATHWAYS IN MAMMALIAN CELLS

When mammalian cells encounter physiological or pathological stress conditions [e.g., oxidative stress, hypoxia, nutrient or growth factor deprivation, viral infections], the integrated stress response (ISR) signaling pathway is activated (Donnelly et al., 2013; Kourtis & Tavernarakis, 2011a; Pakos-Zebrucka et al., 2016). The ISR is mediated by the stress-induced activation of one, or multiple ISR kinases PKR-like ER resident Kinase (PERK), protein kinase R (PKR), general control non-depressible -2 kinase (GCN2), and heme-regulated inhibitor kinase (HRI) (Donnelly et al., 2013; Fulda et al., 2010; Kourtis & Tavernarakis, 2011b; Pakos-Zebrucka et al., 2016). Each of these kinases is activated by a distinct type of stress signal/s (Donnelly et al., 2013; Mirkes, 1997; Pakos-Zebrucka et al., 2016). These 4 kinases converge at the phosphorylation of the α subunit of eukaryotic initiation factor 2 (eIF2α) on serine 51 (Donnelly et al., 2013; Pakos-Zebrucka et al., 2016; Saelens et al., 2001), leading to a transient shut down of protein synthesis thereby allowing cells to return to homeostasis in a timely manner. A small number of specific transcripts escape the global translation shut down during this phase including but not limited to the mRNA transcripts encoding the transcription factor ATF4 (Donnelly et al., 2013; Fulda et al., 2010; Kroemer et al., 2010; Napoletano et al., 2019; Pakos-Zebrucka et al., 2016). While transient eIF2α phosphorylation is protective prolonged activation,, shifts the balance from being pro-survival to pro-apoptotic by ATF4 induction of CHOP, consequently triggering programed cell death i.e.

apoptosis (Doherty & Baehrecke, 2018; Fulda et al., 2010; Los et al., 2002; Ou et al., 2014).

Protein Kinase R (PKR) is an interferon (IFN)-induced serine/threonine kinase that is ubiquitously expressed constitutively at low basal levels (Gal-Ben-Ari et al., 2019; Li et al., 2006; Peters et al., 2009; Sadler & Williams, 2007). Although PKR expression is elevated during viral infections and by IFNs (Donnelly et al., 2013; García et al., 2007; Sadler & Williams, 2007), PKR's kinase activity stays latent until it binds to an activator. PKR can be activated by binding to double stranded (ds) RNA via its two dsRNA binding motifs (dsRBMs) in case of viral infections, or by binding to the PKR's **p**rotein **act**ivator (PACT) in response to oxidative stress, growth factor deprivation, and ER stress (D'Acquisto & Ghosh, 2001; Lee et al., 2007; Li et al., 2006; R. C. Patel & Sen, 1998; Sen & Peters, 2007; Singh & Patel, 2012). The dsRBM containing proteins usually have variable numbers of these motifs and perform functions that range from RNA editing, translational control, protein phosphorylation, and transcription (Daher et al., 2017; V. Gupta et al., 2003; Lee et al., 2007; Li et al., 2006; Singh & Patel, 2012). In addition to dsRNA binding, these motifs also mediate protein-protein interactions in an RNA independent manner (Burugu et al., 2014; Chukwurah et al., 2018; Clerzius et al., 2013; Kok et al., 2007; Sen & Peters, 2007). The two regulatory dsRBM containing proteins PACT and TRBP (i.e., human immunodeficiency virus (HIV-1 transactivation-response (TAR) RNA-binding protein) exert positive and negative effects respectively on PKR in

response to stress signals (Chukwurah & Patel, 2018; Clerzius et al., 2013; Guerline Clerzius, Jean-Francois Gatignol, 2010; Li et al., 2006) (Figure1.5).

Research from our lab has established that PKR activation and its catalytic activity are tightly regulated by PACT and TRBP during oxidative stress (Chukwurah & Patel, 2018) (Figure1.6). At early time points during oxidative stress, PACT is phosphorylated, reducing its affinity for TRBP and increasing PACT-PKR interaction while also promoting PACT-PACT interactions (Chukwurah & Patel, 2018). In response to oxidative stress, PACT undergoes a stress induced phosphorylation at serine 287 in addition to its constitutive phosphorylation on serine 246 and this phosphorylation at serine 287 promotes PKR activation (Chukwurah et al., 2018; Huang et al., 2002; Li et al., 2006; Singh & Patel, 2012). Once phosphorylated on both serine 246 and 287, there is an increase in PACT-PKR as well as PACT-PACT interactions while PKR-TRBP and TRBP-PACT interactions are decreased (Chukwurah et al., 2018). PKR activation is transient in response to oxidative stress and soon after encountering a stress signal PACT activates PKR by a direct association (C. V. Patel et al., 2000; Singh et al., 2011; Singh & Patel, 2012). PKR activity is inhibited by TRBP at later time points after oxidative stress (Chukwurah et al., 2018; Gatignol et al., 2005; Park et al., 1994). Thus, PKR activity is tightly regulated under conditions of cellular stress, in order to maintain the homeostatic balance between cellular recovery and apoptosis. Our results also have established that TRBP mediated downregulation of PKR activity at late time points after stress is very important for cellular survival as prolonged PKR activation induces apoptosis (Chukwurah et

al., 2018; Chukwurah & Patel, 2018). Furthermore, our previous results have also established that TRBP phosphorylation at late time points in response to oxidative stress limits PKR activation by a direct interaction and plays a protective role (Chukwurah & Patel, 2018). Phosphorylation of PACT and TRBP thus plays an important role in regulating their association and dissociation from PKR. Effective inhibition of PKR by overexpression of a phospho-mimic mutant of TRBP was shown to be protective to cells after oxidative stress (Chukwurah & Patel, 2018). These results underline the important role of PKR in activating pro-apoptotic mechanisms in response to oxidative stress.

We have also established that phosphorylated TRBP associates with PKR more efficiently to inhibit its catalytic activity and thus is important to downregulate PKR activation and eIF2α phosphorylation after oxidative stress (Daher et al., 2009; V. Gupta et al., 2003; Singh et al., 2011; Singh & Patel, 2012). In addition to inhibiting PKR by a direct association, phosphorylated TRBP could also inhibit PKR by associating with PACT with higher affinity. The effect of TRBP phosphorylation on TRBP-PACT interactions has not been explored yet, so part of my research was exploring the regulatory role of PKR in determining cellular survival in response to oxidative stress in mammalian cells. In particular, my research was focused on how PKR's negative regulation by TRBP affects cellular apoptosis and if inhibition of PKR activity after oxidative stress can protect the cells from apoptosis. Furthermore, I also investigated if TRBP phosphorylation affects its interactions with PACT in addition to its known effect on PKR interaction to promote cellular survival.

1.5 STRUCTURE OF DISSERTATION

In **Chapter 2** of my thesis, I have focused on investigating if the short-lived *Daphnia* ecotype accumulates more oxidatively damaged proteins than the long-lived ecotype. I compared the overall amount of oxidative damage to proteins in the cytoplasmic and mitochondrial compartments, the activity levels of a few ROS scavenger enzymes, and the relative activity of complex I of the mitochondrial ETC in the short-lived *D. pulex* and the long-lived *D. pulicaria.* This was to understand if shorter lifespan and accelerated aging in *D. pulex* correlated with higher oxidative damage and proteotoxicity as compared to the long-lived *D. pulicaria. D. pulex* exhibited more oxidative damage to proteins than *D. pulicaria* at young and middle ages. This was further supported by the mitochondrial complex-1 activity analysis, which showed that *D. pulex,* has overall reduced levels of mitochondrial complex-1 activity and more oxidative damage to mitochondrial proteins. We next compared the activities of ROS scavenger enzymes SOD and CAT too see if any differences in their activities are indicative of higher ROS load in the short-lived *Daphnia* ecotype. The SOD activity levels in *D. pulex* were much higher relative to *D. pulicaria*. Additionally, when we examined CAT activity, *D. pulex* showed higher levels of CAT activity than *D. pulicaria*, and there was an age-dependent decrease in catalase activity in both ecotypes. The roles of SOD and catalase in determining the lifespan or longevity of an organism has been confusing in *C. elegans* as well as *D. melanogaster.* Similar to these model organisms, higher SOD and catalase activity did not

correlate with longer lifespans in *Daphnia* but rather an inverse correlation was observed. The significance of these results remains to be determined with further studies.

In **Chapter 3,** I transition from looking at the effects of oxidative damage in the invertebrate model *Daphnia* to a mammalian cell culture model to investigate the regulatory role of protein kinase PKR in determining cellular fate in response to oxidative stress. When mammalian cells encounter pathological stress conditions such as oxidative stress, the integrated stress response (ISR) signaling pathway is activated. Our previous results have established that PKR activation and its catalytic activity is regulated very tightly by PACT and TRBP during oxidative stress. At early time points during oxidative stress, PACT is phosphorylated, and this reduces its affinity for TRBP and increases PACT-PKR interactions while also promoting PACT-PACT interactions. We have previously established that TRBP phosphorylated at late time points after oxidative stress binds to and inhibits PKR more efficiently thereby promoting cell survival. In this study, I investigated if phosphorylation of TRBP also enhances its interaction with PACT to bring about additional PKR inhibition. My data establishes that phosphorylation of TRBP has no effect on PACT-TRBP interactions and TRBP's inhibitory actions on PKR are mediated exclusively by its enhanced interaction with PKR. Cells lacking TRBP are more sensitive to apoptosis in response to oxidative stress and show persistent PKR activation as well as eIF2a phosphorylation. These results establish that PKR inhibition by stress induced

TRBP phosphorylation occurs by its direct binding to PKR and is important for preventing apoptosis resulting from sustained PKR activation.

In **Chapter 4,** we explored the role of PKR in stress granules. We focused on the G3BP1- induced stress granules, as recent studies have shown that PKR was involved in eIF2α phosphorylation in these granules because of stress conditions. Therefore, we investigated the mechanisms of PKR recruitment to these granules and asked if PACT it is known activator was also present ass a possible activator of PKR n these granules. Our results showed that overexpression of G3BP1 in cells did indeed lead to stress granule formation. Furthermore, both PKR and PACT were shown to colocalize to these granules. Our protein-protein association immunoprecipitation pulldown assay using both G3BP1 overexpression and endogenous PKR protein additionally supported the colocalization results of the interactions between G3BP1 and PKR. Next, we explored the effects of oxidative stress between G3BP1 and PKR interactions. Interesting we see that G3BP1 associated more with PKR in the absence of stress, however, the association was disrupted as the stress prolonged. This led us to conclude that oxidative stress cause PKR to dissociate from G3BP1 which could then lead to its activation and exit from the granules as was propose by *Reineke et* al, 2015. When we check for direct protein- protein interaction between G3BP1 and PKR using our Yeast 2 hybrid assay, we did not see any interaction as we has expected, however these results could have been as a results of a) the yeast not properly expressing our G3BP1 construct or b)it could be that G3BP1 has a transient 3 party protein in a large stress granule protein

complex that could be responsible for the interactions we has observed in our pull down studies. Overall, these findings of this study can be taken as a first step in elucidating the mechanism by which G3BP1 is able to recruit PKR to SG.

In **Chapter 5**, we discussed our overall conclusions of this dissertation and proposed some future directional studies and new possibilities raised by the current conclusions.

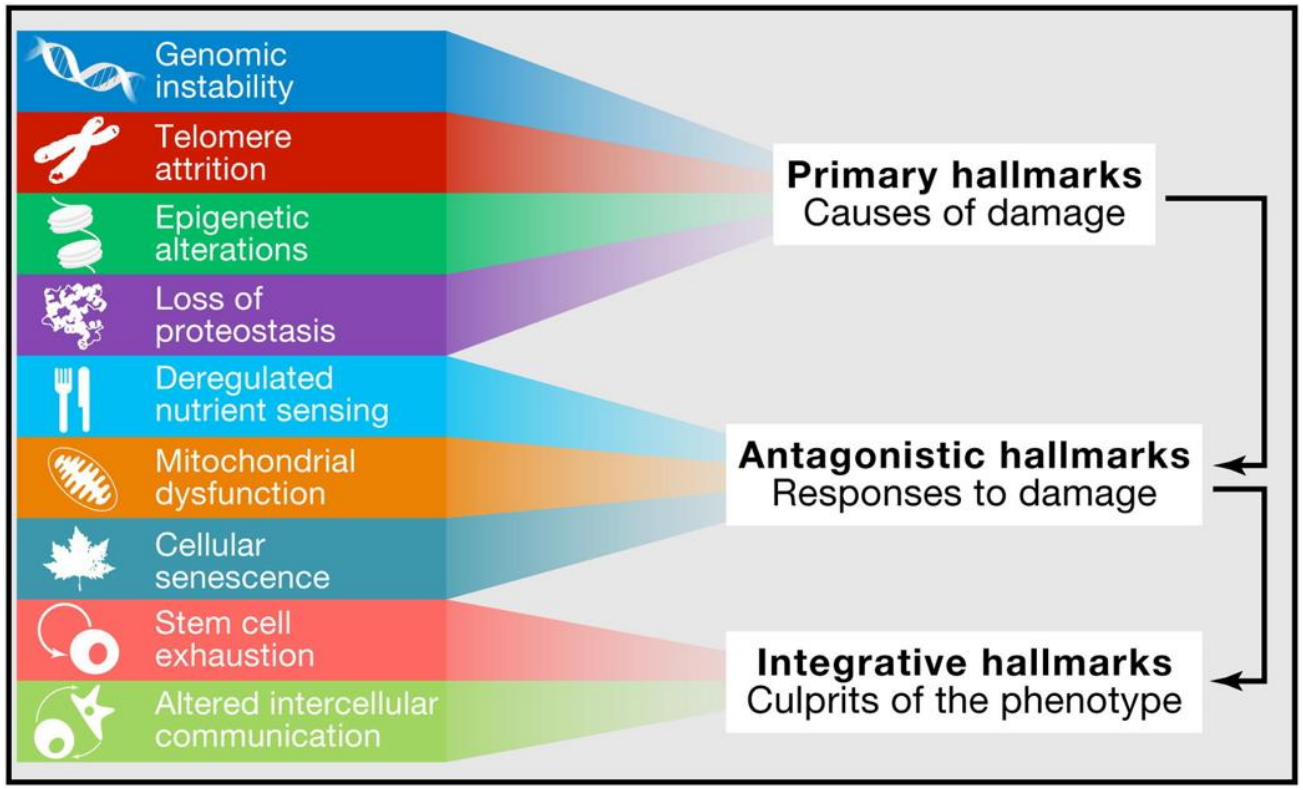

Figure 1.1 Hallmarks of Aging: The nine hallmarks grouped into three categories. The primary hallmarks: considered to be the primary cause of cellular damage. The antagonistic mechanisms: initially mitigate damage but if chronic or exacerbated, become deleterious themselves. The integrative hallmarks: the result of these two groups, responsible for the functional decline associated with aging. *(Figure from Lopez-Otin et. al., Cell, 2013)*

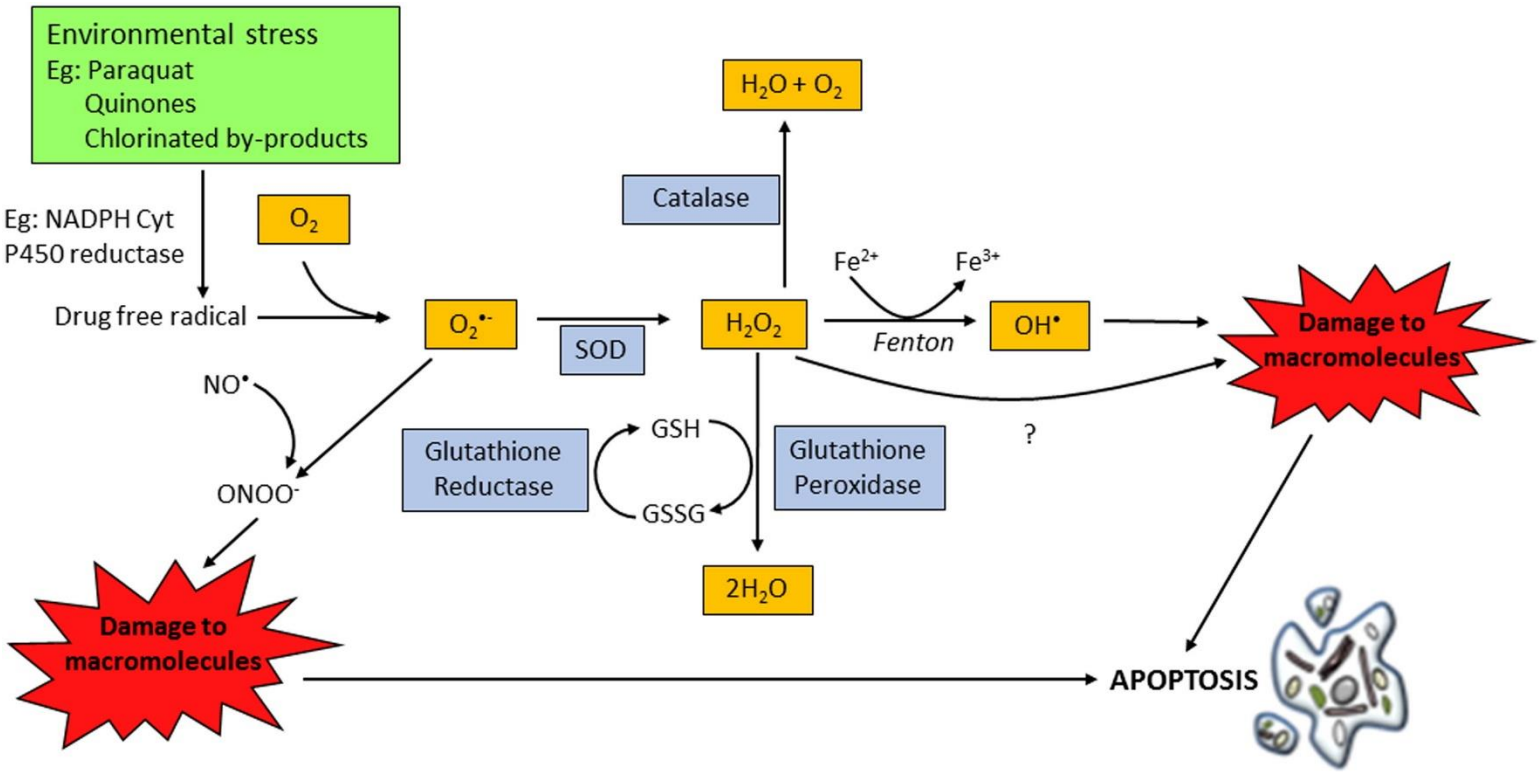

Figure 1.2 Oxidative stress and antioxidant pathway: Reactive oxygen species (ROS), are small molecules that are short-lived and highly reactive in cells. They can be oxygen-derived free radicals like superoxide anion (O_2•−) and the hydroxyl radical (OH•), or non-radical molecules such as hydrogen peroxide (H_2O_2).Ros generation can be attributed to both external stress (environmental derived stressors) and internal stress (derived from normal and abnormal biological process) generate ROS that causes cellular damage to macromolecules and cellular organelles. The generation of ROS in cells exists in equilibrium with a wide variety of antioxidant defenses. These include enzymatic scavengers such as superoxide dismutase (SOD), catalase, glutathione peroxidase and peroxiredoxins, as well as non-enzymatic scavengers such as vitamins C and E, glutathione (GSH), lipoic acid, carotenoids, and iron chelators . *(Figure from Redza-Dutordoir et. al., Mol. Cell Research, 2016)*

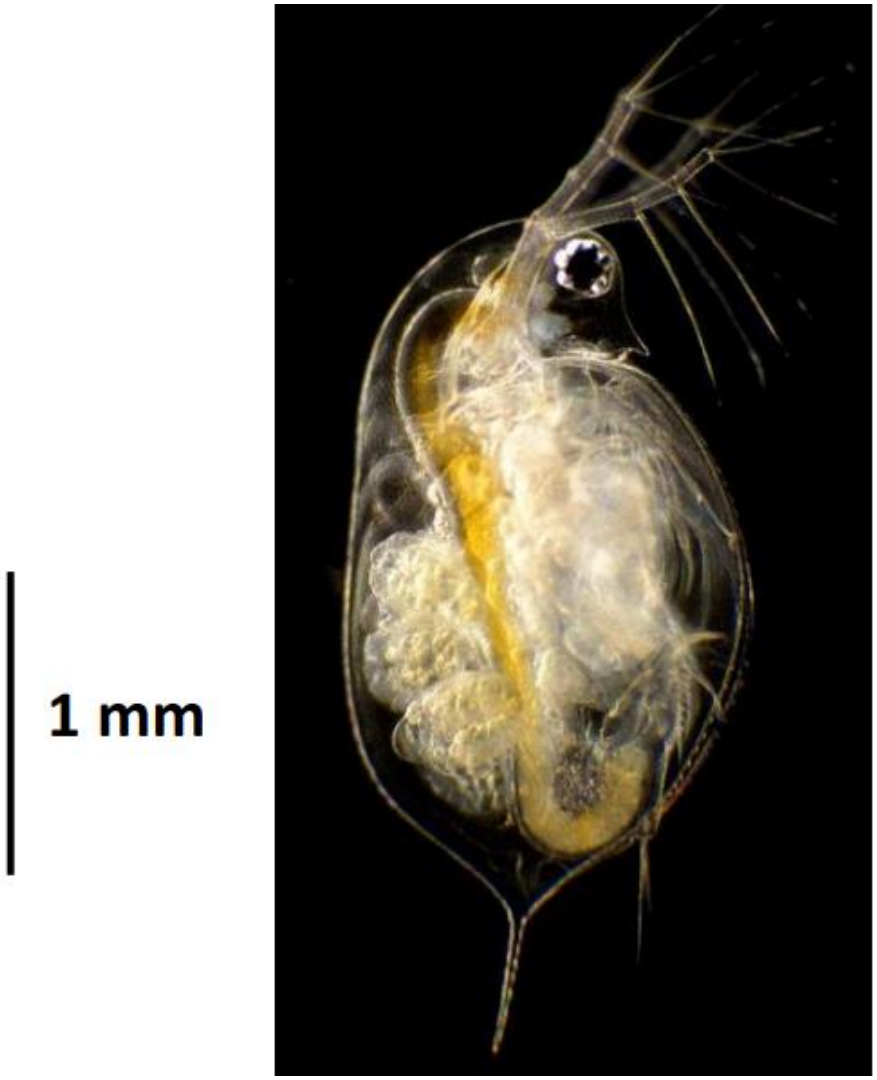

Figure 1.3 *Daphnia pulex,* a freshwater microcrustacean. *Daphnia* is a genus of small planktonic microcrustaceans with adults ranging from 1mm to 5mm in size depending on the species. *Daphnia* are member of the phylum Arthropoda, class Branchiopoda, order Cladocera, family Daphniidae and the ecology of the genus *Daphnia* is the best studied of any other group of organisms.

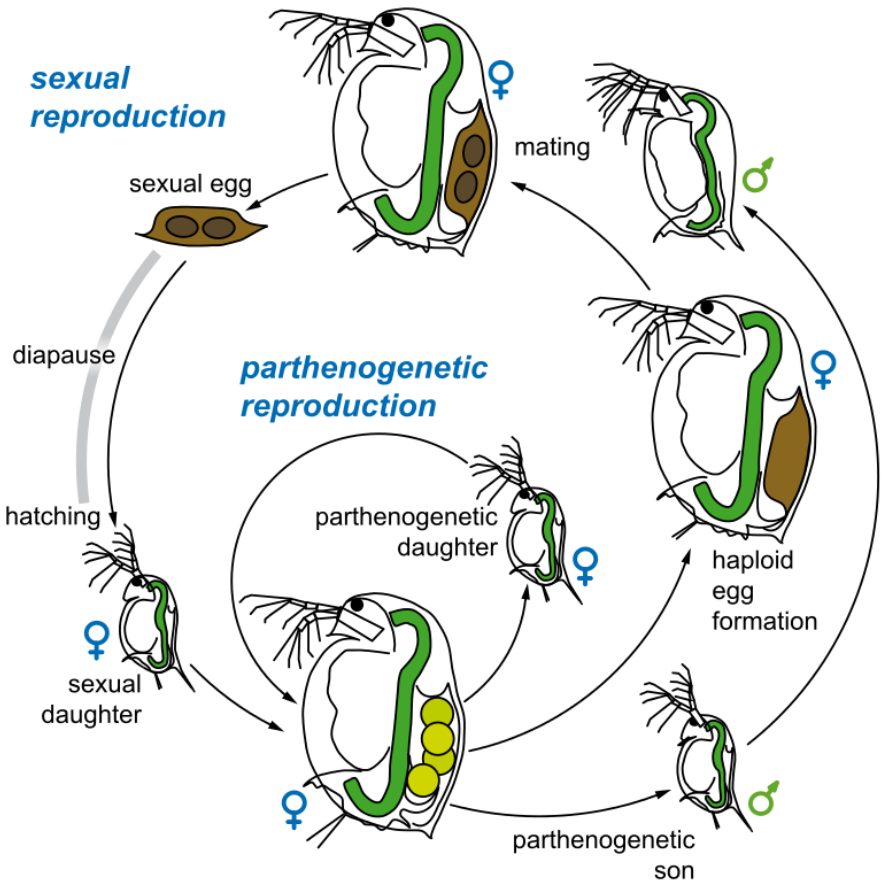

Figure 1.4 *Daphnia pulex* life cycle: This diagram depicts reproductive strategy of the microcrustacean *Daphnia*. Under favorable conditions (left), *Daphnia* reproduce via clonal reproduction, mothers give birth to genetically identical daughters. When conditions become unfavorable (right) for the survival of *Daphnia*, sexual reproduction can be initiated by the birth of male offspring. The males can then mate with females that have developed haploid eggs and the formation of an ephippium takes place with two fertilized resting eggs. This ephippium is resistant to various environmental stressors and once conditions are optimal for *Daphnia* survival, the ephippium can hatch, giving rise to clonally reproducing female offspring.

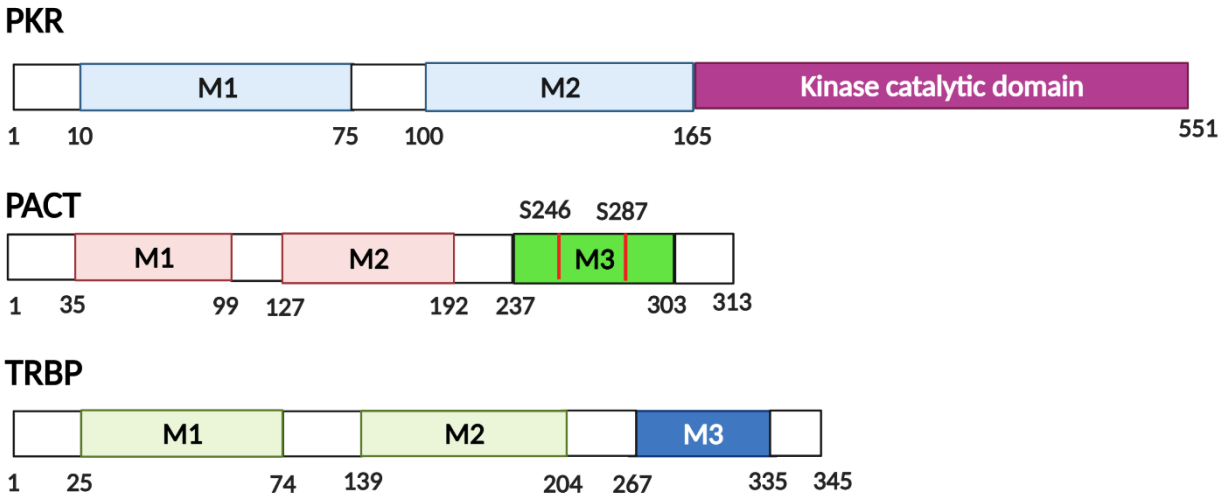

Figure 1.*5* Schematic representation of PKR, PACT and TRBP domains and phosphorylation sites. PKR*:* The light blue boxes represent the two dsRBMs, M1, and M2 , while the dark purple box represents Kinase domain. **PACT**: The light pink boxes represent the two dsRBMs, M1, and M2 , while the green box represents DsRBM M3.The two known phosphorylation sites in PACT serine 246 and serine 287whihc are in the M3 motif region are represented by red lines. **TRBP:** The light green blue boxes represent the two dsRBMs, M1, and M2 , while the dark blue box represents DsRBM M3. Figure was created using BioRender.

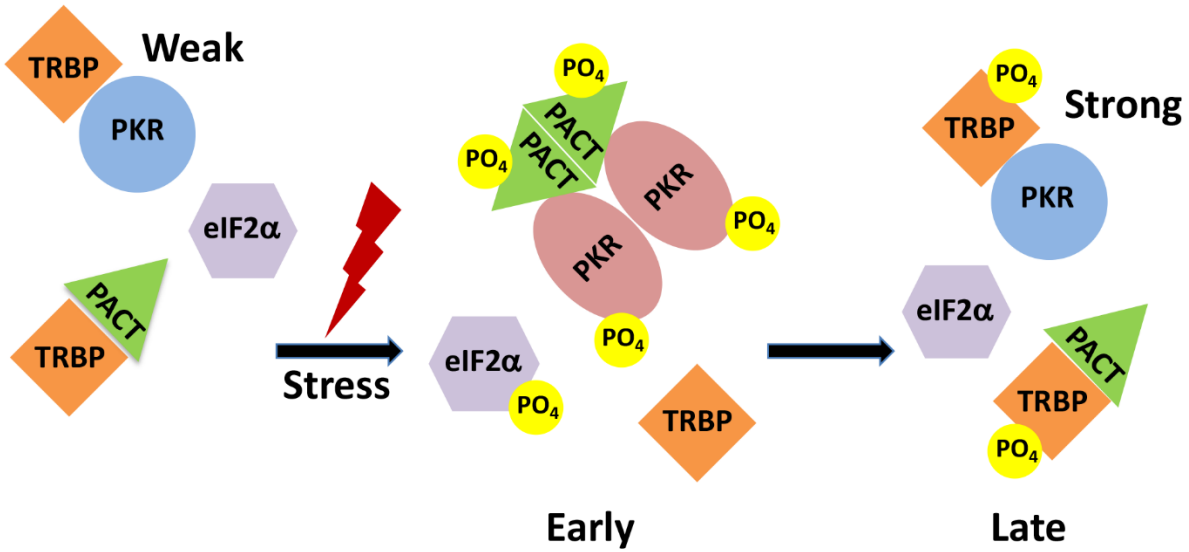

Figure 1.6 A schematic model of PACT and TRBP mediated regulation of PKR in response to oxidative stress. In the absence of stress TRBP heterodimerizes with PKR and PACT, PKR is catalytically inactive and eIF2α is not phosphorylated. At early time points after ER stress, TRBP dissociates from phosphorylated PACT, PACT associates with PKR and activates it catalytically leading to its autophosphorylation and eIF2α phosphorylation. At late time points after stress, TRBP is phosphorylated by ERK and JNK and interacts with PKR with higher affinity to inhibit PKR's catalytic activity. The cells recover by forming TRBP-PKR heterodimers and turning off PKR and eIF2α phosphorylation. Phosphorylated TRBP also associates with PACT similar to unphosphorylated form of TRBP and this further helps to keep PKR inactive**.**

CHAPTER 2

ROLE OF OXIDATIVE DAMAGE IN DETERMINING LIFESPAN IN DAPHNIA[2]

[2] To be submitted as a manuscript to the *Journal of Aging Research*.

2.1 ABSTRACT

Macromolecular damage leading to cell, tissue and ultimately organ dysfunction is a major contributor to the process of aging. Intracellular reactive oxygen species (ROS) resulting from normal metabolism cause most damage to cellular macromolecules and mitochondria play a central role as they are the principal source of ROS. The relationship between naturally occurring variations in mitochondrial (MT) genomes leading to differences in correspondingly less or more ROS and macromolecular damage to change the rate of aging associated organismal decline remains relatively unexplored. MT complex I, a component of electron transport chain (ETC), is a key source of ROS, *NADH dehydrogenase subunit 5 (*ND5) is a highly conserved core protein of the essential subunits that constitute the backbone of complex I. Using the established new freshwater microcrustacean *Daphnia* as a new model organism for aging research, we explored if there are naturally occurring, inherited sequence variations in ND5 that may correlate with a short or long lifespan.

Our results indicate that the short-lived clones have ND5 variants that correlate with reduced complex I activity, increased oxidative damage to proteins, and heightened expression of ROS scavenger enzymes. *Daphnia* offers a unique opportunity to investigate the correlation between inherited variations in components of complex I and differences in ETC efficiencies that can then lead to differences in ROS generation and consequently affect the rate of aging and lifespan. Different populations of *D. pulex* have colonized radically different habitats in geographically separate locations and exhibit extreme differences in

longevity and aging, making such a study possible. The research outlined in this study fully exploits the unique advantages of *Daphnia* as a model system to investigate a direct relationship between inherited mitochondrial efficiencies and rate of organismal aging.

2.2 INTRODUCTION

Understanding the molecular basis of aging is a priority as age is the single most important risk factor for human pathologies such as cancer, diabetes, cardiovascular disorders, and neurodegenerative diseases (Lopez-Otin et al., 2013). Accumulating evidence supports that aging starts with macromolecular damage leading to cell, tissue and ultimately organ dysfunction (Richardson & Schadt, 2014). This intrinsic process can be viewed as an inevitable outcome of the cellular biochemistry and forms a basis from which the diseases of older age originate. The cellular product that causes the most damage is the intracellular reactive oxygen species (ROS) (Fischer et al., 2012). Mitochondria play a central role in regulating the rate of macromolecular damage, as they are the principal source of ROS (Luce et al., 2010; Page et al., 2010; Ray et al., 2012). So far, the contribution of mitochondria to aging has been studied with a view that mitochondrial DNA (mtDNA) is the primary target of the ROS generated by mitochondria. Thus, somatic mtDNA mutations are reported in normal aging, particularly in post-mitotic tissues such as skeletal muscle and neurons, leading to a corresponding decline in the mitochondrial function with age (Khrapko & Turnbull, 2014; Kukat & Trifunovic, 2009; Reeve et al., 2008). Although this decline leads to further ROS production, cellular damage, and aging associated

cellular dysfunction (Lauri et al., 2014); such observations do not imply a causal relationship between inherited variations in mitochondrial efficiencies and variations of aging. The causal relationship between naturally occurring variations in the mitochondrial genomes that can lead to differences in the mitochondrial electron transport chain (ETC) efficiencies could result in correspondingly less or more ROS. Admittedly, macromolecular damage caused by these ROS that can change the rate of age -associated organismal decline has remains relatively unexplored.

The mitochondrial ETC comprises five multi-subunit complexes (complex I- complex V), the last one being the ATP synthase (Sazanov, 2015). Complex I (NADH:quinone oxidoreductase) is the first and largest enzyme, the major electron entry point for the respiratory chain (Sazanov, 2015), and a key source of ROS in mitochondria (St-Pierre et al., 2002) Mutations in complex I subunits are implicated in human diseases and aging (Zapico & Ubelaker, 2013). Of the 44 subunits (human) of the complex I, 38 are encoded by the nuclear genome and 7 by mtDNA (Lauri et al., 2014). The 7 mtDNA-encoded hydrophobic subunits NADH dehydrogenase (ND) 1–6 and 4L (ND1-ND6 and ND4L) are the core subunits that form the major membrane arm of complex I (Brandt, 2006; Janssen et al., 2006). Mutations in ND subunits disrupt either complex I assembly or enzyme activity and cause ~ 20% of cases of isolated complex I deficiency (Bugiani et al., 2004). In humans, variations in ND5 sequence are associated with mitochondrial encephalomyopathy, lactic acidosis, and stroke-like episodes (MELAS) (Liolitsa et al., 2003) as well as some symptoms of

Leigh's syndrome (Brecht et al., 2015; Hashimoto et al., 2015; Ma et al., 2013), and Leber's hereditary optic neuropathy (LHON) (Huoponen et al., 1993; Mayorov et al., 2005; Pulkes et al., 1999; Zhang et al., 2012). Many fatal pathological conditions such as Leigh syndrome, leukoencephalopathy, LHON, mitochondrial myopathy, encephalopathy, MELAS, and Parkinson's disease, and cancer are associated with mutations in the ND genes including the ND5 gene (Copeland & Longley, 2014; Vartak et al., 2014). ND5 mutations cause mitochondrial dysfunction due to a decrease in complex I efficiency and increased ROS generation (Blok et al., 2007). However, very few studies have been done to relate naturally occurring, non-pathogenic ND5 sequence variations to ETC efficiencies, and ROS generation that can affect rate of aging, senescence, and life span.

In this study, we identified naturally occurring ND5 sequence variations in geographically distinct populations of the freshwater microcrustacean, *Daphnia pulex* and examined its correlation with complex I enzyme activity and level of oxidative damage to total and mitochondrial proteins. We also investigated the activities of ROS scavenging antioxidant mechanisms in the short- and long-lived *Daphnia*. Our results indicate that lower activity of complex I possibly leading to higher levels of ROS leads to correspondingly high levels of oxidative damage to proteins. Although there is a corresponding increase in activities of ROS scavenging antioxidant mechanisms, the short-lived clones show an imbalance between ROS production and removal thus accumulating damaged proteins possibly leading to a shorter lifespan. The results are important because they

demonstrate the effects of naturally occurring single amino acid sequence variations in ND5 on longevity. Our study demonstrates that *Daphnia* is an excellent model system that offers significant advantages with its unique clonal reproduction, availability of genome manipulation techniques, and naturally existing ecotypes with varied lifespans to understand natural determinants of lifespan.

2.3 MATERIALS AND METHODS

***Daphnia* Cultures:** *D. pulex* clones used in this study were isolated from ponds and lakes in southwest Michigan in 2008 and have since been cultured in the laboratory. No specific permissions are required to collect zooplankton from these public-access waterbodies in Michigan. *D. pulex* clones are neither endangered nor protected. For further details on the source populations, see Dudycha (Dudycha, 2004). *Daphnia* are maintained at a temperature of 20 C with a photoperiod of 12:12 L:D (12 hours of light followed by 12 hours of dark) within a Percival growth chamber. *Daphnia* were maintained at a concentration of 3 to 5 animals per 250 mL beaker in 200 mL of COMBO, artificial lake water. *Daphnia* were cleared of young and transferred to a new beaker with fresh water on alternate days. They were fed every day with vitamin supplemented algae *Ankistrodesmus falcatus* at a concentration of 20,000 cells/mL. To generate experimental animals, even-aged cohorts were begun by placing neonates individually in 100 mL of COMBO. Experimental animals were otherwise maintained as in the source cultures.

Survivorship curves: We compared survivorship of the 11 different clones using previously described methods for *Daphnia* in (Kim et al, 2014). Experimental conditions were 20°C, a 12:12 L:D photoperiod, with animals kept in individual 150-mL Pyrex beakers in 100 mL COMBO hardwater artificial lake water (Kilhaam et al, 1998). Two generations were maintained under experimental conditions prior to initiating the life table to minimize maternal effects variation. Experimental individuals were fed 20,000 cells/mL Ankistrodesmus falcatus daily, a food level that produces normal aging processes in *Daphnia* (Dudycha, 2003). Individuals were transferred to fresh beakers and COMBO every other day, and survivorship was observed daily until all experimental animals died. For each clone, n = 60 females (Shumpert et al, 2015).

ND5 sequence analysis and cloning of *Daphnia* ND5 ORF: Primers were designed to PCR amplify the *Daphnia* ND5 ORF sequences of all our long- and short-lived *Daphnia* clones using MacVector based on the published *D. pulicaria* genome on the wfleabase.org. For each PCR reaction, 10 ng genomic DNA was used with 50 pmoles each of the forward and reverse primers designed to amplify the ND5 PCR product using the Promega GoTaq PCR kit. The following conditions were used for PCR: Lid 95°C, 95° C for 2 min (initial denaturation), denaturation at 95° C for 15 s, annealing at 55° C for 15 s, extension at 72° C for 15s for 24 cycles on the Eppendorf Scientific gradient Mastercycler®. PCR products were separated on a 1 % agarose gel. The PCR products were sent out for sequencing (Eton Bio). Both DNA sequences and the deduced protein sequences were aligned using MacVector and compared to the reference

Daphnia mitochondrial genome. The protein sequences were checked for any amino acid sequence changes.

Primer sequences used were as follows:

Primer: ND5 Forward: 5'-GAGGTGGTCCGCATTCTTTA-3'

Primer :ND5 Reverse: 5'-AAAGTCAAGTAGCGCGGGTA-3

Blue Native gel electrophoresis

***Daphnia* cell/tissue lysate isolation preparation:** All water was removed from the tubes containing the *Daphnia*, the organisms were washed once with 1 mL cold PBS and the organisms were homogenized using a tight-fitting pestle. We homogenized 100-200 individuals in 100 µL of NativePAGE® Sample buffer, 5% Digitonin containing protease inhibitor cocktails (Sigma and Calbiochem) following the manufactures protocol for the NativePAGE® Sample Prep Kit (BN206, BN 2008, Life Technologies) and then centrifuged at 20,000 x g for 30 minutes at 4°C. The supernatant was aliquoted into sterile microcentrifuge tubes and stored at -80°C until use. The protein concentration was determined using the BCA kit (Pierce). To determine the activity of mitochondrial complex 1 in the two ecotypes of *Daphnia* at different ages, we utilized the blue native gel kit from Life Technologies (NativePAGE™ Novex® Bis-Tris Gel system, BN1001BOX, BN1002BOX, BN1003BOX and BN1004BOX). After mitochondrial proteins were extracted, two Gels were run side by side; 1) a clear native gel used for the in-gel activity assay and 2) a blue native gel for staining with Coomassie blue G250.

Blue Native (BN-PAGE): Mitochondrial protein extracts prepared in 1X Native PAGE™ Sample Buffer and detergents were subsequently run on a 4-16% Blue Native polyacrylamide gradient gel following the manufactures protocol (Invitrogen, Native PAGE Gel system). Immediately prior to electrophoresis, NativePAGE™ 5% G-250 Sample Additive was added to the samples and the NativeMark™ Unstained Protein Standard (Invitrogen, LC0725) was used for as the markers. Two types of NativePAGE™ Running Buffers are used for native gel electrophoresis with NativePAGE™ Novex® Bis-Tris Gels. NativePAGE™ 20X Running Buffer (BN2001) and the NativePAGE™ 20X Cathode Buffer Additive (BN2002), contains 0.4% Coomassie G-250 (added to NativePAGE™ Running Buffer to generate the Cathode Buffer) which were purchased and prepared according to the manufactures protocol. The dark cathode buffer (Dark Blue Cathode Buffer contains 0.02% G-250) was used for the Blue native gel. The manufacturer's instructions for performing electrophoresis using the Invitrogen Mini-Gel Tank (Invitrogen, A25977) was followed with the gel being run in the cold room at 4°C. First at 150 V for 60 minutes, then it was increased to 250 V for the remainder of the run (30–90 minutes). After electrophoresis was completed a fast Coomassie G-20 staining was performed by first placing the gel in 100 mL Fix solution (40% methanol, 10% acetic acid) and microwaving on high (950–1100 watts) for 45 seconds, next the gel was on an orbital shaker for 15 minutes at room temperature. Finally, to destain the gel, we added 100 mL destain solution (8% acetic acid) and microwaved on high (950–1100 watts) 45 seconds. The final round of shaking was done on an orbital shaker at room

temperature until the desired background was obtained. The gel was then washed with water and photographed using a White Light Transilluminator FB-WLT-417 (FisherBiotech, Fisher Scientific).

In-gel complex I activity assays

Clear-Native (CN)-PAGE : The protocol used for the for the BN-PAGE was used for the CN-PAGE, with the major changes being the use of a light Cathode buffer (made by adding less NativePAGE™ Cathode Buffer Additive (20X) to the NativePAGE™ Running Buffer). The gel was first run in the light cathode buffer at 150 V for 30 minutes. After 30 minutes, the light cathode buffer was changed to the clear cathode/running buffer to prevent the excessive blue color of the Coomassie Blue dye from interfering with the color of the in-gel activity assay.

Mitochondrial complex 1 (in-gel) activity was detected using a modified method first explained by *Witting et al, 2007* and simplified by Wang et al, 2017. The gel was then incubated for 30 minutes in 20 mL of the Complex 1 activity substrate buffer (2 mM Tris-HCL at pH 7.4, 0.1mg/mL NADH disodium salt trihydrate (Abcam, ab146315 and 2.5mg nitrotetrazolium blue (NTB) (Abcam, ab146262) according to the protocol describe by *Wang et al, 2017*. To stop the reaction once the desired purple color for complex 1 activity was obtained to fix the gel, a 10% acetic acid solution was used. The gel was then washed with water and photographed using a White Light Transilluminator FB-WLT-417 (FisherBiotech, Fisher Scientific).

Detection of Protein Carbonyls via Oxyblot: The oxidation status of proteins from various Daphnia clones was determined using the Oxyblot protocol from

EMD Millipore. This assay is based upon the fact that reactive oxygen species induces carbonyl group formation in proteins at specific residues. These carbonyl groups can then be derived into 2,4-dinitrophenylhydrazone (DNP-hydrazone) by 2,4-dinitrophenylhydrazine (DNPH). The altered groups are detected following SDS PAGE and Western Blot Analysis with an antibody that detects the DNP-hydrazone group of oxidized proteins. *Daphnia* protein samples were harvested using RIPA buffer and protein concentration was determined using a BCA protein quantification kit (thirty individual *Daphnia* were used for each aged set of both ecotypes). To first derivatize the carbonyl group into DNP-hydrazone, 20 µg of each protein sample was placed in a fresh tube (the samples were diluted such that 5 µL of each sample was used). Then 5 µL of 12% SDS was added to the tube to denature the proteins and 10 µL of 1X DNPH solution was added to the tube. The tubes were then incubated for 15 minutes at room temperature. The derivation reaction was stopped by adding 7.5 µL of neutralization solution to each tube. Note that we performed each Oxyblot with duplicate samples, one that had been derivatized another that served as a control, was not derivatized into DNP-hydrazone. The 20µg samples were then loaded onto a 12% polyacrylamide gel and western blot analysis was performed using chemiluminescent ECL plus (Pierce)for detection of protein on a GE Typhoon LAS 4000 (antibody used was provided with the Oxyblot kit, recognizes DNP-hydrazone, dilution 1:2000) (Schumpert *et al,* 2014). The images were analyzed and quantified using the program ImageQuant.

Hydrogen peroxide Assay: Hydrogen peroxide amounts were determined for each aged set of *Daphnia* using the Pierce Quantitative Peroxide Assay Kit (Lipid). This assay is based upon the oxidation of ferrous iron to ferric iron which is performed directly by the hydrogen peroxide contained within the sample. Once the iron is in the ferric state, it can bind directly to a xylenol orange dye which produces a violet color that can be measured spectrophotometrically at a wavelength of 560 nm. We first standardized the assay using various amounts of hydrogen peroxide (30% w/v) and then performed the assay with *Daphnia* samples. Ten individual *Daphnia* were homogenized in 100 µL of PBS and centrifuged at 13,200 rpms for 10 minutes. The supernatant was placed in a new microcentrifuge tube and used for the assay. Note for each experiment 3 biological replicates and 3 technical replicates were performed. To perform the assay, we added 20 µL of sample with 200 µL of the working reagent supplied with the kit in a 96 well plate. The plate was incubated at room temperature for 20 minutes before being read on a plate reader (Bio-Tek) using Gen5 software. Note that all concentrations of hydrogen peroxide were normalized to one microgram of protein which was determined using a BCA kit from Pierce.

Catalase Activity Assay: Catalase activity was detected using a modified method first developed by Beer and Sizer (Beers & Sizer, 1952; Enzor & Place, 2014). This spectrophotometric method utilizes the fact that the absorbance of hydrogen peroxide concentration can be detected at 240 nm. The higher the amount of catalase present, the faster the absorbance representative of hydrogen peroxide will be diminished (Beers & Sizer, 1952). Seven individual

Daphnia from each ecotype at the 3 different ages were homogenized in 30 microliters of 67 mM Phosphate Buffer Solution (PBS). Note for each experiment 3 biological replicates and 3 technical replicates were performed. The homogenate was centrifuged at 13,200 rpms for 5 minutes and the cleared supernatant was kept and used in the Catalase Activity Assay. The assay was initiated by adding 300 microliters of PBS-hydrogen peroxide solution (comprised of 160 µL of 30% hydrogen peroxide and 99.84 mL of 67 mM PBS) into a clear bottom well 96 well black plate (UV-star plate from Greiner Bio-one). Then 5 µL of *Daphnia* homogenate was added to the PBS-hydrogen peroxide solution in the well, mixed and read on a 96 well plate reader (Bio-Tek) using Gen5 software. Numerous reads were taken over a duration of 5 minutes with reads occurring every 47 seconds. We then calculated the slope of the diminishing hydrogen peroxide amounts and calculated the activity of catalase based upon the following equation where S is equal to the slope describing the diminishing hydrogen peroxide absorbance, V is volume of PBS-hydrogen peroxide solution added per well, and Ɛ is the molar extinction rate of hydrogen peroxide at 240 nm (0.0436 mL μmol^{-1} cm^{-1} at 240 nm) (Enzor & Place, 2014).

$$Catalase\ Activity = S(\frac{V}{\text{Ɛ}})$$

For each aged *Daphnia* set, we also determined the protein content of the samples using BCA kit from Pierce and present the data as units of catalase per microgram of protein. Note we also performed standard calculations based upon commercial catalase isolated from bovine liver (sigma). For the standard

calculation, we serially diluted the catalase and performed the assay at various concentrations to standardize the assay.

SOD Activity Assay: To determine the activity of SOD in the two ecotypes of *Daphnia* at different ages, we utilized a kit from Sigma (Sigma SOD Assay kit 19160). This kit is based upon an altered tetrazolium salt WST-1, which will be reduced by superoxide anion to form a formazan dye which can then be detected spectrophotometrically at 450 nm wavelength. The presence of SOD will reduce the amount of superoxide anion and thus diminishing the amount of dye produced lowering the absorbance detected at 450 nm. For each aged set of *Daphnia*, we homogenized 10 individuals in 100 µL of PBS and then centrifuged at 13,200 rpms for 10 minutes. The supernatant was kept and used as the samples for the SOD Activity Assay. Note for each experiment 3 biological replicates and 3 technical replicates were performed. To perform the assay, 20 µL of *Daphnia* homogenate was added to the well of a 96 well plate. Then 200 µL of WST working solution was added to the well and mixed followed by the addition of 20 µL of Enzyme Working Solution. The plate was then incubated for 20 minutes at 37 C before being read using a plate reader (Bio-Tek) at 450 nm using Gen5 software. The amount of SOD needed to inhibit 50% of the reduction of the WST-1 dye is defined as one unit of SOD (Enzor & Place, 2014). Note that the amount of protein was determined for each sample and the activity of SOD is reported as units of SOD per microgram of protein. To standardize the assay, we also performed the experiment using varying amount of commercially available SOD (Sigma).

Statistics: To determine statistical significance when analyzing the various assays performed in this study, we executed a two tailed Student's T-test, assuming equal variance. Each figure legend denotes p values as set forth by brackets and special characters. Note that our alpha level was p=0.05

2.4 RESULTS

Genetic variation of lifespan and ND5 sequence variations in *D. pulex* clones

The median lifespan in 11 clones of *D. pulex* was determined by several replicate experiments with the average lifespan defined as the age at which 50% of the individuals in the population died. As seen in Figure 2.1 A, median lifespans differ greatly (~ 15 to 85 days) among various clones. Once we had established the survivorship curves, we narrowed down our selection of clones for all the future experiments. We chose RW20 and WF6 to represent our short-lived daphnia clones and XVI-11 to represent our long-lived clone. We next investigated if specific inherited variations of ND5 could be causative of differences in the ETC efficiencies that can then lead to differences in ROS generation and consequently affect the rate of aging and lifespan. ND5 was chosen for initial analysis, as it is used extensively for understanding evolutionary relationships among *Daphnia* populations (Cristescu et al., 2012; Xu et al., 2012). We sequenced a 1050 bp region of ND5 gene from the 11 indicated clones to identify specific amino acid variations associated with characteristic short or long lifespans. When we aligned the 11 deduced ND5 protein sequences in the order of increasing life spans (Figure 2.1 B), a striking pattern emerged. First, the two

shortest-lived clones carry a proline at position 307 whereas all other clones have a leucine. Secondly the two longest lived clones carry a leucine at position 320 whereas all other clones carry a phenylalanine, and thirdly, the three longest lived clones carry a leucine at position 354 whereas all other clones carry a phenylalanine. Lastly, these variations are in the conserved C-terminal domain important for ND5 enzymatic activity.

MT complex I activity is diminished in the short-lived clone

To test if the differences in ND5 sequence correlates with enzymatic activity of complex I, we compared complex I enzymatic activity in two representative clones relative to total amount of complex I. We prepared MT protein extracts from mixed-age populations of WF6 short-lived clone and lake XVI-11 long-lived clone. We separated the individual ETC complexes by Blue Native polyacrylamide gel electrophoresis using a 4-16% gradient gel as described by Wittig *et al* (Wittig & Schägger, 2009). Next, we measured the enzymatic activity of complex I, using an in-gel activity assay as described by Wang *et al.* using NADH as the complex I substrate (Wang et al., 2007). If complex one activity is intact, it shows as a purplish dark blue band indicating active complex I. Such in-gel assay is used to measure complex I enzymatic activity as the complex remains catalytically active in native gels. As seen in Figure 2.2 A, (lanes 4-6), the short-lived WF6 clone showed significantly less complex I enzymatic activity when compared to the long-lived XVI-11 clone (lanes 1-3). The band intensities were measured and normalized to the band intensities of total amount of complex I (blue native panels) and are shown in

Figure 2.2 B. The short-lived WF6 showed about 59% reduction in complex I activity compared to XVI-11. Although additional sequence variations in other components of complex I that we have not investigated here also may contribute to the reduced enzymatic activity, these results show a significant correlation of complex I activity and lifespan.

Differences in the level of oxidative damage to proteins in the short-lived and long-lived clones

To test if the short-lived clone generated more oxidative stress in cells, we compared the levels of oxidative protein damage at various ages in two representative clones. As shown in Figure 2.3 (A and B), the short-lived RW20 clone showed high levels of oxidative damage at a young age of 1 week (lane 1) that remained high throughout life (lanes 3 and 5, M and O). In contrast, the long-lived clone lake XVI-11 showed dramatically less oxidative damage at a young age (lane 2) as well as during middle age (lane 4) and the old population showed oxidized protein levels (lane 6) that were comparable to the 1-week-old RW20 clone (lane 1). Similarly, it can be seen in Figure 2.4 that MT extract from a mixed population of short-lived WF6 clone showed more oxidative damage to proteins, when compared to the MT extract from a mixed population of long-lived XVI-11 clone. These results demonstrate that not only do the short-lived and long-lived clones vary in their MTDNA encoded ND5 protein, but these differences could also be playing a role in the difference in their lifespans. As the short-lived clone WF6 had less complex I enzymatic activity (Figure 2.2) known

to generate higher ROS accumulation, it would result in increased oxidative damage in both the cells as well as in the mitochondria.

Differences in the ROS scavenger mechanisms in short- and long-lived clones

To investigate additional factors leading to the difference in oxidative damage to proteins, we compared the activity of the ROS scavenger enzymes superoxide dismutase (SOD) and catalase (CAT) in the short- and long-lived clones. SOD and CAT are ROS scavenging enzymes known to play a central role in the antioxidant defense systems in all organisms (Höhn et al., 2017). SOD enzymes convert the toxic superoxide radical into hydrogen peroxide (another ROS) and molecular oxygen depending on the cellular context (Balaban et al., 2005; Peng et al., 2014). Furthermore, the short-lived RW-20 displays significantly higher levels of SOD activity at young and middle ages, 10.9 and 14.5 units per microgram of protein, respectively (Figure 2.5). As opposed to this, the long-lived clone XVI-11 at equivalent ages shows only 1.9 and 0.9 units per microgram of protein, respectively. At old age in RW20, the SOD activity declines drastically to levels similar to old XVI-11 *with* 1.3 and 0.9 units per microgram of protein, respectively. Of note, XVI-11 exhibits relatively low amounts of SOD activity at all ages examined with very little change through the lifespan indicating lower amounts of ROS accumulation as ROS production is known to induce expression of SOD.

As the short-lived RW20 showed high level of oxidative damage to proteins at all ages during lifespan (Figure 2.3 and 2.44) and had elevated levels

of SOD activity (Figure 2.5), we next examined the relative levels of hydrogen peroxide, the SOD scavenging reaction product that is also a ROS, in both short- and long-lived clones. Hydrogen peroxide causes oxidative damage in macromolecules including proteins (Balaban et al., 2005; Peng et al., 2014) and eleven distinct mitochondrial sites have been identified that can produce it in addition to the SOD enzyme reaction. As is shown in Figure 2.6, the short-lived RW20 contains relatively high levels of hydrogen peroxide with little change during the lifespan. The young, middle, and old RW20 organisms showing 153.6, 139.7, and 147.9 µM hydrogen peroxide per microgram protein, respectively. In contrast, the long-lived XVI-11 *clone* contains high levels of hydrogen peroxide only in young organisms(139.3 µM hydrogen peroxide per microgram protein), which declines drastically by middle age and is kept relatively low in old organisms (46.5 and 41.1 µM hydrogen peroxide per microgram protein respectively).

We then investigated catalase activity, another ROS scavenger enzyme that converts hydrogen peroxide to water and molecular oxygen (Balaban et al., 2005; Lopez-Otin et al., 2013; Peng et al., 2014). We used a catalase activity assay as previously described (Beers & Sizer, 1952; Enzor & Place, 2014). We initially standardized the assay using commercially available catalase (Sigma) and optimized the assay parameters for *Daphnia* samples. Particularly, young RW20 exhibit the highest catalase activity with an average of 63.4 units of CAT per microgram of protein with a decline to 30.9 units per microgram of protein at middle age and thereafter staying at 30.4 units of CAT per microgram of protein

in older age (Figure 2.7). In XVI-11 the same overall trend is observed with higher amounts of catalase being in young organisms before declining in middle age and staying relatively unchanged in old organisms (44.6 to 10.4 to 7.7 units of CAT per microgram of protein), respectively. However, the amount of catalase activity is significantly lower in XVI-11 at equivalent time points compared to RW20 and as ROS is known to induce catalase expression, this possibly means lower overall levels of ROS in XVI-11.

2.5 DISCUSSION

Multiple studies from several model organisms reveal a complex relationship between harmful ROS and aging. The role of oxidative damage and the effects of ROS on aging is not as straightforward as originally envisaged. Initial studies performed in *D. melanogaster* depicted ROS as being quite detrimental to organisms and was cited as being a major factor for the aging process (Clancy & Birdsall, 2013; Eleftherianos & Castillo, 2012; Orr & Sohal, 1994). Other studies indicated that high ROS levels do not necessarily cause shorter lifespan and that overexpression of certain scavenger enzymes known to mitigate effects of ROS showed no effect on longevity (Clancy & Birdsall, 2013; Eleftherianos & Castillo, 2012; Lopez-Otin et al., 2013; Orr et al., 2003). A current theory poses that the presence of ROS is necessary for survival and can be thought of as molecules similar to AMP and NAD+, molecules that are necessary in a strict physiological range and are essential for proper homeostasis (Lopez-Otin et al., 2013). It is plausible that when ROS levels are elevated beyond this physiological range, they become detrimental to the organism by damaging

macromolecules, with the most crippling damage to proteins. Hekimi *et al* suggest that ROS acts as a stress response signaling cascade that is not initially causative of aging and several ROS, particularly hydrogen peroxide, have been shown to be essential signaling molecules (Hekimi et al., 2011; Lopez-Otin et al., 2013). Thus, in our present study we sought to examine the overall amount of oxidative damage to proteins, the activity levels of several ROS scavenger enzymes, and an associated ROS concentration level in young, middle, and old *Daphnia* of two closely related *Daphnia* pulex clones with vastly different lifespans, RW20 or WF6 for short-lived and XVI-11 for long-lived clones.

Some of the previous studies have demonstrated DNA and lipid damage from ROS are not likely involved as large causative agents for the aging process (Clancy & Birdsall, 2013; Edman et al., 2009). Therefore, we decided to examine oxidative damage in proteins. My data shows that, WF6 and RW20 (short-lived Daphnia) exhibit more oxidative damage to proteins than XVI-11 (long-lived Daphnia) at young and middle-ages but the amount of damage is comparable in old organisms of both clones. What is causing the difference in oxidative damage to proteins? Based on our results, the naturally occurring ND5 sequence variations observed in short-lived RW20 and WF6 correlate with reduced complex I activity, which is known to lead to higher ROS generation. Thus, the short-lived clones generate more ROS and that correlates well with higher amounts of oxidative damage to both cytoplasmic and mitochondrial proteins. Thus, we can correlate the natural variations in mitochondrial ND5 sequence to

lower complex I activity, increased oxidative damage to proteins leading to shorter lifespans.

The ROS scavenger enzyme SOD activity levels were much higher in the short-lived RW20 than long-lived XVI-11. This enzyme is known to mitigate the extremely toxic free radical superoxide anion; however, the product of the enzymatic reaction that rids the cells of these toxic species is hydrogen peroxide which is another toxic ROS. Therefore, the high amount of SOD activity in RW20 may not be beneficial for the organism as the enzyme produces a toxic product that could further damage cellular macromolecules, especially proteins. The hydrogen peroxide species is much more stable than superoxide anion and could have a lasting detrimental effect on various macromolecules and can be converted into another toxic ROS, the hydroxyl radical (Hekimi et al., 2011). We also analyzed the levels of hydrogen peroxide in short- and long-lived clones at young middle and old ages. The short-lived RW20 did in fact have higher levels of hydrogen peroxide levels than XVI-11 and these higher levels are maintained throughout life. Note that SOD activity diminishes in old age of RW20, but the hydrogen peroxide levels remain high. As mitochondrial respiration could be less efficient with age and more ROS is known to be produced from aberrant ETC reactions, that could be the cause of the high level of hydrogen peroxide in old RW20 (Johnson et al., 1999; Lopez-Otin et al., 2013). The long-lived XVI-11 also displayed higher amounts of hydrogen peroxide in young organisms which diminished by middle age and was maintained low through old age. To follow this up, we examined CAT activity, the enzyme which would convert hydrogen

peroxide into water and molecular oxygen and thus can potentially alleviate some of the ROS induced stress in the cells. The results indicated that although RW20 showed higher amounts of catalase activity there was much higher amounts of hydrogen peroxide as well. This explains why, the short-lived RW20 contains higher amounts of oxidative damage to proteins, being unable to cope with the ROS produced during normal metabolism throughout the lifespan.

It is also important to note that there are other types of ROS and ROS scavenging enzymes that we did not assay in this study, including hydroxyl anions and glutathione peroxidases (Doonan et al., 2008; Harding et al., 1996; Marí et al., 2009; Nathan & Cunningham-Bussel, 2013). Thus, whether free radicals and ROS are causative of aging, or act as a signaling molecules in response to other aging related insults, we can detect differences in MT complex I activity, ROS levels, ROS scavenging enzymes, and oxidative damage to proteins between the short- and long-lived clones of *D. pulex.* In order to evaluate the direct causal relationship between lifespan and naturally occurring sequence variations in ND5 and possibly other MT genes as well as nuclear genomes, various mitochondrial genomes would need to be manipulated on different nuclear backgrounds. This is certainly possible by setting up genetic crosses as *Daphnia* also can reproduce sexually and isogenic males can be produced relatively easily.

A crosstalk between the ROS network and the heat shock response has been observed and is important for aging process and longevity (Calabrese et al., 2003; Pappolla et al., 1996; Tower, 2011). In a previous study, we had

examined the proteotoxic response known as the heat shock response in *short- and* long-lived clones and found that the short-lived clone stops responding to heat stress by middle age whereas the long-lived clone can still respond to heat shock in middle age by inducing the expression of heat shock protein 70, a molecular chaperone (Schumpert et al., 2014). Thus, the ability to respond to proteotoxic heat stress varies between the short- and long-lived clones of *Daphnia* and may contribute to the observed differences in the longevity. Other ROS not analyzed in this work, such as the hydroxyl ions and their associated scavenging enzymes can be analyzed in future to determine their role in oxidative damage and lifespan. More importantly, we could further analyze the effects of exogenous treatment with antioxidants on lifespan extension, rate of aging, or sex-dependent aging (Barata et al., 2005; Constantinou et al., 2019, Kim et al, 2014) using our *Daphnia* model system.

A.

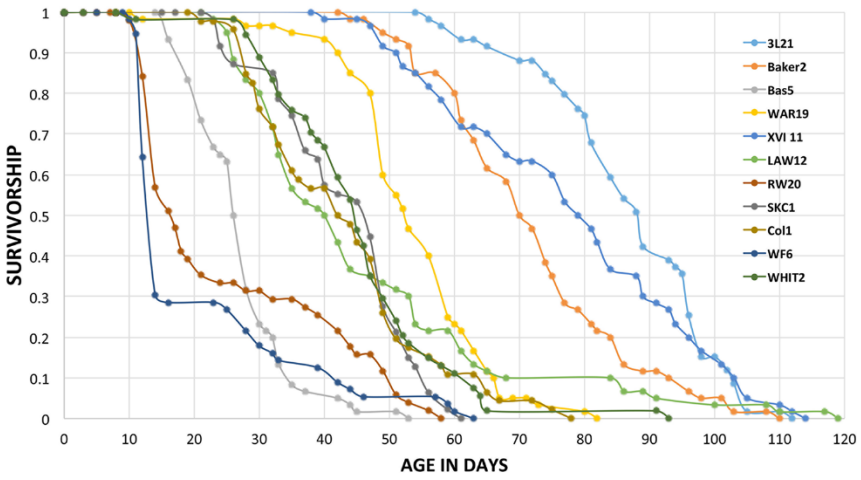

B.

ND5 sequence alignment

```
301                                                          360
|                                                            |
GPILSWPNFPAPVLIFLPVFLKWGALFFVGVSLLVMLSLQGLTYSYKWGAVSKFSGLMWF RW20      20 DAYS
GPILSWPNFPAPVLIFLPVFLKWGALFFVGVSLLVMLSLQGLTYSYKWGAVSKFSGLMWF WF6       20 DAYS
GPILSWLNFPAPVLIFLPVFLKWGALFFVGVSLLVMLSLQGLTYSYKWGAVSKFSGLMWF WHIT2     35 DAYS
GPILSWLNFPVPVLIFLPAFLKWGALFFVGVSLLVMLSLQGLTYSYKWGAVSKFSGLMWF BAS5      35 DAYS
GPILSWLNFPAPVLIFLPVFLKWGALFFVGVSLLVMLSLQGLTYSYKWGAVSKFSGLMWF SKC1      50 DAYS
GPILSWLNFPVPVLIFLPAFLKWGALFFVGVSLLVMLSLQGLTYSYKWGAVSKFSGLMWF LAW12     50 DAYS
GPILSWLNFPAPVLIFLPVFLKWGALFFVGVSLLVMLSLQGLTYSYKWGAVSKFSGLMWF COL1      60 DAYS
GPILSWLNFPVPVLIFLPAFLKWGALFFVGVSLLVMLSLQGLTYSYKWGAVSKFSGLMWF WAR19     65 DAYS
GPILSWLNFPAPVLIFLPVFLKWGALFFVGVSLLVMLSLQGVTYSYKWGAVSKLSGLMWF BAKER2    75 DAYS
GPILSWLNFPAPVLIFLPVLLKWGALFFVGVSLLVMLSLQGVTYSYKWGAVSKLSGLMWF XVI-11    75 DAYS
GPILSWLNFPAPVLIFLPVLLKWGALFFVGVSLLVMLSLQGVTYSYKWGAVSKLSGLMWF 3L2-1     85 DAYS
****** ************ ******************************** ******
                                                     ecotype   average
                                                               life span
```

Figure 2.1 Adult survivorship curves and ND5 sequence alignments. A. **Genetic differences of adult survivorship among populations of *D. pulex*.** Each line represents a specific clone. Pond clones: RW20, WF6, WHIT2, SKC1, and Col1. Lake clones: Bas5, LAW12, WAR19, Baker, XVI-11, and 3L21. B. **ND5 sequence alignments in the order of increasing life spans.** Only a short relevant region of the sequence alignments is shown. Red font with yellow highlighting: amino acids specific to the short-lived clones, red font with green highlighting: amino acids specific to the long-lived clones, blue font: positions where amino acid changes are present. Figure 2.1 A was contributed by Eun-Seok Kim and Jeffry Dudycha.

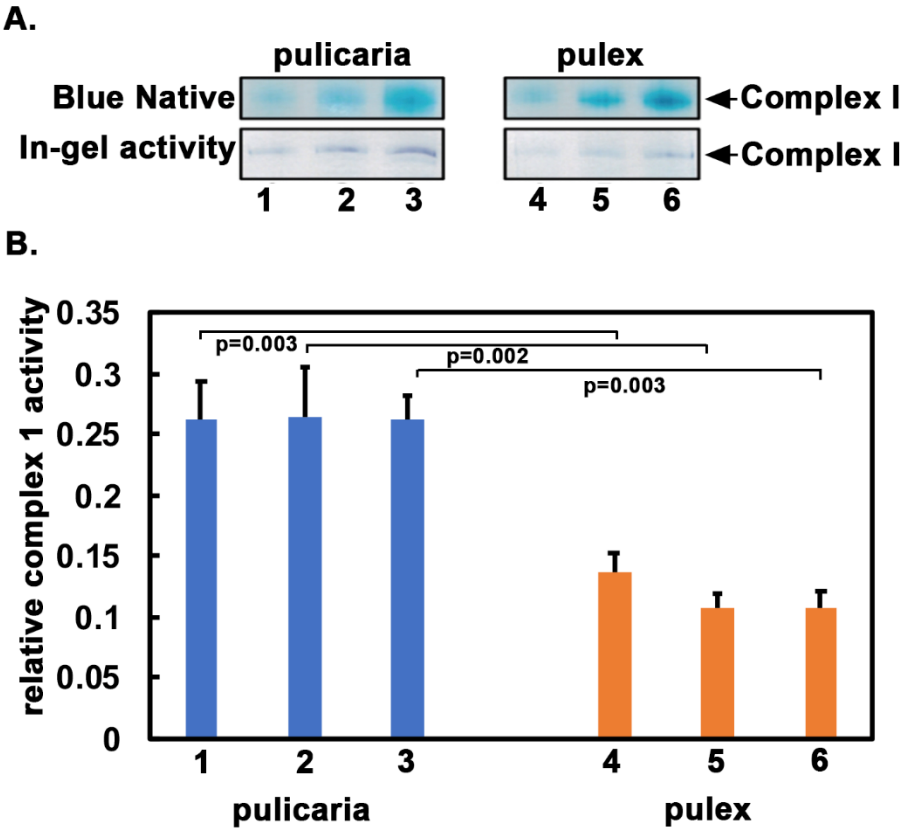

Figure 2.2 Complex 1 activity from clones *WF6* and *XVI-11.* A. Blue Native gels and in-gel activity assay for complex-I. Extracts made at various ages from short-lived WF6, and long-lived XVI-11 clones were run on Blue Native gel for total amount of complex 1 and a duplicate gel was stained for measuring complex 1 activity. Lanes 1- 3: 15μg, 30μg, and 45μg of total *extract* prepared from WF6 mitochondria and lane 4-6: 15μg, 30μg, and 45μg of total extract prepared from XVI-11 mitochondria. **B. Quantification of relative activity of complex I.** The band intensities of total complex-I and in-gel activity were measured and the complex I activity relative to total amount of complex I was calculated. The p-values are as indicated.

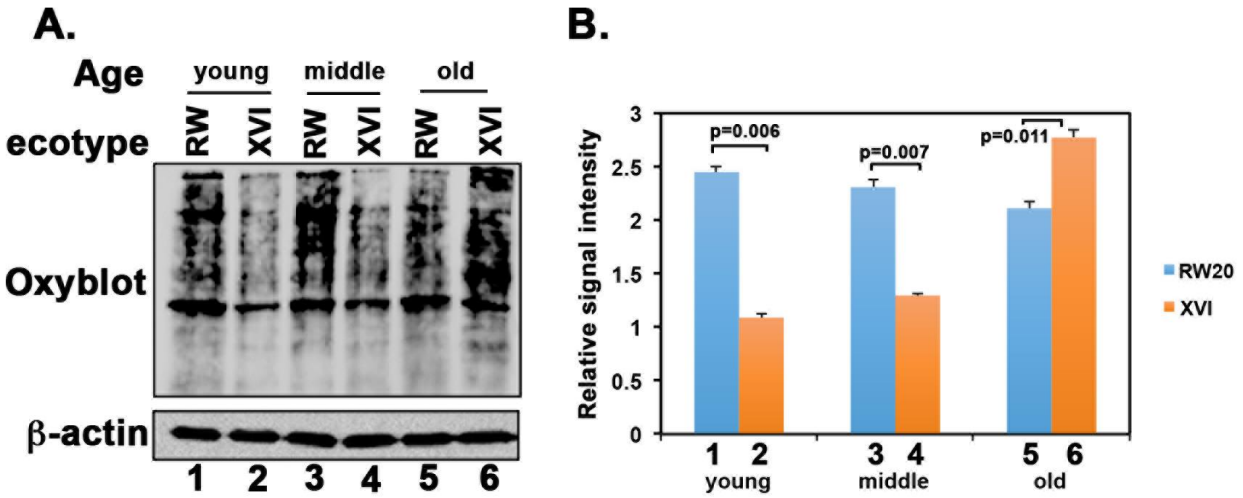

Figure 2.3 Oxidative damage to cellular proteins. A. Protein carbonyl levels were measured with the Oxyblot kit (Millipore). Using total cellular extracts, the carbonyl groups in the protein side chains were derivatized to 2,4-dinitrophenyl hydrazine (DNP). Western blot analysis was performed with an antibody against DNP. Equal loading was assessed using an anti-β actin antibody (Sigma). Y: young (1 week for both clones), M: middle aged (2 week for short-lived RW20 and 4 weeks for long-lived XVI-11) and O: old age (3 week for short-lived RW20 and 8 weeks for long-lived XVI-11). **B.** Bar graph represents the signals obtained from the analysis of the average of 3 blots from various samples after normalization to the β-actin bands. Blue corresponds to short-lived RW20 and orange corresponds to the long-lived XVI-11.

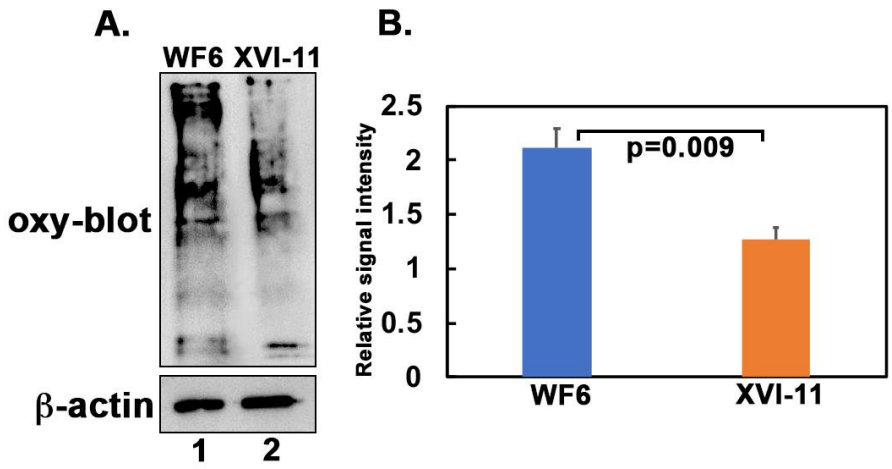

Figure 2.4 Oxidative damage to MT proteins. A. Protein carbonyl levels were measured with the Oxyblot kit (Millipore). Using mitochondrial protein extracts, the carbonyl groups in the protein side chains were derivatized to 2,4-dinitrophenyl hydrazine (DNP). Western blot analysis was performed with an antibody against DNP. Equal loading was assessed using an anti-β actin antibody (Sigma). Lane 1: MT extract from mixed age populations of WF6 with about equal individuals from ages 1 week-3 week of the short-lived WF6 and lane 2: MT extract from mixed age populations of XVI-11 with about equal individuals from ages 1 week-3 week of the long-lived XVI-11. **B.** Bar graph represents the signals obtained from the analysis of the average of 2 blots after normalization to the β-actin bands. Blue corresponds to short-lived WF6 and orange corresponds to the long-lived XVI-11.

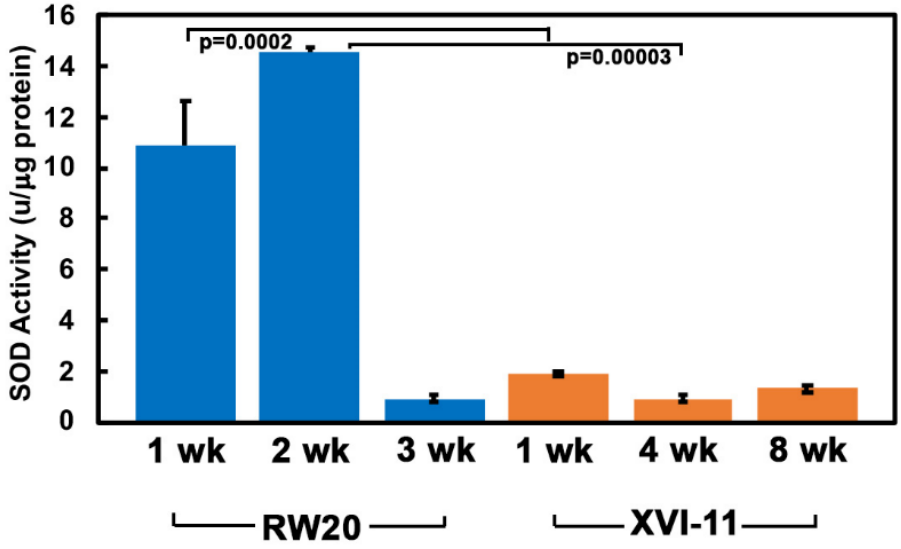

Figure 2.5 Comparison of SOD activity levels in short-lived RW20 and long-lived XVI-11. SOD activity was determined using a colorimetric assay kit (Sigma). The kit was first standardized for use with *Daphnia* samples. All reactions were performed in a 96 well plate and the activity was read on a BioTek Plate reader at a wavelength of 450 nm using the Gen5 software. Note that commercially available SOD was used in the assay to develop a standard curve for SOD activity. Blue bars: SOD activity at indicated ages for short-lived RW20 and orange bars: SOD activity at indicated ages for long-lived XVI-11. Error bars indicate the standard error of the mean. Student T-tests were performed, and the p values are as indicated. This figure was contributed by Dr. Charles A. Schumpert ,

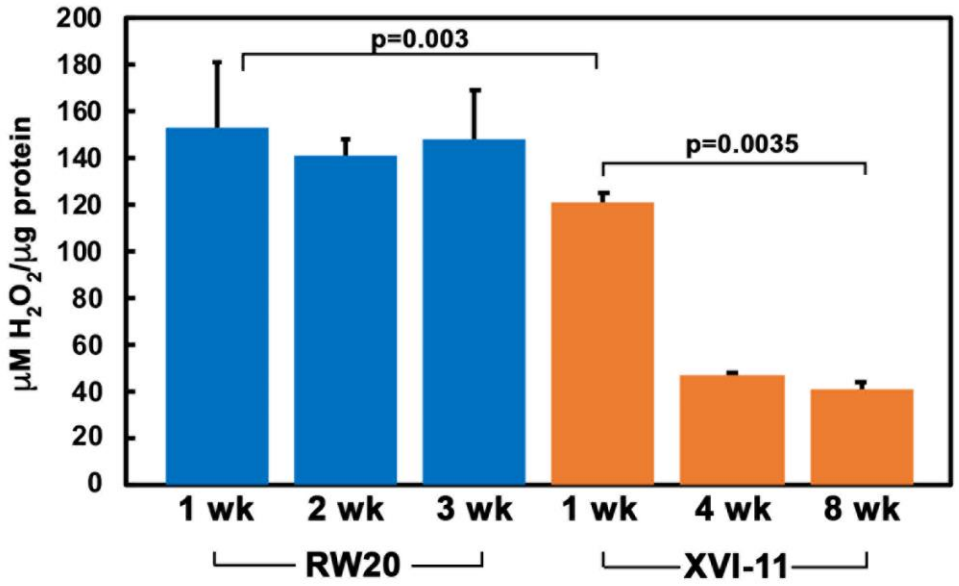

Figure 2.6 Comparison of hydrogen peroxide levels in short-lived RW20 and long-lived XVI-11. Hydrogen peroxide levels were determined at the indicated ages for short-lived RW20 and using a kit available through Pierce. Before the kit, which uses a colorimetric assay, was used with samples from aged *Daphnia*, the kit was standardized for use with *Daphnia* samples (Data not shown). All reactions were performed in a 96 well plate that was read on a BioTek Plate reader at a wavelength of 560 nm using the Gen5 software. Error bars indicate the standard error of the mean. Student T-tests were performed, and the p values are as indicated. This figure was contributed by Dr. Charles A. Schumpert.

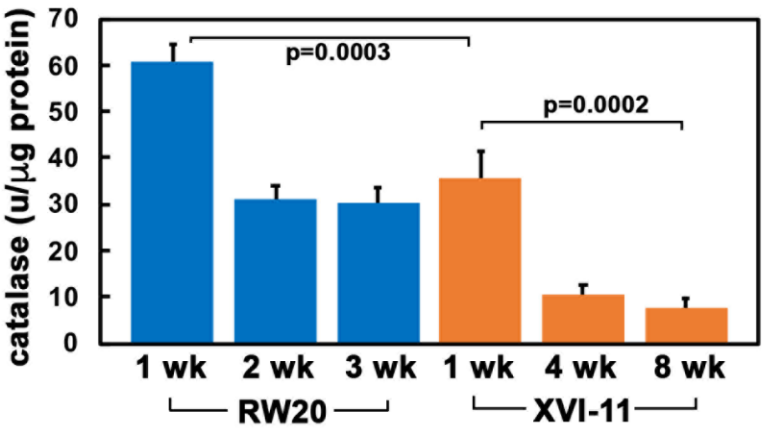

Figure 2.7 Comparison of catalase activity in RW20 and XVI-11. Catalase activity was determined using a previously published protocol based upon the extinction of hydrogen peroxide over a period. All reactions were performed in a 96 well plate that was read on a BioTek Plate reader at a wavelength of 240 nm using the Gen5 software. Plates were read every 47 seconds for a duration of 5 minutes and the extinction of hydrogen peroxide was calculated. The activity of catalase was then calculated based upon the slope of the line representing the disappearance of hydrogen peroxide. Error bars indicate the standard error of the mean and the p-values are as indicated. This figure was contributed by Dr. Charles A. Schumpert.

CHAPTER 3

REGULATION OF PKR ACTIVATION AND APOPTOSIS DURING OXIDATIVE STRESS BY TRBP PHOSPHORYLATION[3]

[3] Ukhueduan, B.O., Chukwurah, E. & Patel R.C. Submitted to *International Journal of Biochemistry and Cell Biology.*

3.1 ABSTRACT

Transactivation response element RNA-binding protein (TRBP or TARBP2) originally identified as a pro-viral cellular protein in human immunodeficiency virus (HIV) replication is also a regulator of microRNA biogenesis and cellular stress response. TRBP inhibits the catalytic activity of interferon-induced double-stranded RNA (dsRNA)-activated protein kinase (PKR) during viral infections and cell stress thereby regulating stress-induced signaling pathways. During cellular stress, PKR is catalytically activated transiently by its protein activator PACT and TRBP inhibits PKR to bring about a timely cellular recovery. We have previously established that TRBP phosphorylated after oxidative stress binds to and inhibits PKR more efficiently promoting cell survival. In this study, we investigated if phosphorylation of TRBP enhances its interaction with PACT to bring about additional PKR inhibition. Our data establishes that phosphorylation of TRBP has no effect on PACT-TRBP interaction and TRBP's inhibitory actions on PKR are mediated exclusively by its enhanced interaction with PKR. Cells lacking TRBP are more sensitive to apoptosis in response to oxidative stress and show persistent PKR activation. These results establish that PKR inhibition by stress induced TRBP phosphorylation occurs by its direct binding to PKR and is important for preventing apoptosis due to sustained PKR activation.

3.2 INTRODUCTION

The double-stranded RNA (dsRNA)-activated protein kinase (PKR) is ubiquitously expressed in mammals and regulates cellular survival and programmed cell death in response to stress signals (Garcia et al., 2006; Meurs et al., 1990; Williams, 1999). PKR is induced at the transcriptional level by interferons (IFNs), which are antiviral cytokines produced during viral infections and thus PKR plays a central role in the innate immune system to protect cells against viruses. Although IFNs induce expression of PKR, its kinase activity remains latent until binding to one of its activators leading to autophosphorylation and catalytic activation (Sadler & Williams, 2007). Active PKR phosphorylates serine 51 of the translation initiation factor, eIF2α, which results in an inhibition of protein synthesis (Katze, 1995; Samuel, 1993). In addition to virus replication stress, other stress signals also result in phosphorylation of eIF2α (Holcik & Sonenberg, 2005) and thus eIF2α phosphorylation serves an important function to block the general protein synthesis allowing cells to either recover from stress or undergo apoptosis when the damage is beyond repair (Pakos-Zebrucka et al., 2016). PKR plays an important role in regulating apoptosis after exposure to several diverse stress signals that include viral pathogens, oxidative stress, endoplasmic reticulum (ER) stress, and growth factor or serum deprivation (Gil et al., 1999; Marchal et al., 2014).

The two well-established activators of PKR, dsRNA, and protein PACT, activate its kinase activity by a direct interaction. During viral infections, the dsRNA produced as a replication intermediate (Garcia et al., 2007), binds to PKR

via two evolutionarily conserved dsRNA-binding motifs (dsRBMs) (Feng et al., 1992; Green & Mathews, 1992; Katze et al., 1991; Patel & Sen, 1992), changing PKR conformation to expose the ATP-binding site (Nanduri et al., 1998; Nanduri et al., 2000) and consequent autophosphorylation (Cole, 2007). These dsRBMs also mediate dsRNA-independent protein-protein interactions with other proteins that carry similar domains (Chang & Ramos, 2005; Patel et al., 1995). For PKR, among the proteins that interact via dsRBMs are **T**AR **R**NA-**b**inding **p**rotein (TRBP), an inhibitor of PKR activity (Benkirane et al., 1997), and PACT, a **P**KR **act**ivating protein (Patel et al., 2000; Patel & Sen, 1998). PKR activation in response to stress signals is tightly regulated by PACT and TRBP, both regulating kinase activity by a direct interaction with PKR as well as with each other (Daher et al., 2009; Singh et al., 2011). PKR, PACT, and TRBP interacting via their respective dsRBMs (Laraki et al., 2008), form both heterodimers as well as homodimers to regulate PKR activity tightly during stress response. The stress-induced phosphorylation of PACT reduces the PACT-PACT and PACT-PKR interactions to bring about a timely and transient PKR activation (Singh et al., 2011; Singh & Patel, 2012). This regulates the general kinetics as well as level of eIF2α phosphorylation thereby influencing the cellular response to stress either as recovery and survival or elimination by apoptosis (Vaughn et al., 2015). Any perturbation either in the kinetics or relative duration of PKR activity brings disastrous consequences for cellular recovery culminating in apoptosis.

Both PACT and TRBP have three dsRBMs, of which the first two dsRBMs interact with dsRNA, while the third carboxy-terminal dsRBM does not it lacks the

conserved lysine residues required for dsRNA-binding. All three dsRBMs mediate interactions with other proteins which include PKR, PACT, Dicer, and Merlin for TRBP (Daniels & Gatignol, 2012; Daniels et al., 2009; Laraki et al., 2008). In the absence of viral infections and stress signals, TRBP inhibits PKR both by interacting with dsRNA (Benkirane et al., 1997; Park et al., 1994) and PACT thus sequestering them away from PKR as well as by forming PACT-TRBP and PKR-TRBP heterodimers (Daher et al., 2009; Daher et al., 2001). Importantly, the stress-induced serine 287 phosphorylation of PACT regulates PKR activity by decreasing its interaction with TRBP causing rapid PKR activation following exposure to stress signals (Daher et al., 2009; Singh et al., 2011).

TRBP phosphorylation also regulates PKR activity in response to oxidative stress to bring about a timely downregulation of PKR activity to promote cellular recovery and survival. Using various biochemical assays, we recently determined that TRBP also gets phosphorylated in response to oxidative stress. Our results established that ERK1/2 and JNK phosphorylate TRBP at late time points after oxidative stress and this significantly enhances TRBP's ability to interact with and inhibit PKR to promote cell survival. However, it remained unknown if TRBP phosphorylation affects its association with PACT after oxidative stress. In this study, we examined this using phospho-mimic and phospho-defective mutants of TRBP and PACT. Our results indicate that unlike TRBP-PKR interactions, TRBP phosphorylation does not have any effect on TRBP-PACT interactions. Thus, the downregulation of PKR activity after oxidative stress is mainly achieved by a

direct, and enhanced interaction of phosphorylated TRBP with PKR. Furthermore, the TRBP null cells are more sensitive to oxidative stress-induced apoptosis and the PKR activation and consequent eIF2α phosphorylation persists for longer duration in the absence of TRBP indicating the importance of a timely, TRBP dependent downregulation of PKR activity after oxidative stress.

3.3 MATERIALS AND METHODS

Reagents, Cell Lines and Antibodies: TRBP+/+, TRBP-/-. PACT+/+, PACT-/- MEFs and HeLa cells were cultured in Dulbecco's Modified Eagle's Medium (DMEM) containing 10% fetal bovine serum and penicillin/streptomycin. Transfections were performed with Effectene Transfection Reagent (Qiagen) according to the manufacturer's protocol. Sodium arsenite, phosphatase inhibitor cocktail (Phosphatase Inhibitor Cocktail 2 – P5726), were purchased from Sigma Aldrich. Antibodies used are as follows: PKR: anti-PKR (human) monoclonal (71/10, R&D Systems), p-PKR: antiphospho- PKR (Thr-446) monoclonal (Abcam, [E120]), eIF2α: anti-eIF2α polyclonal (Invitrogen, AHO1182), p-eIF2α: anti-phospho-eIF2α (Ser-51) polyclonal (CST, #9721), PACT: Anti-PACT monoclonal (Abcam, ab75749), Cleaved PARP: anti-Cleaved-PARP monoclonal (CST, #32563), β-Actin: Anti- β-Actin-Peroxidase monoclonal (Sigma-Aldrich, A3854). The construction of all plasmid constructs has been described before in detail (Chukwurah & Patel, 2018).

DNA Fragmentation analysis: 5 X 10^6 TRBP+/+ and TRBP-/- MEFs described in "Reagents, Cell Lines and Antibodies" were treated with 5, 10 or 20 μM sodium arsenite for 48 h. Cells were collected and washed with ice cold 1X PBS and

lysed in 100 µl of lysis buffer (10mM Tris-HCl pH 7.5, 10mM EDTA, and 0.5% Triton-X 100) for 5 minutes on ice. Lysates were centrifuged at 13200 rpm for 5 minutes and were incubated with 100 µg Proteinase K at 37^{o}C for 2 hours. 5 µl of 6M NaCl and 110 µl of isopropanol were subsequently added to the lysates which were then incubated at -20^{o}C overnight. The precipitated DNA was then collected by centrifugation at 14,000 rpm for 5 minutes. After the isopropanol was removed from each sample, the DNA was dissolved in 20 µl TE Buffer (10 mM Tris-HCl pH 7.5, 10 mM EDTA). The DNA was incubated with 20 µg/mL RNase A at 37^{o}C for 1 hour before analysis on a 1.5% agarose gel.

Western blot analysis: TRBP+/+ or TRBP-/- MEFs were treated with 25µM sodium arsenite and harvested at indicated time points. Cells were washed twice with ice cold 1× PBS. Harvested cells were lysed in western lysis buffer (2% Triton X-100, 20 mM Tris–HCl pH 7.5, 100 mM KCl, 200 mM NaCl, 4 mM $MgCl_2$, 40% Glycerol, and phosphatase inhibitor cocktail 2 (Sigma) at 1:100 dilution) for 5 minutes on ice. Lysates were centrifuged at 13,200 rpm for 2 minutes. Protein concentration in the supernatant was quantified using Bradford reagent. Western blot was performed with the indicated antibodies (cleaved PARP1, p-eIF2α, p-PKR, eIF2α, PKR) and western blot images were analyzed using the ImageQuant LAS 4000 (Amersham).

Caspase3/7 activity assay: Both TRBP +/+ and TRBP -/- MEFs were seeded at a concentration of 300,000 cells/mL of DMEM and treated with a concentration of 25 µM of sodium arsenite over a 24-h time course. Samples were collected at indicated time points and mixed with equal parts Promega Caspase-Glo 3/7

reagent (Promega G8090) and incubated for 45 min. Luciferase activity was measured and compared to cell culture medium alone and untreated cells as the negative controls.

Yeast Two-Hybrid Interaction Assay: To test TRBP-PACT interaction, wt PACT or DA mutant was expressed as a GAL4 DNA-activation domain fusion protein from the pGADT7 vector and the AAAA and DDDD TRBP point mutants were expressed as GAL4 DNA-binding domain fusion proteins from the pGBKT7 vector. The AAAA TRBP and DDDD TRBP pGBKT7 and pGADT7 empty vector, wt PACT/pGADT7 or DA PACT/pGADT7 construct pairs were co-transformed into AH109 yeast cells (Clontech) and the transformed yeast cells were plated on double dropout SD minimal medium lacking tryptophan and leucine. To check for the transformants' ability to grow on quadruple dropout media, transformed yeast cells were grown to an OD_{600} of 2 in YPD media (yeast extract, peptone, and dextrose). 500 µl of each culture was pelleted and resuspended in an appropriate amount of distilled water to yield an OD_{600} of 10. Serial dilutions were then made to yield OD_{600} values of 1, 0.1, and 0.01. 10 µl of each dilution was then spotted onto quadruple dropout SD minimal media lacking adenine, histidine, tryptophan, and leucine in the presence of 100 mM 3-amino-1,2,4-triazole (3-AT). Plates were incubated at 30^{o}C for 3 days.

Mammalian two-hybrid interaction assay: In all cases, wt PACT, DA PACT ORFs were sub-cloned into pSG424 expression vector such that it created an in-frame fusion to a GAL4 DNA binding domain (GAL4-DBD), and DDDD or AAAAA TRBP ORFs were sub-cloned into pVP16AASV19N expression vector such that

it maintains an in-frame fusion to the activation domain of the herpes simplex virus protein VP16 (VP16-AD). COS-1 cells were then transfected with: (i) 250 ng each of the GAL4-DBD and the VP16-AD constructs, (ii) 50 ng of pG5Luc a firefly luciferase reporter construct, and (iii) 1 ng of pRLNull plasmid (Promega), to normalize for transfection efficiencies. Cells were harvested 24-h post transfection and assayed for both firefly and renilla luciferase activities using Dual Luciferase® Reporter Assay System (Promega).

In vivo ^{32}P orthophosphate labeling to analyze phosphorylation kinetics of PACT and PKR: For analyzing phosphorylation of PACT and PKR, HeLa cells grown in 6 well dishes were kept in phosphate-free DMEM containing 10% serum for 1 h before the sodium arsenite treatment. The sodium arsenite treatment was done in 1 mL phosphate-free medium in the presence of 0.5 μCi/mL of ^{32}P-orthophosphoric acid (Perkin Elmer). At indicated time points after the arsenite treatment, cell extracts were prepared in 100 μl buffer (20 mM Tris-HCl pH 7.5, 100 mM KCl, 100 units/mL aprotinin, 0.2 mM phenylmethylsulfonyl fluoride, 20% glycerol, 0.1% Triton X-100, and phosphatase inhibitor cocktail, Sigma). PACT and PKR were immunoprecipitated from 200 μg total protein extract using the anti-PACT and anti-PKR antibody resp. and protein A Sepharose (Sigma) in 500 □L of the lysis buffer at 4°C for 2h. The beads were washed in 500 μl of low salt buffer four times and PACT and PKR bound to the beads was analyzed by SDS-PAGE followed by phosphorimager analysis. Another sample, similarly, immunoprecipitated was used for western blot analysis with anti-PACT and anti-PKR monoclonal antibodies.

Apoptosis assay using DNA condensation as marker: PACT +/+ and PACT -/- MEFs were grown to 60% confluency in six-well plates and co-transfected with 250 ng of empty vector pcDNA3.1-, flag-TRBP AAAA/ pcDNA3.1-, or flag-TRBP DDDD/pcDNA 3.1⁻ and 250 ng of pEGFPC1 (Clontech) using Effectene (Qiagen). The cells were observed for GFP fluorescence 24 hours after transfection using an inverted fluorescence microscope (EVOS® FL Imaging System). Cells were treated with 25 μM sodium arsenite, and cellular morphology was monitored at every 2 h. 12 hours after treatment, the cells were rinsed with ice-cold phosphate buffered saline (PBS) and fixed in 2% paraformaldehyde for 10 minutes. Cells were washed twice in ice-cold PBS and permeabilized with 0.1% Triton-X for 10 minutes, after which the cells were washed twice in ice-cold PBS. Cells were stained with the DAPI nuclear stain (4,6-diamidino-2-phenylindole) at 0.5 μg/mL in PBS for 10 minutes at room temperature in the dark. The cells were rinsed once with PBS and viewed under the fluorescent microscope. At least 300 GFP-positive cells were counted as apoptotic or live based on their morphology. Cells showing normal flat morphology were scored as live, while cells showing cell shrinkage, membrane blebbing, rounded morphology and nuclear condensation with intense fluorescence as apoptotic. The percentage of cells undergoing apoptosis (*Percent apoptosis*) was calculated using the formula: (EGFP- expressing cells with intense DAPI nuclear staining/Total EGFP-expressing cells) × 100

3.4 RESULTS

TRBP inhibits oxidative stress-induced apoptosis

To evaluate TRBP's effect on the cellular response to oxidative stress, we evaluated the response of TRBP-/- mouse embryonic fibroblasts (MEFs) with that of TRBP+/+ MEFs. To compare the relative apoptosis in TRBP+/+ and TRBP-/- cells, we used DNA fragmentation analysis in response to sodium arsenite treatment. DNA fragmentation is a late marker of apoptotic cells as the DNA is cleaved by caspase-activated DNases (CADs) into nucleosomal fragments of 180 bp (Nagata et al., 2003). In Figure 3.1 A, the TRBP-/- MEFs showed high levels of DNA fragmentation in response to sodium arsenite (lanes 8-10). In comparison, the TRBP+/+ cells have no detectable DNA fragmentation after exposure to sodium arsenite (lanes 3-5). These results indicate that TRBP+/+ cells are significantly protected from oxidative stress-induced apoptosis.

To further assess the protection from cellular apoptosis by TRBP, we compared the cleavage of Poly-ADP Ribose Polymerase (PARP1) in response to arsenite in TRBP-/- and TRBP+/+ MEFs. The 116 kDa protein PARP1 is cleaved into an 89 kDa fragment by Caspase-3 in response to apoptosis-inducing stimuli (Tewari et al., 1995). We assessed PARP1 cleavage in both sets of cells after treatment with arsenite in a time dependent manner (Figure 3.1 B). There is a significant level of cleaved PARP1 in the TRBP-/- cells at 6-24h (lanes 7-10). In contrast to this, the TRBP+/+ cells cleaved PARP1 is barely detectable (lanes 2-5). These results demonstrate that TRBP protects the cells from apoptosis in

response to oxidative stress and caspase-3 activation and subsequent PARP1 cleavage is significantly elevated in cells lacking TRBP.

To further validate these results, we performed caspase 3/7 activity assays under the same treatment conditions to measure apoptosis. In TRBP-/- MEFs we detect caspase activity at 12 h which steadily increases till 24 h post-treatment (Figure 3.1 C, red bars). In contrast, the TRBP+/+ MEFs demonstrate no increase in caspase activity at any of the time points post-treatment (Figure 3.1 C, blue bars). This further supports that the TRBP-/- fibroblasts are significantly more susceptible to oxidative stress and exhibit increased apoptosis as compared to TRBP+/+ cells possibly due to a failure to restore homeostasis.

PKR as well as eIF2α phosphorylation stays on for a prolonged duration in TRBP -/- cells

To elucidate the underlying mechanism driving heightened sensitivity to oxidative stress in TRBP-/- MEFs, we performed western blot analysis on cells treated with arsenite and probed for markers of cellular stress response. We compared the kinetics of both eIF2α phosphorylation and PKR activation in the TRBP+/+ and TRBP-/- MEFs. In TRBP+/+ MEFs we observe a low basal level of eIF2α phosphorylation in the untreated cells (Figure 3.2, lane 1) followed by increased eIF2α phosphorylation at 0.5–4 h post treatment (lanes 2–5) and then restoration to basal levels by 8 h (lane 5). In contrast to this, in the TRBP-/- MEFs, we observe a similar increase in eIF2α phosphorylation 0.5 h-4h after treatment (lanes 9-12), however, the eIF2α phosphorylation is sustained even at 8 and 12 h post treatment (lanes 13-14). We also studied the time course of PKR

activation in TRBP +/+ and TRBP-/- MEFs under the same conditions. In wt MEFs we observe PKR activation at 0.5 h after arsenite treatment that is sustained until 4 h (lanes 2-5) and shows a decrease by 8 h (lane 6). In contrast , the TRBP-/- MEFs exhibit a dramatically prolonged presence of activated PKR (lanes 9-14) after treatment with arsenite. Although PKR phosphorylation is detected similar to TRBP+/+ MEFs at 0.5 h after arsenite treatment (lane 9), it is sustained at 8 and 12 h after treatment unlike the TRBP+/+ MEFs. These results indicate that in the absence of TRBP, PKR and eIF2α stays phosphorylated for a prolonged time, thus suggesting that TRBP is required for a timely downregulation of PKR activation following oxidative stress.

Phosphorylation status of TRBP does not change its ability to interact with PACT

Our previous research has established that TRBP is phosphorylated by MAPK/ERK 1/2 at four serines (S142,S152, S283, and S286) starting at 8 h after oxidative stress. Of these sites, S142 and S152 have also been previously shown to be phosphorylated by JNK (Kim, Yeo, et al., 2014). Our research has shown that a phospho-mimic TRBP point mutant (TRBP DDDD) generated by substituting aspartic acid for serine at these four sites interacts with PKR much stronger than the phospho-defective TRBP mutant (TRBP AAAA) generated by substituting alanine for serine. These findings and our other apoptosis studies established that TRBP is involved in the downregulation of PKR's kinase activity after oxidative stress. Furthermore, the results in Fig. 3.2 support our earlier findings and indicate that TRBP plays a central and important role in regulating

cell survival in response to oxidative stress. It is possible that TRBP's phosphorylation changes its affinity for PACT in addition to a change in its affinity for PKR. Previous research has established that PACT is constitutively phosphorylated at serine 246 and becomes additionally phosphorylated at serine 287 in response to stress. Figure 3.3 A shows a schematic representation of phosphorylation sites in TRBP and PACT that are important for stress-dependent regulation of PKR activity.

To test if phosphorylated TRBP interacts with PACT more strongly to further aid in PKR inhibition at late time points after oxidative stress, we first wanted to determine the PACT phosphorylation kinetics after arsenite treatment. We examined this by in vivo ^{32}P-orthophosphate labeling of proteins phosphorylated in response to arsenite treatment in HeLa cells. As seen in Fig. 3.3 B, both PKR and PACT are rapidly phosphorylated after treatment with arsenite at 15 min (lane 2) and their phosphorylation stays high until 30 min (lanes 2-3) and then gradually decreases (lanes 4-6) to undetectable levels at 8 h (lane 7). Importantly, the PACT phosphorylation kinetics matches the PKR phosphorylation status as we had reported earlier in response to arsenite. In this earlier study, we did not examine the later time points when PKR's kinase activity is downregulated. The results shown in Figure 3 A demonstrate that at 8 h after oxidative stress, the stress-induced phosphorylation of PACT on serine 287 is downregulated. Based on these results, we determined that it would be meaningful to examine if the phospho-mimic (TRBP-DDDD) and phospho-defective (TRBP-AAAA) mutants of TRBP interact with different affinities with

PACT and its mutant DA PACT that has a substitution of aspartic acid for serine 246 and a substitution of alanine for serine 287. The DA PACT mutant thus mimics the phosphorylation state of PACT at 8 h after arsenite treatment. Additionally, both DDDD and AAAA TRBP mutants interact similarly with wt PACT as well as with DA PACT in the yeast two-hybrid interaction assay, thus indicating that the phosphorylation status of TRBP does not affect the strength of its interaction with PACT (Figure 3.3 C). In Figures 3 C and D, the interaction of DDDD and AAAA TRBP with wild type (wt) PACT serves as a positive control as we have demonstrated this interaction before. It is important to note that the DDDD TRBP mutant which mimics the natural form of TRBP at 8 h after arsenite treatment, interacts with PACT with significant affinity and will thus aid in PKR downregulation except that TRBP-PACT interaction is not modulated by TRBP's phosphorylation status. We further tested this using the mammalian two-hybrid system to examine if there are any differences in strengths of interaction between DA PACT and DDDD or AAAA TRBP mutants. As seen in Figure 3.3 D, no differences were observed in the luciferase reporter activity for AAAA and DDDD TRBP indicating that similar to yeast two-hybrid data in Figure 3.3 C, the phosphorylation status of TRBP does not change the affinity of its interaction with PACT in mammalian cells.

These results indicate that phosphorylation of TRBP at late time points after exposure to oxidative stress primarily works via a direct interaction with PKR and although the interaction of phosphorylated TRBP with PACT may aid in

this process, it is not a primary driver of PKR downregulation observed at later time points.

Both the phospho-mimic and phospho-defective TRBP mutants can protect mammalian cells equally well in absence of PACT

Given that TRBP phosphorylation status does not change its interaction with PACT, it is proposed that both phosphor-defective (AAAA) and phosphor-mimetic(DDDD) TRBP mutants will be able to protect mammalian cells from apoptosis in response to oxidative stress equally well even in the absence of PACT. To test this, we first compared the response of PACT+/+ and PACT -/- MEFs to oxidative stress by assaying for the caspase3/7 activity in PACT+/+ and PACT-/- MEFs after arsenite treatment. As seen in Figure 3.4 A, arsenite treatment induced an increase in caspase 3/7 activity in a time-dependent manner in both PACT+/+ (blue bars) and PACT-/- (red bars) MEFs. In agreement with our previously published data, PACT-/- cells showed reduced caspase 3/7 activation. These results confirm our previous results that PACT activates PKR in response to oxidative stress and the absence of PACT delays pro-apoptotic signaling in PACT -/- cells.

To test the ability of AAAA and DDDD TRBP mutants to protect cells in the absence of PACT, we transfected PACT-/- MEFs to transiently overexpress TRBP mutants and measured the apoptosis of transfected cells after arsenite treatment. Flag-tagged expression constructs of AAAA or DDDD TRBP in pcDNA3.1- or empty vector pcDNA 3.1- were co-transfected with pEGFPC1 to identify cells that were transfected. 24h after transfection, the cells were treated

with 25 μM sodium arsenite and 12 h after treatment, the cells were fixed and stained with DAPI nuclear stain. We used nuclear condensation as the hallmark sign of apoptosis as indicated by the intense DAPI nuclear fluorescence (Smyth & Berman, 2002). There is a significant amount of apoptosis at 30.43% in PACT+/+ and 19.7% in PACT-/- MEFs (Figure 3.4 B, blue bars) after arsenite treatment in the empty vector (pcDNA3.1-) transfected cells. Cell death is significantly reduced with the co-transfection of both AAAA phospho-defective (16.4% in PACT+/+ and 10.82% in PACT-/-, red bars) and DDDD phospho-mimic TRBP (15.32 % in PACT+/+ and 11.89% in PACT-/-, green bars) Figure 3.4 C. These results indicate that both AAAA and DDDD TRBP offer protection to mammalian cells even in the absence of PACT. These results further substantiate that TRBP's actions to attenuate PKR activation at late time points after oxidative stress mainly take place via its direct interaction with PKR. The apoptosis data thus agrees well with the interaction data in Figure 3.3, further confirming that although the phosphorylated TRBP remains capable of interacting with PACT, its major inhibitory effect on PKR activity is via enhancement of its direct interaction with PKR.

TRBP's interaction with PKR in strengthened by TRBP phosphorylation as established by our previous research, and the MAPK/ERK 2 mediated TRBP phosphorylation ensures a timely downregulation of PKR activity. Figure 3.4 C shows the fluorescence microscopy images in PACT-/- cells that demonstrate intense DAPI fluorescence in arsenite treated empty vector transfected cells (panel b, white arrow). Overexpression of AAAA TRBP (panel d) as well as

DDDD TRBP (panel f) shows cells with a lack of nuclear condensation (white arrows) in response to arsenite. Although the experiment was done in both PACT+/+ and PACT-/- MEFs, the microscopy images are shown only for PACT-/- cells in Figure 3.4 C but the data in Figure 3.4 B includes the quantification of apoptosis in both PACT +/+ and PACT-/- cells.

3.5 DISCUSSION

PKR plays an important role in regulating cellular survival in response to stress signals and its kinase activity is regulated by PACT and TRBP, PACT acting positively to activate PKR and TRBP acting negatively to ensure appropriate strength and duration of PKR activation (Daher et al., 2009; Patel et al., 2000; Singh et al., 2011). Immediately after oxidative stress, at early time points PACT activates PKR by a direct interaction to trigger inhibition of protein synthesis via eIF2α phosphorylation (Patel et al., 2000; Singh et al., 2011; Singh et al., 2009). Stress-induced PACT phosphorylation immediately after oxidative stress reduces the PACT-TRBP interactions while increasing PACT-PACT and PACT-PKR interactions, thereby leading to PKR dimerization and activation (Singh et al., 2011; Singh et al., 2009). Our previous results also demonstrated that TRBP is phosphorylated by ERK 1/2 and JNK in response to oxidative stress at later time points and the phosphorylated TRBP inhibits PKR's kinase activity more efficiently than its unphosphorylated form to protect cells from apoptosis. Phosphorylated TRBP interacts with PKR more strongly than the unphosphorylated TRBP and forms TRBP-TRBP homomeric interactions less efficiently than the unphosphorylated form. Our data established that in addition

to GADD34 induction after oxidative stress (Kazemi et al., 2004; Rojas et al., 2015), TRBP plays a central role in the downregulation of PKR activity. Thus, PKR activity during cell stress is dictated not only by stress-induced changes in interactions between PACT and PKR, but also by interactions between PKR and TRBP. TRBP interacts with both PACT and PKR and although we established that TRBP phosphorylation enhances its affinity for PKR while reducing the TRBP-TRBP interactions, its effect of PACT-TRBP interaction was not investigated previously. In this study, we examined if TRBP phosphorylation controls PKR activity also by interacting more strongly with PACT. Based on our results presented here, we conclude that phosphorylated TRBP regulates PKR activity negatively at late time points after oxidative stress via a direct increase in its interaction with PKR and not by an increased interaction with PACT. The downregulation of PKR activity at late time points after oxidative stress is important for cell survival as demonstrated by our results that cells lacking TRBP are very sensitive to apoptosis in response to oxidative stress. This increased sensitivity to apoptosis results from PKR staying active at late time points after oxidative stress and consequently eIF2α remaining phosphorylated and inactive for a longer duration causing a dysregulated cellular homeostasis.

Most strikingly, despite a high degree of homology between TRBP and PACT, the stress-induced phosphorylation affects their protein-protein interactions quite differently. The dsRBM motifs in PKR, TRBP, and PACT carry the characteristic alpha-beta-beta-beta-alpha fold with two well-established functions; to bind structured RNA molecules and to mediate protein-protein

interactions with other proteins that possess the same motif (Chang & Ramos, 2005; Fierro-Monti & Mathews, 2000). The dsRBM is conserved evolutionarily and most eukaryotic, prokaryotic, and viral proteins with dsRBMs contain a variable number of copies of these motifs. Proteins that contain dsRBMs regulate many diverse cellular processes such as RNA editing, nucleocytoplasmic transport, RNA localization, RNA interference, innate immunity, and translational regulation (Saunders & Barber, 2003). In addition to dsRNA, dsRBMs also recognize non-RNA targets (proteins and DNA), and act in combination with other dsRBMs and non-dsRBM motifs to play a regulatory role in catalytic processes (Barber, 2009). Our work presented here demonstrates one more level of regulation to the versatility of the dsRBM as it demonstrates that phosphorylation sites that reside outside the dsRBM can influence the strength of protein-protein interactions mediated via the dsRBMs. This points to a fruitful area for future studies examining the phosphorylation sites outside the conserved motifs that could mediate significant changes in protein interactions possibly by changing overall conformations of the interacting partners or the positioning of individual dsRBMs. The role of phosphorylation and other post-translational modifications in regulating interactions with RNA or proteins for the other members of this diverse family of proteins also remains to be investigated in future.

Based on our data, we can add more information to our previous schematic model for TRBP-mediated downregulation of PKR activity at late time points after oxidative stress. As depicted in Figure 5, under conditions of no

oxidative stress, unphosphorylated TRBP interacts both with PKR and PACT, thus preventing PKR activation and eIF2α phosphorylation. In response to oxidative stress, TRBP dissociates from phosphorylated PACT, PKR gets activated by phosphorylated PACT homodimers and eIF2α is phosphorylated to bring about a transient protein synthesis inhibition. At this early time point, TRBP remains unphosphorylated but at late time points, ERK1/2 and JNK phosphorylate TRBP, leading to significantly increased and stronger TRBP-PKR interactions that bring about efficient PKR inactivation, and eIF2α is dephosphorylated. Phosphorylated TRBP retains its ability to interact with PACT but unlike for PKR interaction, TRBP phosphorylation does not change its affinity for PACT. Thus, the stress-induced phosphorylation of PACT and TRBP affects their protein interactions quite differently. PACT phosphorylation enhances PACT-PACT and PACT-PKR interactions while decreasing PACT-TRBP interactions whereas TRBP phosphorylation enhances TRBP-PKR interactions and decreases TRBP-TRBP interactions while leaving the affinity of PACT-TRBP interactions unchanged.

First identified as a protein that facilitates HIV replication, TRBP also regulates many cellular pathways such as innate immune responses, miRNA biogenesis, RNA interference and cellular response to stress. By contributing to multiple pathways in the cell, TRBP mutations or its dysregulated expression affects oncogenesis and cancer progression. Both depletion and overexpression of TRBP results in malignancy suggesting that a fine balance of TRBP function is required for maintaining normal cellular function. In this regard, this work and

previous research on post-translational modifications of TRBP are indicative of its several important implications. Kim et al. have reported previously that phospho-TRBP efficiently inhibits PKR during M-G1 transition to regulate cell cycle (Kim, Lee, et al., 2014). According to this study, TRBP is phosphorylated by JNK at S142 and S152 by JNK during M phase thus enhancing its inhibitory actions on PKR. Paroo et al have reported that ERK mediated phosphorylation of TRBP on S142, S152, S283, and S286 in response to mitogenic signaling is accompanied by a coordinated increase in the levels of growth-promoting miRNAs and a reduction in the levels of tumor suppressor let-7 miRNA (Paroo et al., 2009). TRBP phosphorylation has also been reported in response to metabolic stress and inhibition of TRBP phosphorylation during metabolic stress reduces inflammation and improves systemic insulin resistance and glucose metabolism (Nakamura et al., 2014; Nakamura et al., 2015). However, the precise function of TRBP and PKR in high-fat diet-induced obesity and associated metabolic and inflammatory complications remains unclear and controversial (Lancaster et al., 2016). Most importantly, TRBP plays an important pro-viral function in HIV infected cells by regulating PKR activity and promoting HIV replication (Burugu et al., 2014; Clerzius et al., 2011). The effect of TRBP phosphorylation that has remained unexplored in HIV-infected cells may reveal novel ways to suppress HIV replication or latency in future. Oxidative stress is known to affect the miRNA expression profiles and regulate cellular apoptosis in various disease conditions including cancer and the effect of TRBP phosphorylation on stress-induced changes in miRNA expression also remain to be explored.

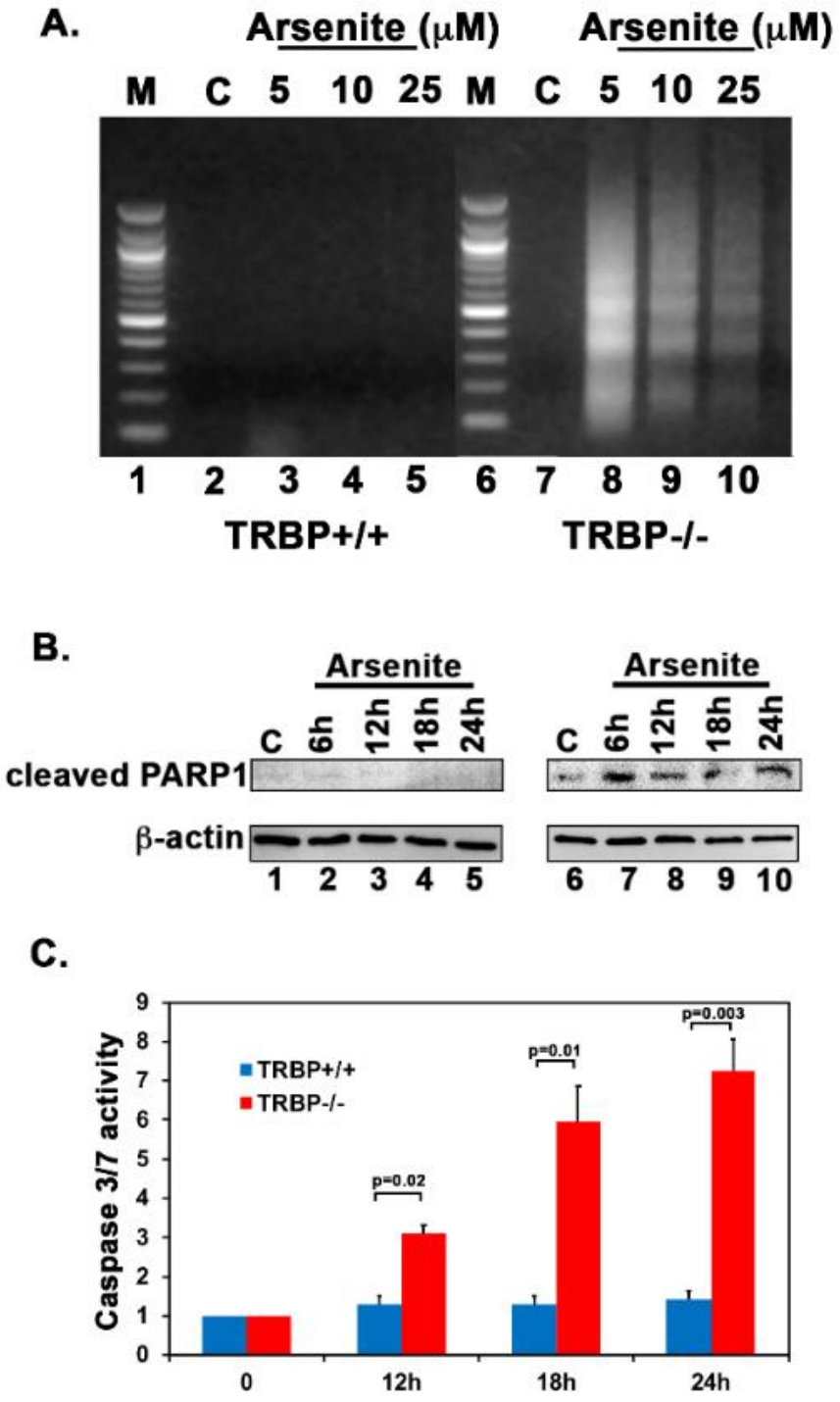

Figure 3.1 TRBP protects cells from arsenite-induced apoptosis. (A) DNA Fragmentation Analysis. TRBP+/+ (Lanes 2-5) or TRBP-/- MEFs (Lanes 7 -10) were treated with either 5 μM, 10 μM, or 25 μM sodium arsenite for 48 hours, fragmented DNA was isolated and analyzed. Lane 1 and 6: size markers, 100-bp ladder, Lanes 2 & 7: untreated controls, lanes 3 & 8: 5 μM arsenite, lanes 4 & 9: 10 μM arsenite, lanes 5 and 10: 25 μM arsenite. **(B) Analysis of PARP1 cleavage in response to arsenite**

treatment. TRBP+/+ and TRBP-/- MEFs were treated with 25 μM sodium arsenite for the indicated time points, and western blot analysis using anti-poly ADP-ribose polymerase (PARP1) antibody specific for the cleaved PARP1 was performed on cell lysates containing 30 μg of total protein to assess increases in PARP1 cleavage. Western blot was also performed with anti-β actin antibody to ensure equal protein in all lanes. (C) **Caspase-Glo 3/7 activity.** TRBP+/+ and TRBP-/- MEFs were treated with 25 μM sodium arsenite and the caspase 3/7 activities were measured at indicated time points. Blue bars: TRBP+/+ MEFs, and red bars: TRBP-/- MEFs. The data is an average of three independent experiments and the p values are as indicated.

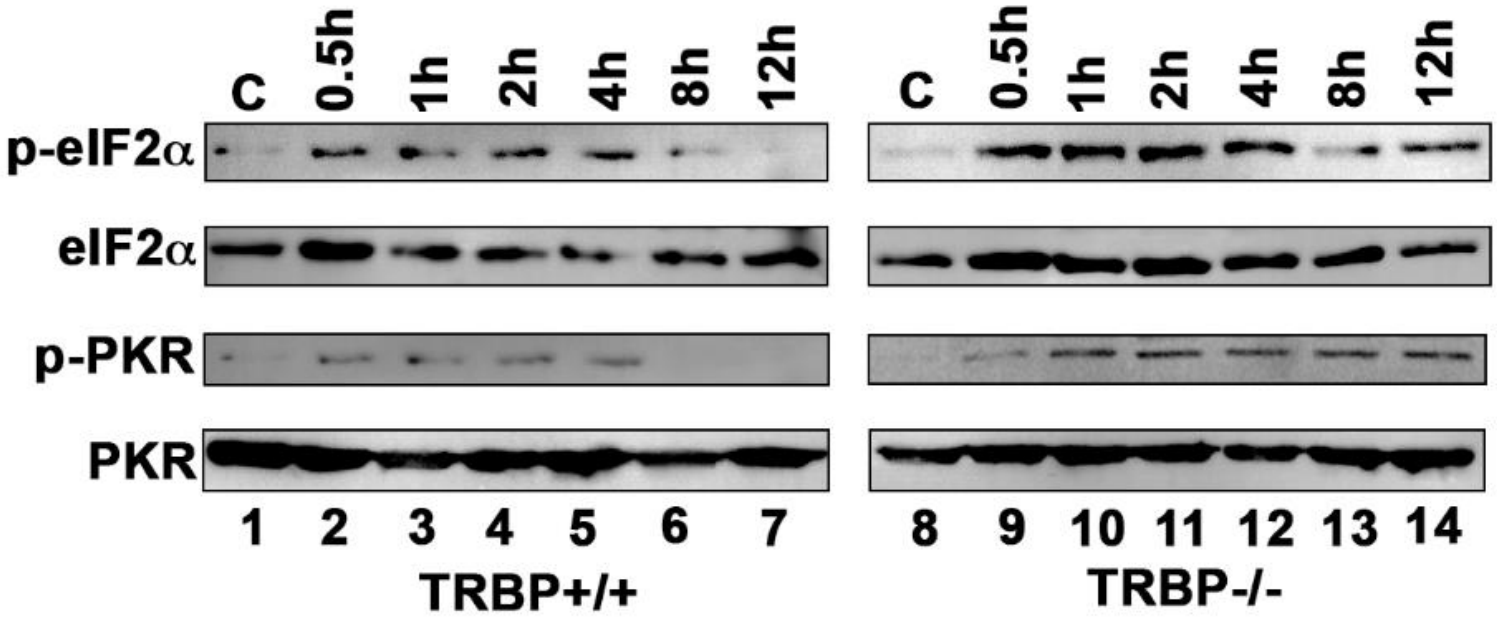

Figure 3.2 PKR activation and eIF2-α phosphorylation in response to arsenite in TRBP+/+ and TRBP/- MEFs. Whole cell extracts prepared from TRBP+/+ and TRBP-/- MEFs treated with 25 μM sodium arsenite at indicated time points were analyzed. Blots were probed for p-eIF2α, total eIF2α, p-PKR, and total PKR. Best of three representative blots are shown. Total eIF2α and total PKR signals also serve as loading controls to ensure equal amounts of protein was loaded in each lane.

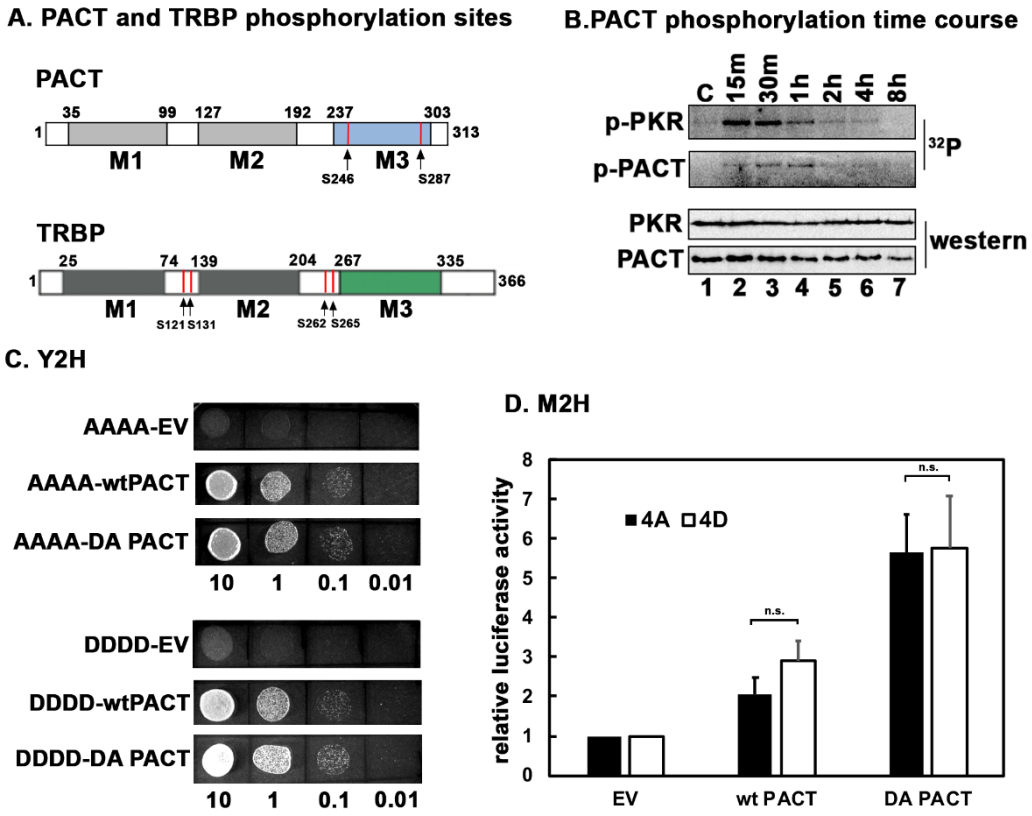

Figure 3.3 TRBP interaction with PACT. (A) Schematic representation of PACT and TRBP domains and phosphorylation sites. PACT: The grey and blue boxes represent the three dsRBMs, M1, M2 and M3. The two known phosphorylation sites in PACT serine 246 and serine 287 are represented by red lines. TRBP: The dark grey and green boxes represent the three dsRBMs, M1, M2, and M3. Red vertical lines represent previously identified ERK 1/2 phosphorylation sites at S142, S152, S283, and S286. **(B) PACT and PKR phosphorylation kinetics in response to arsenite.** HeLa cells were treated with 25 μM sodium arsenite for indicated time periods in phosphate-free medium containing ^{32}P-orthophosphate. PACT and PKR from 500 μg of cell extracts prepared at indicated times after treatment were immunoprecipitated with anti-PACT and anti-PKR monoclonal antibodies. Phosphorylation status of immunoprecipitated PACT and PKR was examined by SDS-PAGE followed by phosphorimager analysis. Aliquots of cell lysates were also examined for total PKR and PACT by western blot analyses. **(C) The phospho-mimetic as well as phospho-defective TRBP interact with PACT with similar affinities.** Empty vector pGAD424, wtPACT/pGAD424, or DA PACT/pGAD424 and either AAAA TRBP/pGBKT7 or DDDD TRBP/pGBKT7 were co-transformed into AH109 yeast cells and selected on SD double dropout media (-tryptophan, - leucine). Ten microliters of transformed yeast cells (OD_{600} = 10, 1, 0.1, 0.01) were spotted on SD quadruple dropout media (-tryptophan, - leucine, - histidine) containing 100 mM 3-amino-1,2,4-triazole (3-AT). Plates were incubated for 3 days at 30° C. **(D) Mammalian two-hybrid assays.** COS-1 cells were transfected with 250 ng of each of the two test plasmids encoding proteins to be tested for interaction, 50 ng of the reporter plasmid pG5Luc, and 1 ng of plasmid pRL-Null to normalize the transfection efficiency. Cells

were harvested 24 h after transfection, and cell extracts were assayed for luciferase activities. The plasmid combinations are as indicated, TRBP was expressed as a GAL4 DNA-binding domain fusion protein (bait) and all PACT proteins were expressed as VP16-activation domain fusion proteins (preys). The experiment was repeated twice with each sample in triplicate, and the averages with standard error bars are presented. The p values were not significant (n. s.) indicating no significant differences in the interactions.

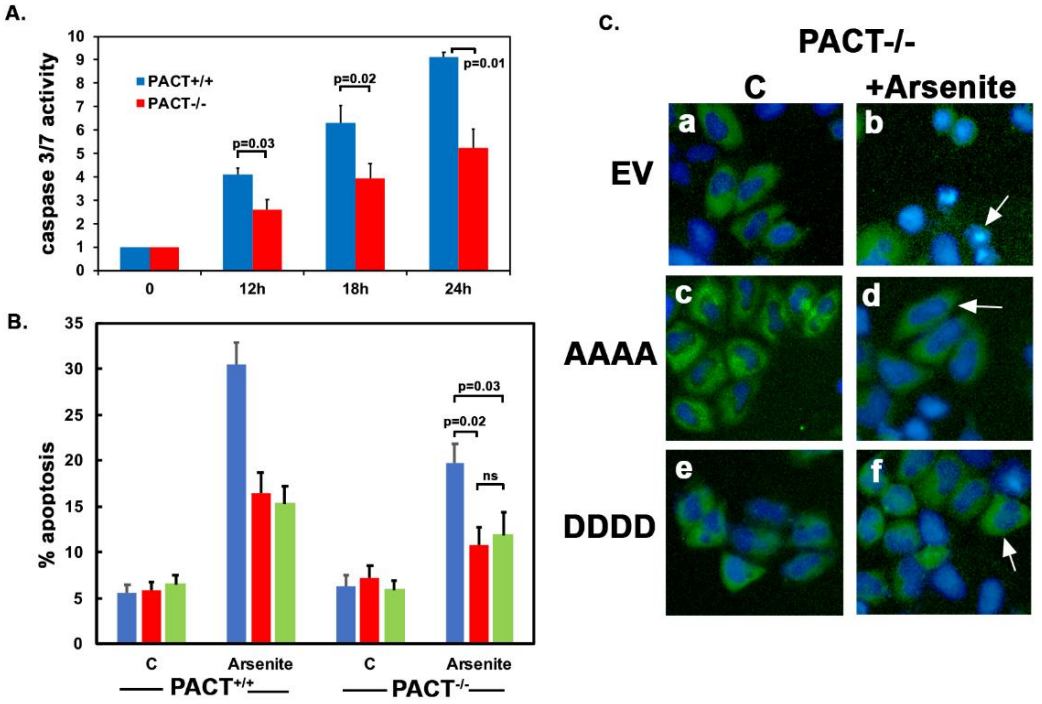

Figure 3.4 TRBP protection of cells from apoptosis in response to arsenite is independent of PACT.
(A) Caspase-Glo 3/7 activity. PACT+/+ and PACT-/- MEFs were treated with 25 μM sodium arsenite and the caspase 3/7 activities were measured at indicated time points. Blue bars: PACT+/+ MEFs, and red bars: PACT-/- MEFs. The data is an average of three independent experiments and the p values are as indicated. **(B and C) Expression of phospho-mimic or phospho-defective TRBP protects PACT-/- MEFs equally well during oxidative stress.** PACT+/+ and PACT-/- MEFs were transfected with 200 ng pEGFPC1 (EV) alone (blue bars), 200 ng each of pEGFPC1 and Flag TRBP AAAA/pcDNA 3.1^{-}(orange bars), or 200 ng each of pEGFPC1 and Flag TRBP DDDD/pcDNA 3.1^{-}(green bars). 24 hours after transfection, the cells were treated with 25 μM sodium arsenite for 12 h, fixed and stained with DAPI nuclear stain. Only the pictures from PACT-/- MEFs are shown in C as PACT+/+ pictures look very similar except for higher level of apoptotic cells after arsenite treatment. At least 300 EGFP-positive cells were scored as apoptotic or live based on nuclear condensation indicated by intense DAPI nuclear staining and cell morphology. The percentage of cells undergoing apoptosis (% apoptosis) was calculated using the formula: (EGFP-expressing cells with intense DAPI nuclear staining/Total EGFP-expressing cells) x 100. This data is represented in B. Bars represent averages ± S.D. from two independent experiments. The p values are as indicated, ns: not significant.

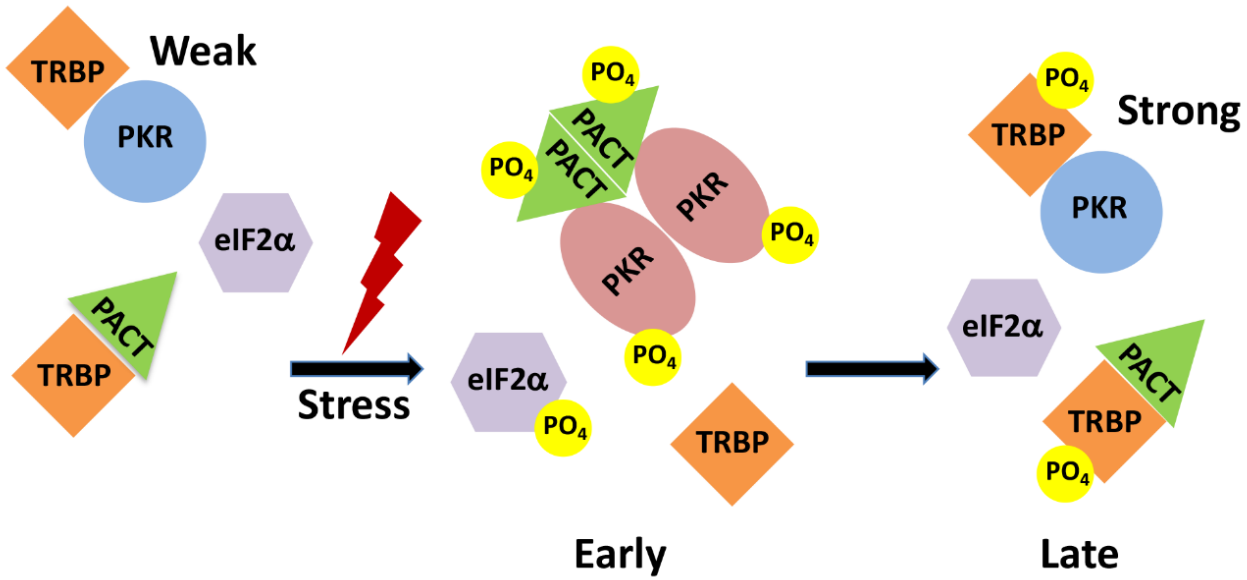

Figure 3.5 A schematic model of PKR, PACT, TRBP interactions in response to oxidative stress. As previously established, in the absence of stress TRBP heterodimerizes with PKR and PACT, PKR is catalytically inactive and eIF2α is not phosphorylated. At early time points after ER stress, TRBP dissociates from phosphorylated PACT, PACT associates with PKR and activates it catalytically leading to its autophosphorylation and eIF2α phosphorylation. At late time points after stress, TRBP is phosphorylated by ERK and JNK and interacts with PKR with higher affinity to inhibit PKR's catalytic activity. The cells recover by forming TRBP-PKR heterodimers and turning off PKR and eIF2α phosphorylation. Phosphorylated TRBP also associates with PACT similar to unphosphorylated form of TRBP and this further helps to keep PKR inactive.

CHAPTER 4

REGULATION OF PKR ACTIVATION IN STRESS GRANULES DURING OXIDATIVE STRESS[4]

[4] Ukhueduan, B.O., & Patel, R.C. To be submitted 2022

4.1 ABSTRACT

Alterations that disrupt stress granule (SG) formation or prolong SG assembly and maintenance have been linked to the acquisition of neuro-degenerative diseases such as ALS (Amyotrophic Lateral Sclerosis) and FTLD (frontotemporal lobar degeneration). SGs sequester stalled pre-initiation components necessary for mRNA translation to protect them from damage and to keep them readily available for protein synthesis when stress signals have been dissipated. Ras GTPase-activating protein-binding protein 1 (G3BP1), a well-characterized SG nucleating protein, activates stress granule formation, and many viruses including HIV prevent stress granule formation by cleaving G3BP1 to prevent a protein synthesis block and replicate efficiently.

The double-stranded (ds) RNA-activated protein kinase (PKR) is activated by dsRNA during viral infections and by PACT in response to non-viral stress signals, is one of the four protein kinases which inactivates the α subunit of eukaryotic translation initiation factor 2 (eIF2α) by phosphorylating it. Previous studies have shown that PKR is present in G3BP1-induced stress granules, creating a biochemical link between the virus-activated innate immune response and the integrated stress response pathway. In this study, we examined if a) the mechanism of PKR recruitment to SG is by a direct interaction between G3BP1 and PKR and b) if PACT is also present in the G3BP1-induced SG as the possible activator of PKR. Our results establish that G3BP1 is associated with PKR in unstressed cells, however, their interaction is reduced after oxidative stress. This result uncovers some key differences in G3BP1-PKR interactions

during viral and non-viral stress signals. It also demonstrates the possibility that G3BP1 recruits PKR to the SG at the early stages of stress response, but after PKR activation within the SG , PKR and G3BP1 dissociate. As the regulation of PKR activation in SG in response to oxidative stress is still not fully understood, these findings could also be considered as a promising link between understanding the dynamic role of SG in viral and non-viral stress response pathways.

4.2 INTRODUCTION

When cells experience extrinsic stresses such as viral infection, oxidative damage, or heat shock, the proteotoxicity resulting from damaged or misfolded proteins triggers a specific stress response. One of the first outcome is a temporary halt in protein synthesis, which aids in cellular recovery (Fulda et al., 2010; Pakos-Zebrucka et al., 2016). However, if the cells cannot recover from the stress, they activate the cell death pathway which kills affected cells leading to acquisition of diseases (Doherty & Baehrecke, 2018; Mirkes, 1997; Napoletano et al., 2019). A temporary block in protein synthesis induces the formation of stress granules (White et al., 2007). Stress granules sequester stalled pre-initiation components (i.e., mRNAs stalled in translation initiation, various translation initiation factors, a variety of RNA-binding proteins, and many non-RNA-binding proteins) necessary for mRNA translation to protect them from damage and also to keep them readily available for protein synthesis when stress signals have been dissipated (Protter & Parker, 2016; Reineke et al., 2012, 2015; White et al., 2007). Once the stress has been cleared, the stress

granules get disassembled and protein translation can commence, which then results in restoration of cellular homeostasis (Protter & Parker, 2016; Reineke et al., 2012, 2015; White et al., 2007).

Mutations that disrupt stress granule formation or prolong stress granule assembly and maintenance have been linked to the acquisition of neuro-degenerative diseases such as ALS (Amyotrophic Lateral Sclerosis) and FTLD (Frontotemporal Diseases, such as dementia) (Eiermann et al., 2020; Lloyd, 2013; Paul et al., 2018). This is thought to result from the neuron-specific functions of stress granules that effect mRNA localization and translation which is essential for normal neuronal function even under unstressed conditions (Paul et al., 2018). Additionally, stress granules also contain several proteins that aid in transitioning from smaller granules to larger aggregates (Eiermann et al., 2020; Reineke et al, 2017; Reineke et al., 2015; Reineke & Lloyd, 2015; Yang et al., 2020). Therefore, characterizing the protein-protein interactions within stress granules can help us resolve the role of stress granules in neuro-degenerative diseases, cellular immunity, and cellular stress response.

The Ras GTPase Activating Protein Binding Protein (G3BP) has 3 different isoforms (G3BssP1, G3BP2a, and G3BP2b) (Bidet et al., 2014; Reineke et al., 2012, 2015; Yang et al., 2020). Each isoform differs from the other by the number of the PXXP motif found in the central region of the protein (Figure 1) (Reineke et al, 2017; Reineke et al., 2012; Yang et al., 2020). G3BP1, G3BP's most well-characterized isoform is a nucleating protein that activates stress granule formation, and many viruses including HIV prevent stress granule

formation to prevent a protein synthesis block and replicate efficiently (Protter & Parker, 2016; Reineke et al., 2012, 2015; Yang et al., 2020). In addition to the PxxP motifs, G3BP1 also contains glutamine and glycine rich domain, an RNA recognition motif (RRM) and an N-terminal NTF2-like domain (Figure 1) (Yang et al., 2020). The NTF2-like domain is the most highly conserved motif of the G3BP sequence indicating its involvement in several G3BP functions (Figure 1) (Bidet et al., 2014; Eiermann et al., 2020; Yang et al., 2020).

Protein Kinase R (PKR) contains two evolutionarily conserved double-stranded (ds) RNA binding motifs (dsRBMs): dsRBM1 (amino acid residues 10-72) and dsRBM2 (amino acid residues 100-165) which mediate its interactions with dsRNA generated during viral infection as well as with other dsRBM-containing proteins (Donnelly et al., 2013; Eiermann et al., 2020; Sadler & Williams, 2007; Sen & Peters, 2007). PKR's kinase catalytic domain is towards the C-terminal (residues 165-551) as shown in Figure 1 (Daher et al., 2017; Donnelly et al., 2013; Sadler & Williams, 2007). In the absence of virus infections PKR is activated by PACT (Sen & Peters, 2007; Singh et al., 2009), also a double stranded RNA binding protein. PKR is one of the four protein kinases which inactivates the eukaryotic translation initiation factor 2α- by phosphorylating the α-subunit (eIF2α) in response to cellular stressors (Donnelly et al., 2013; Pakos-Zebrucka et al., 2016; Peters et al., 2009). The eukaryotic initiation factor eIF2-α is required for initiation of translation for most mRNAs and inactivation of eIF2α leads to a global shut down of protein synthesis and

prolonged inactivation of eIF2α leads to cell death by apoptosis (Mirkes, 1997; Pakos-Zebrucka et al., 2016).

PACT is a dsRNA-binding protein that was originally identified as a PKR-interacting protein in a yeast two-hybrid screen (Bennett et al., 2004; De La Cruz-Herrera et al., 2017; Marques et al., 2008; Patel & Sen, 1998; Singh et al., 2011). PACT is a 313 amino acid long protein containing three dsRNA-binding and dimerization motifs homologous to those present in PKR and other dsRNA-binding proteins; of which the two amino-terminal motifs M1 and M2 are true dsRBMs that exhibit dsRNA-binding activity (Figure 1) (Li et al., 2006; Patel & Sen, 1998; Singh et al., 2011). M1 and M2 are essential for binding to the corresponding M1 and M2 dsRBMs of PKR and the third motif M3 is essential for activation of PKR during cellular stress and binds to a specific region in the kinase domain of PKR with low affinity (Huang et al., 2002; Li & Sen, 2003; Peters et al., 2009; Vaughn, 2015). Within PACT's dsRBM3 are two serine residues (serine 246 and serine 287) that serve as sites for phosphorylation (Figure 1) (Huang et al., 2002; Peters et al., 2009; Singh et al., 2011). While S246 is constitutively phosphorylated, S287 is only phosphorylated under conditions of cellular stress (Peters et al., 2009; Singh et al., 2011; Vaughn, 2015).

Previous studies have shown that PKR is present in G3BP1-induced stress granules, creating a biochemical link between the innate immune response and the integrated stress response pathway as PKR is an interferon-induced kinase which also gets activated under viral stress conditions (Eiermann

et al., 2020; Reineke & Lloyd, 2015). Furthermore, recently published co-localization experiments using G3BP1, PKR and eIF2α have shown that PKR and eIF2α are both present in G3BP1-induced stress granules (Reineke et al., 2012, 2015; Reineke & Lloyd, 2015; Singh et al., 2009). In addition , PKR gets phosphorylated and catalytically activated within the larger stress granules leading to the phosphorylation of eIF2α and triggering the downstream effects of eIF2α phosphorylation (Bidet et al., 2014; Reineke et al., 2012, 2015). However, the mechanism by which PKR gets recruited and activated within G3BP1 induced stress granules has not yet been fully elucidated.

In this study, we examined if a) the mechanism of interaction between G3BP1 and PKR recruitment to stress granules is by direct protein-protein interaction and b) if PACT is also present in these G3BP1 induced stress granules as the possible activator of PKR. Our results establish that G3BP1 associates with PKR in unstressed cellular conditions, however, their interaction decreases after oxidative stress. This result uncovers key differences in G3BP1-PKR interactions during viral and non-viral stress signals. Our results also show that PACT is present in G3BP1 induced stress granules, creating a possibility that it could serve as PKR activator during both viral and oxidative stress response pathways.

4.3 MATERIALS AND METHODS

Cell lines and antibodies: HeLa cells were cultured in Dulbecco's modified Eagle's medium (DMEM) containing 10% Fetal Bovine Serum and penicillin/streptomycin. Transfections were performed with Effectene Transfection

Reagent (Qiagen) according to the manufacturer's protocol. Sodium arsenite (S-7400) and phosphatase inhibitor cocktail (Phosphatase Inhibitor Cocktail 2 – P5726) were purchased from Sigma Aldrich. The following antibodies were used: Mouse monoclonal anti-Flag M2- Peroxidase (Sigma-Aldrich A8592), mouse monoclonal anti-PKR (human) (71/10, R&D Systems), mouse monoclonal anti-G3BP1 (Santa Cruz , SC-365338). The secondary antibody used was goat anti-mouse IgG HRP (Sigma-Aldrich A3682).

Plasmid construction*:* pG3BP1-GFP-2N plasmid construct was generously provided by Dr. Richard E. Lloyd (Department of Molecular Virology and Microbiology, Baylor College of Medicine, Houston, Texas, USA) and the pG3BP-GFP-2N expression plasmid construct have been previously described in his past studies using G3BP1(Reineke et al., 2012) After the sequence of G3BP1-pGEMT Easy was verified, G3BP1 was then subcloned into the pGBKT7 and pGADT7 (Takara Bio USA, Inc) yeast expression vectors at the NdeI and BamHI restriction sites. To generate a Flag-G3BP1/pcDNA 3.1- expression construct, G3BP1 insert from pG3BP1-GFP-2N was subcloned into a Flag BSIIKS+ construct with NdeI-BamHI then Flag- G3BP1 in BSINS+ was then subcloned into pcDNA 3.1- in order to put a Flag- tag at its amino terminus with XbaI and BamHI. The PKR/pmCherryC1 and PACT/pmCherryC1 constructs was generated by subcloning the PKR (K296R) and PACT ORFs from Flag PACT/pcDNA3.1- and Flag K2(6R/pcDNA3.1 -) . The PKR/ pmCherryC1 construct was generated by sub-cloning the PKR ORF with the (kinase inactivated domain) K296R mutation from K296R PKR/pCDNA3.1- .

Fluorescent microscopy*:* Hela cells were grown to 30% confluency on coverslips in six-well plates and co-transfected with 250 ng of empty vector pEGFP-G3BP1 and 250 ng of pmCherryC1 K296R PKR or PACT (TakaraBio) using Effectene (Qiagen). The cells were observed for GFP fluorescence 24 hours after transfection using an inverted fluorescence microscope (EVOS® FL Imaging System, Thermo Fisher Scientific). 12 hours after treatment, the cells were rinsed with ice-cold phosphate buffered saline (PBS) and fixed in 2% paraformaldehyde for 10 minutes. Cells were washed twice in ice-cold PBS and permeabilized with 0.1% Triton-X for 10 minutes, after which the cells were washed twice in ice-cold PBS. Cells were stained with the DAPI nuclear stain (4,6-diamidino-2-phenylindole) at 0.5 µg/mL in PBS for 10 minutes at room temperature in the dark. The cells were rinsed once with PBS and viewed under the fluorescent microscope (Leica DMI 3000B) IF images were captured using the Leica DFC 345FX camera.

G3BP1-PKR co-immunoprecipitation assay*:* HeLa cells were co-transfected in 6-well culture dishes with 250 ng each of (Flag G3BP1/ pcDNA 3.1$^-$ or Flag PACT/ pcDNA 3.1$^-$, using the Effectene reagent (Qiagen). 24 hours after transfection, cell extracts were prepared in co-IP buffer (150 mM NaCl, 30 mM Tris-HCl pH 7.5, 1 mM MgCl2, 10% Glycerol, 0.4% Igepal). Flag G3BP1 and Flag PACT were immunoprecipitated with anti-Flag mab-agarose (Peroxidase (Sigma-Aldrich A8592) in co- IP buffer. The agarose beads were washed 5 times in co-IP buffer. The bound proteins were then analyzed by western blot analysis with ,

PKR antibody (anti-PKR (human) monoclonal (71/10, R&D Systems)), and anti-Flag (Sigma) antibody.

Co-Immunoprecipitation Assays with Endogenous Proteins: HeLa cells were treated with 1 mM of Sodium arsenite over a 0, 5,10,20 and 30-minute time course. Cells were then harvested and lysed in IP buffer ((20 mM Tris-pH 7.2 HCl pH 7.5, 150 mM NaCl, 1 mM EDTA, 1% Triton X-100, 20% Glycerol). PKR was immunoprecipitated from the prepared lysates overnight at 4^{o}C using 100 ng anti-PKR antibody (71/10, R&D Systems) conjugated to 10 µL protein A sepharose beads (GE Healthcare). Immunoprecipitates were then washed 3 times in 500 µL of IP buffer followed by resuspension and boiling for 5 minutes in 2x LaemmLi buffer (150 mM Tris–HCl pH 6.8, 5% SDS, 5% β-mercaptoethanol, 20% glycerol). Samples were then resolved on 10% SDS-PAGE denaturing gel and transferred to PVDF membranes which were probed with anti-G3BP1 antibody to determine co-IP efficiency and anti-PKR antibody to determine equal amounts of PKR were immunoprecipitated. Input blots of whole cell extract without immunoprecipitation are shown to indicate equal amounts of protein in each sample. Western blot images were analyzed using the Typhoon FLA 7000 and ImageQuant LAS 4000 (GE Health).

Yeast two-hybrid interaction assay: To compare the strength of G3BP1 protein with PKR protein interactions, PKR was expressed as a GAL4 DNA-activation domain fusion protein from the pGAD424 vector, and G3BP1 and K296R PKR were expressed as GAL4 DNA-binding domain fusion proteins from the pGBKT7 and pGBT9 vector, respectively. K296R pGAD424 /K296R pGBT9 and K296R

pGAD424/ G3BP1 pGBKT7 were co-transformed into AH109 yeast cells (TakaraBio), and the transformed yeast cells were plated on double dropout SD (synthetic defined) minimal medium lacking tryptophan and leucine. To check for the transformants' ability to grow on triple dropout media, transformed yeast cells were grown to an OD_{600} of 2 in liquid growth medium. A 500 µl aliquot of each culture was pelleted and resuspended in an appropriate amount of distilled water to yield an OD_{600} of 10. Serial dilutions were then made to yield OD_{600} values of 1, 0.1, and 0.01. A 10 µl aliquot of each dilution was then spotted onto triple dropout SD minimal media lacking histidine, tryptophan, and leucine. Plates were incubated at 30^{o}C for 3 days to 4 days.

4.4 RESULTS

Overexpression of G3BP1 causes SG formation and both PKR and PACT co-localize to these SGs

Overexpression of cellular proteins such as G3BP1 induced SG formation (Reineke et al., 2012). To confirm that our G3BP1 expression construct induces SG formation, and assess co-localization of PKR and PACT to SG, we co-transfected HeLa cells with mCherry-PKR or mCherry-PACT and eGFP-G3BP1 expression constructs. After 24 hours, the transfected cells were observed under a fluorescence microscope for SG formation. Since wt PKR overexpression induces apoptosis very rapidly, we used a catalytically dead PKR mutant for all experiments using full length as indicated by white arrows, overexpression of G3BP1 Figure 4.2 (panel A and D) did indeed lead to formation of SG of various sizes. Next, we looked for the colocalization of both mCherry-PKR and mCherry-

PACT within these SG. As indicated by the overlay panels for both mCherry-PKR (Figure 4. 2 panel C) and mCherry PACT (Figure 4.2 panel F), both PKR and PACT colocalize to SG. These results demonstrate that G3BP1 overexpression alone induces SG formation in the absence of stress. Furthermore, it shows that both PKR and PACT are present in SGs.

PKR interacts with G3BP1: co-immunoprecipitation of endogenous PKR with FLAG-G3BP1

Since we demonstrate that G3BP1 overexpression in cultured cells induces SG formation and both PKR and PACT colocalize within these stress granules (Figure 4.2), we next asked if there is a direct association between PKR and G3BP using a co-immunoprecipitation (Co-IP) assay (Figure 4.3). HeLa cells were transfected with either FLAG-tagged G3BP1 (FLAG-G3BP1) or FLAG-tagged PACT (FLAG-PACT) which serves as a positive control since it is a known PKR-interacting protein. FLAG- PACT and Flag-G3BP1 proteins were immunoprecipitated using an anti-Flag monoclonal antibody (mAB) conjugated agarose beads and the co-immunoprecipitation of endogenous was investigated by western blot analysis of immunoprecipitates using anti-PKR mAb (Figure 4.3). PKR shows a strong interaction with G3BP1 (Co-IP panel: lane 2) under unstressed conditions, compared to FLAG-PACT Co-IP panel lane 1 Co-IP. The weak interaction between PACT-PKR can be explained by the absence of a stressor because PACT is known to interact with PKR strongly in presence of a stress signal. Lanes 3 and 4 (IP panels) showed that both Flag tagged G3BP1, and PACT were efficiently immunoprecipitated. Furthermore, there were equal

amounts for endogenous PKR present in each sample as shown by the input blot (lanes 1 and 2). HeLa cells effectively expressed both FLAG- G3BP1 and FLAG-PACT (Figure 4.3, input blot lanes 3 and 4). Overall, these results show that PKR interacts with G3BP1, and this interaction with occurs under unstressed conditions in mammalians cells when G3BP1 is overexpressed.

Oxidative stress causes dissociation of PKR from G3BP1

Past research in our lab has shown that oxidative stress induces PKR activation and consequent phosphorylation of eIF2α (Singh et al., 2012; Chukwurah et al., 2018). Prolonged eIF2α phosphorylation leads to cell death via the apoptosis pathway. Since we have established that G3BP1-induced SGs recruit PKR, we next questioned what effect oxidative stress (treatment with sodium arsenite) has on the interaction between G3BP1 and PKR. To determine if oxidative stress affects G3BP1-PKR interaction, we transfected HeLa cells with FLAG-G3BP1 and compared G3BP1-PKR interaction at the indicated time points after sodium arsenite treatment. the intensity of the basal level band of PKR immunoprecipitated was low in the control untreated cells while a higher intensity band for the basal level of FLAG-G3BP1 co-IP panel, thus confirming the interaction between G3BP1 and PKR before stress is applied. However, this interaction was not maintained after arsenite treatment as there was less G3BP1 co-immunoprecipitated (Figure 4.4, lanes 2-4) even though more PKR was pulled down compared to unstressed conditions (compare lane 1 to lanes 2-4 in IP panel). There were equal levels of both FLAG-G3BP1, and PKR in all samples (figure 4.4, input blot lanes 3 and 4) . These results align with those from a

previous study by Reineke and colleagues showing that that PKR is recruited transiently to G3BP1-induced SGs. Additionally, my data show that cellular stress reduces the interaction between G3BP1 and PKR in a time dependent manner.

Oxidative stress causes dissociation of G3BP1-PKR interaction

Next, we asked if the oxidative stress-induced dissociation of PKR from G3BP1 could be replicated using endogenous levels of proteins expression (i.e., without overexpression) Therefore, we repeated the experiments described in the previous section using HeLa cell extracts prepared after treatment with sodium arsenite at the indicated time points. Endogenous PKR was immunoprecipitated with anti-PKR antibody and protein A-sepharose and the co-immunoprecipitation of endogenous G3BP1 was assessed by western blot analysis with anti-G3BP1 antibody. There was very little PKR immunoprecipitated in control without any PKR antibody (lane 1) but PKR antibody immunoprecipitated PKR efficiently (lane 2) in the absence of arsenite treatment (Figure 4.5). Also, endogenous G3BP1 efficiently co-immunoprecipitated in the absence of stress (lane 2, co-IP panel). After arsenite treatment, there is a time-dependent decrease in G3BP1 coimmunoprecipitation with small amount still co-immunoprecipitating at 5 min (co-IP panel, lane 3) but decreasing to undetectable levels at 10 and 20 min (co-IP panel, lanes 4-5) . PKR was immunoprecipitated efficiently in lanes 3-5 (IP panel) indicating that G3BP1 is not co-immunoprecipitated with PKR after stress. The input blot which served as our controls for the experiment, show that there were equal amounts of endogenous G3BP1, and PKR proteins present in our samples. These results demonstrate

that oxidative stress disrupts the interaction between G3BP1 and PKR in a time dependent manner with a total abrogation of their interaction 20 minutes after dress.

G3BP1 does not directly interact with PKR in yeast two-hybrid assay

The co-localization and co-immunoprecipitations assays indicated that G3BP1 and PKR are in the same complex of proteins. To determine if G3BP1 and PKR interacts directly without the involvement of a third partner such as PACT, we used a yeast two-hybrid system to investigate the interaction between G3BP1 and PKR. Since the expression of active PKR in S. *cerevisiae* suppresses yeast growth, a dominant negative form of PKR (K296R) whose catalytic activity has been silenced but still retains the protein-protein interaction abilities of PKR was used in place of wild type PKR. We introduced G3BP1 into a pGBKT7 yeast expression vector to create a G3BP1-Gal4 DNA binding domain fusion protein and introduced K296R PKR into a pGAD424 yeast expression vector to create a K296R-Gal4 activation domain fusion protein. We did not observe any interaction between G3BP1, and PKR as compared to the strong interaction seen between two PKR molecules, PKR-PKR homodimer formation which was used as a positive control (Figure 4.6). This indicates that either G3BP1 might not be expressing in our yeast system correctly or that the interactions seen between G3BP1 and PKR might be mediated via a third protein such as PACT

4.5 DISCUSSION

In this study, our goal was to investigate the interaction between G3BP1 and PKR within G3BP1-induced SGs. We wanted to understand which proteins are involved in the recruitment of PKR to the SG. As PKR is an interferon inducible stress response kinase (Donnelly et al., 2013; Sen & Peters, 2007), the ability of G3BP1-induced SG to recruit PKR and possibly other innate immune transcriptional components indicates that G3BP1 can serve both as an antiviral and stress response activator protein. Our colocalization results indicated that overexpression of G3BP1 did lead to SG formation as was previously described by (Reineke et al., 2012; Reineke & Lloyd, 2015). Furthermore, both PKR and PACT co-localize to these SG (Figure 2). As SGs are centers for protection and storage of translationally silenced messenger RNPs (mRNPs), translation initiation factors, 40S ribosomal subunits, and RNA-binding proteins (Cao et al., 2020; Eiermann et al., 2020; Protter & Parker, 2016; White et al., 2007), that form in response to cellular stressors that inhibit protein synthesis, the role of PKR in these SG is of great importance. While the recruitment of innate immune proteins to SGs does not always activate the innate immune response (Reineke et al, 2017; Meyer et al., 2018; Protter & Parker, 2016), the additional presence of PACT as shown by the colocalization images in these SGs does support the notion that G3BP1 might also be an activator of non-immune based cellular stress response pathway. It is a well-established that PACT's interaction with PKR during stress response leads to PKR activation and phosphorylation of

eIF2α leading to a global shutdown of protein translation in cells (Peters et al., 2009; Sadler & Williams, 2007; Singh et al., 2009).

To determine if G3BP1 plays a role in recruitment of PKR to G3BP1-induced SG, we transfected mammalian cells with flag-G3BP1, and Flag-PACT then looked for interaction with endogenously expressed PKR via a coimmunoprecipitation assay. As PACT only interacts with PKR under conditions of non-viral stress (Singh et al., 2009), it served as a good control for testing PKR protein associations. Our results showed that the flag-G3BP1 protein did express beautifully in our cells and PKR interacts with G3BP1. Interestingly, the co-IP of PKR with overexpression of FLAG-G3BP1 showed G3BP1 having a stronger interaction with PKR in non-stress conditions compared to the Flag-PACT overexpression. This made sense as we did not expect to see interactions between PACT and PKR in the absence of stress. While it could be hypothesized that the overexpression of G3BP1 itself could be a simulation of a stressful cellular condition as supported by the formation of SG, we next wanted to test the strength of the interaction we had seen between G3BP1 and PKR under oxidative stress conditions. Therefore, we decided to treat mammalian cells expressing our Flag-G3BP1 protein with sodium arsenite which is a known oxidative stress inducer. We also added a time course so we can assess if the G3BP1 and PKR interaction changes with time after oxidative stress. When we used PKR antibody for our pull-down assay, we found that as stress increased in duration the amount of PKR that was immunoprecipitated also increased with the highest amounts seen at 30-minute post treatment with sodium arsenite (Figure

4.4). However, the opposite could be said for the Flag- G3BP1 which seemed to show a reduction in the amount coimmunoprecipitated with PKR as time of stress increased. Especially when looking at the same 30 minutes post stress, the protein signal in the G3BP1 CO-IP panel seems almost nonexistent compared to the dark PKR protein signal seen in the IP panel. This is an interesting new finding as it demonstrates the possibility that G3BP1 does recruit PKR to the SG at the early stages of stress response, but as the stress persists, PKR might be getting activated, leading to its dissociation from G3BP1. This can further explain the increase in eIF2α phosphorylation that was also reported by Reineke et al, in large G3BP1-induced stress granules containing PKR (Reineke et al., 2012; Reineke & Lloyd, 2015). They had shown that PKR gets activated in the granules and leaves, but they could not explain the clear mechanism of PKR recruitment and activation. It is important to note that these conclusions are based on the data we currently have at this stage and more experiments including looking at phospho-PKR and phospho-eIF2α will need to be carried out in other to fully confirm these conclusions.

To get a much more accurate understanding of this new finding about the protein-protein association between G3BP1 and PKR in response to oxidative stressor, applicability of these new results was then tested using endogenous proteins. Similar to our previous results with Flag-G3BP1 overexpression, our results from the endogenous protein pulldown assay also showed that oxidative stress causes dissociation of interaction between G3BP1 and PKR (Figure 4.5). Together, these basic findings are consistent with the research showing the

presence of PKR in G3BP1-induced SG and the possible hypothesis that G3BP1 might be directly recruiting PKR to these granules as a way for its activation and increase in its downstream activities. One concern about these findings is that in coimmunoprecipitation studies, whole protein complexes that include other proteins could have played a role also in the recruitment of PKR to these G3BP1-induced SG. Additionally, these unknown proteins could also have been pulled down during our experiments and could possibly be the reason for the G3BP1-PKR associations we had seen.

One of the potential limitations to our co-immunoprecipitation assay is that a whole complex of proteins interacting together gets pulled down, and so, we decided to test for the direct protein-protein interactions between G3BP1 and PKR using a yeast two-hybrid system. Expression of active wild type PKR in S. cerevisiae suppresses yeast growth, thus a dominant negative form of PKR (K296R) whose catalytic activity has been silenced but still retains the protein-protein interaction abilities of PKR was used in place of wild type PKR. The results showed that G3BP1 had no interaction with PKR (Figure 4.6). It is difficult to explain this result within the current context of protein interaction, because there might be numerous possible reasons as to why the yeast experiments showed no interaction results. One of this possible explanation could be that their interaction may not be direct. Alternatively, it should simply mean that our G3BP1 yeast constructs were not expressing or expressing at low levels leading to the negative results. Whatever the case might be, it is most evident by the

results that more experiments or a different assay such as a mammalian two-hybrid assay should be used to probe this unanswered question.

In summary, the findings of this study can be taken as a first step in elucidating the mechanism by which G3BP1 is able to a) recruit PKR to SG b) activate PKR within these SG and c) which other proteins play important roles and are essential for PKR activation. As the regulation of PKR activation in SG in response to oxidative stress is still not fully understood, these findings could also be considered as a promising link between understanding the dynamic role of SG in viral and non-viral stress response pathways.

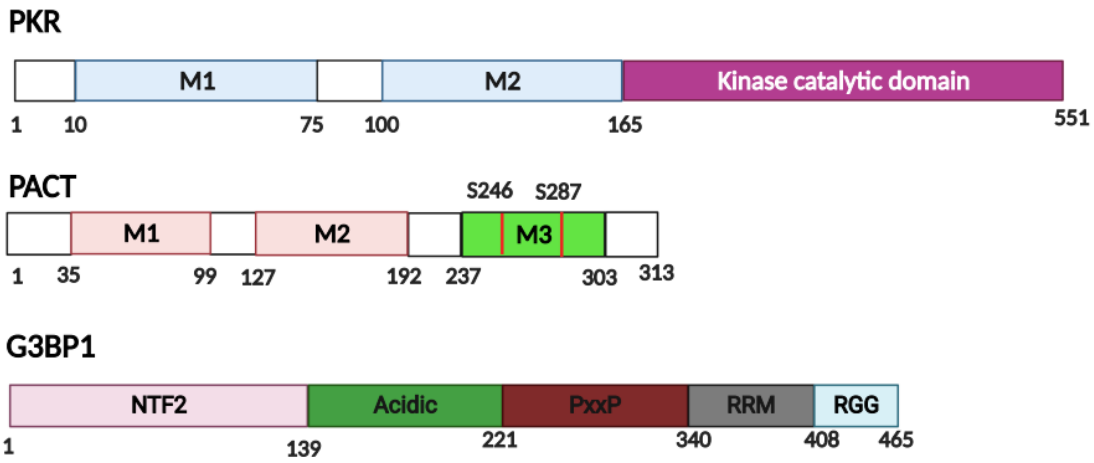

Figure 4.1. Schematic representation of PKR, PACT and G3BP1 domains. PKR: light blue boxes represent the two dsRBMs M1 and M2, and the purple box represents PKR's kinase catalytic domain. **PACT:** The light brown boxes represent the two dsRBMs, M1 and M2 and the light green box represents M3 motif that is important for protein–protein interactions and PKR activation. The two known phosphorylation sites in PACT serine 246 and serine 287 are also represented by the red lines located with the M3 motif.**G3BP1:** Ras-GTPase-activating protein Binding Protein 1 showing the NTF2 (Nuclear Transport Factor 2)-like domain that binds FGDF motifs in other proteins (light purple box), Acidic motif (dark green box), PxxP motif which is proline-rich and very hydrophobic (dark brown box), the RRM domain; RRM represents the RNA recognition motif (dark gray box) and the RGG, containing repeats of the arginine-glycine-glycine, a peptide motif used for RNA/Protein Binding (light teal box). Figure was created using BioRender.

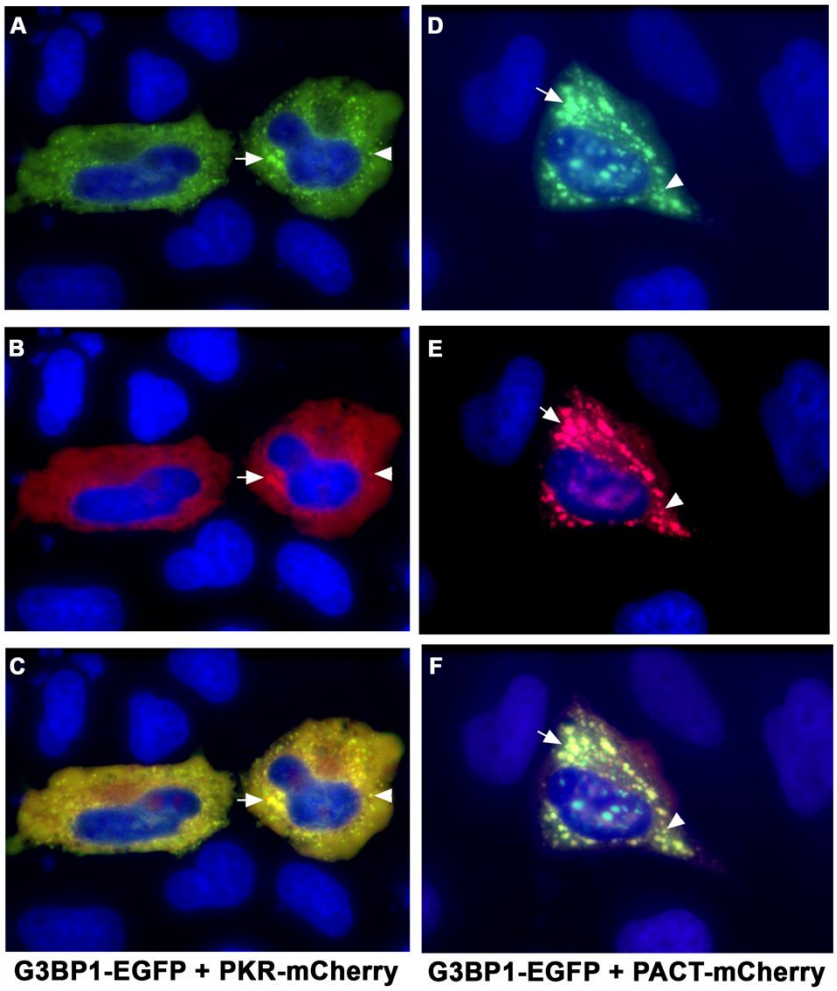

Figure 4.2 Overexpression of G3BP1 causes SG formation and both PKR and PACT co-localize to these SG. HeLa cells were co-transfected with pmCherry-PACT and pEGFP-G3BP1 or pmCherry-PKR and pEGPF-G3BP1. Expression of proteins was examined 24h after transfection using a fluorescence microscope. **a:** overlay of pEGFP-G3BP1 fusion protein (Green) and DAPI nuclear stain (blue) **b:**overlay of pmCherry-PKR (red) and DAPI nuclear stain (blue),**c:** overlay of pEGFP-G3BP1 fusion protein (green), DAPI nuclear stain (blue) and pmCherry-PKR (red) **d:**overlay of pEGFP-G3BP1 fusion protein (green) and DAPI nuclear stain (blue), **e:**overlay of pmCherry-PACT (red) and DAPI nuclear stain (blue), **f:**overlay of pEGFP-G3BP1 fusion protein (green), pmCherry-PACT fusion protein(red) and DAPI nuclear stain (blue).The white arrows are pointing to the SGs.

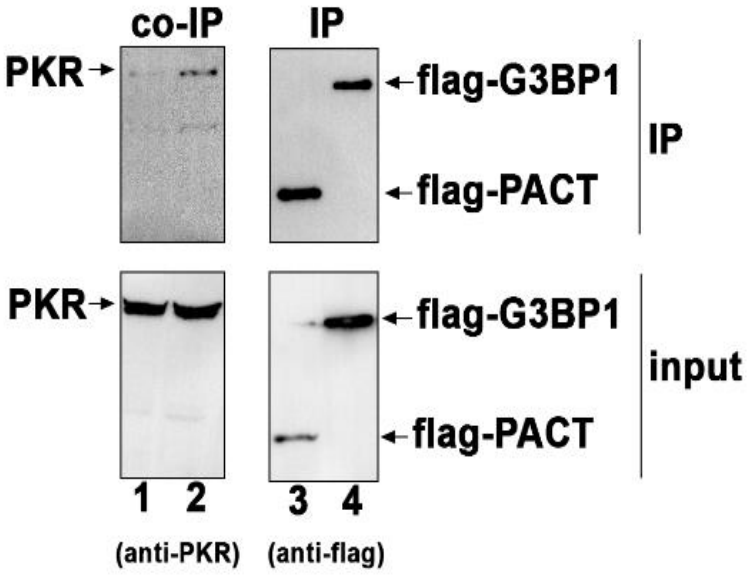

Figure 4.3 PKR interacts with G3BP1: co-IP of endogenous PKR with flag-G3BP1. HeLa cells were transfected with either Flag-G3BP1/pcDNA 3.1- or Flag-PACT/pcDNA 3.1-. The cells were harvested 24h after transfection. Flag PACT and Flag-G3BP1 was immunoprecipitated using anti-Flag monoclonal antibody conjugated agarose beads. The co-immunoprecipitation of endogenous PKR was analyzed by western blot analysis with an anti-PKR antibody (IP: xPKR panel). Blot was subsequently stripped and re-probed with anti-Flag antibody to ensure Flag-PACT and Flag-G3BP1 immunoprecipitation from each sample (Input: x Flag panels). Input panels show western blot analysis for Flag tagged proteins and endogenous PKR.

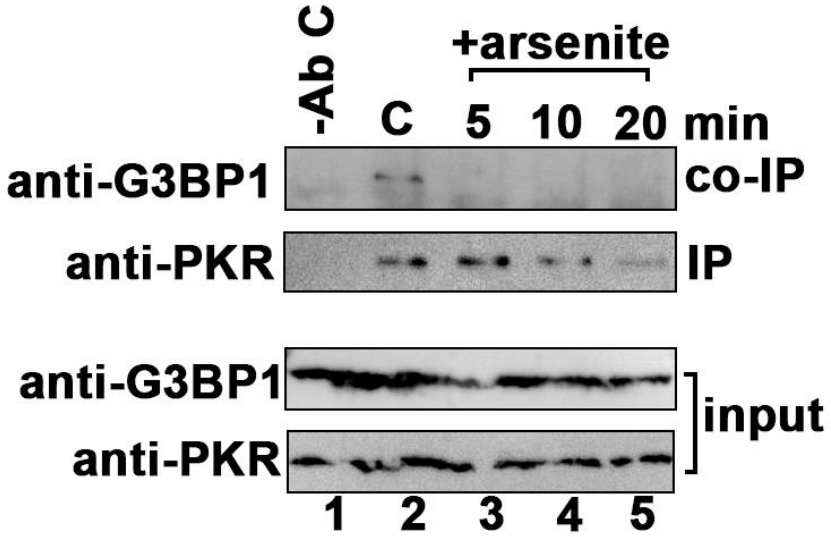

Figure 4.4 Oxidative stress causes dissociation of interaction between G3BP1 and PKR: flag-G3BP1 overexpression and co-IP of PKR with flag-G3BP1*:*HeLa cells were transfected with Flag G3BP1/pcDNA 3.1-. The cells were treated with 1mM sodium arsenite 24 h after transfection and harvested at 0, 10, 20 and 30 minutes after treatment. Flag G3BP1 was immunoprecipitated using anti-Flag monoclonal antibody conjugated agarose beads. The co-immunoprecipitation of PKR was analyzed by western blot analysis with an anti-PKR antibody (co-IP: panel). Blot was subsequently stripped and re-probed with anti-Flag antibody to ensure equal Flag-G3BP1 immunoprecipitation from each sample (IP: x Flag panel). Equal Flag-G3BP1 expression and PKR in all samples was tested by western blot analysis of equal amounts of cell extract with anti-PKR and anti-Flag antibodies (Input panels).

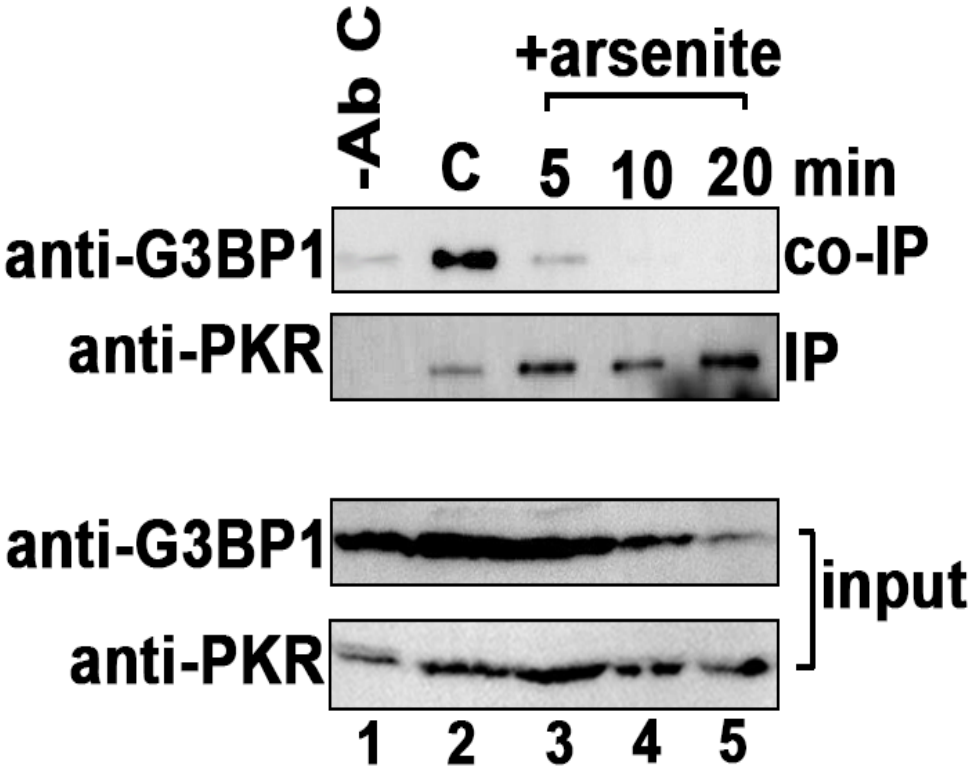

Figure 4.5. Oxidative stress causes dissociation of interaction between G3BP1 and PKR: endogenous G3BP1 co-IP with PKR. HeLa cells were treated with 1 mM sodium arsenite and the cell extracts were prepared at the indicated times after treatment. The endogenous PKR protein was immunoprecipitated using anti-PKR mAb and protein A-Sepharose, which immunoprecipitates total PKR. The immunoprecipitates were analyzed by western blot analysis with anti-G3BP1 monoclonal antibody (co-IP panel). The blot was stripped and re-probed with anti-PKR mAB to ascertain an equal amount of PKR was immunoprecipitated in each lane (IP panel). Input blot: Western blot analysis of total proteins in the extract with anti-G3BP1 and anti-PKR mAbs showing equal amount of G3BP1 and PKR in all samples.

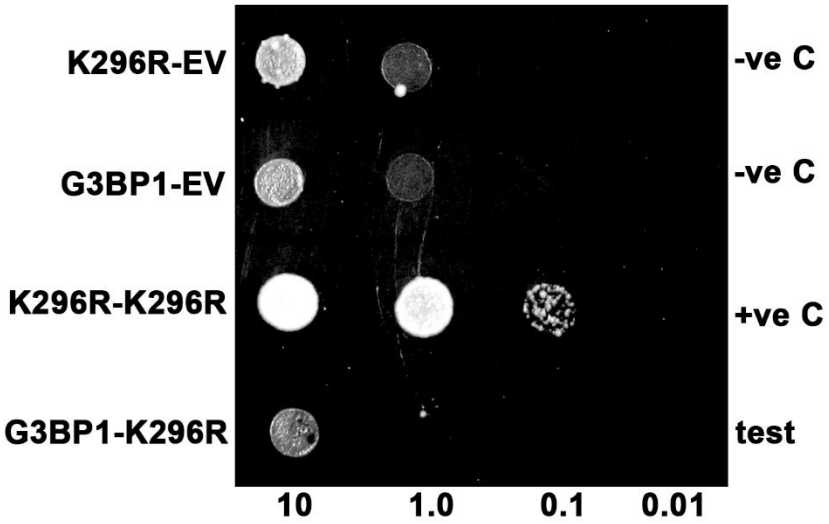

Figure 4.6. G3BP1 does not directly interact with PKR- their interaction could be via PACT. (1) Empty vector pGAD424 and PKR (K296R)-pGBT9, (2) G3BP1/pGBKT7 and empty vector pGAD424, (3) PKR (K296)/pGBT9 and PKR (K296)/pGAD424, (4) G3BP1/pGBKT7 and PKR (K296)/pGAD424 were co-transformed into AH109 yeast cells and selected on SD double dropout media (- tryptophan, - leucine). Ten microliters of transformed yeast cells grown in liquid medium (OD600 = 10, 1, 0.1, 0.01) were spotted on SD triple dropout media (- tryptophan, - leucine, - histidine). Plates were incubated for 4 days at 30 C. Co-transformation of PKR (K296R)/pGBT9 + empty vector pGAD424 and G3BP1/pGBKT7 + empty vector pGAD424 served as negative controls.

CHAPTER 5

GENERAL DISCUSSION

This dissertation focuses on understanding pathways that regulate cellular response to oxidative stress. Under the oxidative stress umbrella, this thesis is divided into two parts; 1) evaluating if oxidative stress contributes to aging and lifespan differences using *Daphnia* as a model and 2) exploring the regulatory role of PKR in determining cellular survival in response to oxidative stress. Both extrinsic and intrinsic oxidative stressors can lead to cell death via apoptosis when there is an imbalance between the production of reactive oxygen species (ROS) and their efficient removal by antioxidant mechanisms. This work explores the effect of such an imbalance on protein function and aging at an organismal level and how protein-protein interactions regulate responses to oxidative stress at a cellular level with major implications on cell survival.

In **Chapter 2**, we took a closer look at the effects of oxidative stress in short-lived and long-lived clones of *Daphnia pulex.* By comparing the overall amount of oxidative damage to proteins in the cytoplasmic and mitochondrial compartments, we demonstrated that short-lived clones had higher levels of oxidative damage to proteins at all ages throughout their lifespan. We next looked at the activity levels of some of two ROS scavenger enzymes (SOD and CAT) as they might contribute to the observed lifespan differences between the *Daphnia* clones. We found the same overall trend in the SOD and CAT enzyme activity in our daphnia ecotypes. In general, the activity of both CAT and SOD was higher in the short-lived clone indicating the presence of higher ROS as compared to the long-lived clone. Furthermore, the amount of catalase activity was significantly lower in the long-lived clone at equivalent time points compared

to the short-lived clone. Finally, the relative activity of complex I of the mitochondrial ETC was more robust in the long-lived clone as compared to the short-lived clone, leading us to conclude that, the short-lived clones have a higher amount of oxidative damage to proteins compared to the long-lived clone possibly due to higher production of ROS contributed by compromised complex I activity. Other types of ROS and ROS scavenging enzymes that we did not assay in this study, including hydroxyl anions and glutathione peroxidases need to be investigated in future studies.

In **Chapter 3**, we transitioned from studying oxidative stress at an organismal level to a cellular level. We investigated the regulatory role of protein kinase PKR in determining cellular fate in response to oxidative stress. We further characterized the mechanism of how phosphorylation of TRBP, a known PKR inhibitor, brings about PKR inhibition after oxidative stress. This work was built upon our earlier work that phosphorylation of TRBP at late time points after oxidative stress makes TRBP a more efficient PKR inhibitor. Previously we had established that phospho-TRBP interacts more strongly with PKR than unphosphorylated TRBP and thus brings about PKR inhibition more efficiently. In the current study we explored if phospho-TRBP also interacts with PKR activator PACT more strongly to bring about additional PKR inhibition by preventing PACT's association with PKR. Our results show that, phosphorylation of TRBP has no effect on PACT-TRBP interactions and TRBP's inhibitory actions on PKR are mediated mainly via its enhanced interaction with PKR. Furthermore, TRBP null cells are more sensitive to oxidative stress-induced apoptosis. PKR

activation and consequent eIF2α phosphorylation in TRBP null cells persisted for longer duration when compared to the wild type cells indicating the importance of a timely, TRBP dependent downregulation of PKR activity after oxidative stress. In the future it will be beneficial to study the effect of TRBP phosphorylation in HIV-infected cells in terms of HIV-viral reservoir and latency in reemergence of infection. This area in cellular stress response has remained unexplored and may reveal some novel ways to suppress HIV replication in adults, transmission via infant breastfeeding and overall disease remission.

In **Chapter 4,** we explored the newly emerging role of PKR in oxidative stress-induced cellular cytoplasmic bodies called stress granules (SGs). SGs sequester stalled pre-initiation components necessary for mRNA translation to protect them from damage and make them readily available for protein synthesis when stress signals have been dissipated. We examined a) if the mechanism of PKR recruitment to SGs is by a direct interaction between G3BP1 and PKR and b) if PACT is also present in SGs as the possible activator of PKR. Our results establish that G3BP1 is associated with PKR in unstressed cells, however, their interaction is reduced after oxidative stress. This demonstrates that G3BP1 does recruit PKR to the SGs at the early stages of stress response, but PKR activation within SGs may lead to its dissociation from G3BP1. The findings of this study can be taken as a first step in elucidating the mechanism by which G3BP1 is able to a) recruit PKR to SG, and b) which protein may work to activate PKR within these SG. As the regulation of PKR activation in SG in response to oxidative stress is still not fully understood, future studies in this area will reveal a link

between understanding the dynamic role of SG in viral and non-viral stress response pathways.

REFERENCES

CHAPTER 1 REFERENCES

Balaban, R. S., Nemoto, S., & Finkel, T. (2005). Mitochondria, oxidants, and aging. *Cell*, *120*(4), 483-495. https://doi.org/10.1016/j.cell.2005.02.001

Barata, C., Navarro, J. C., Varo, I., Riva, M. C., Arun, S., & Porte, C. (2005). Changes in antioxidant enzyme activities, fatty acid composition and lipid peroxidation in Daphnia magna during the aging process. *Comp Biochem Physiol B Biochem Mol Biol*, *140*(1), 81-90. https://doi.org/10.1016/j.cbpc.2004.09.025

Beers, R. F., Jr., & Sizer, I. W. (1952). A spectrophotometric method for measuring the breakdown of hydrogen peroxide by catalase. *J Biol Chem*, *195*(1), 133-140.

Blok, M. J., Spruijt, L., de Coo, I. F., Schoonderwoerd, K., Hendrickx, A., & Smeets, H. J. (2007). Mutations in the ND5 subunit of complex I of the mitochondrial DNA are a frequent cause of oxidative phosphorylation disease. *J Med Genet*, *44*(4), e74. https://doi.org/10.1136/jmg.2006.045716

Brandt, U. (2006). Energy converting NADH:quinone oxidoreductase (complex I). *Annu Rev Biochem*, *75*, 69-92. https://doi.org/10.1146/annurev.biochem.75.103004.142539

Brecht, M., Richardson, M., Taranath, A., Grist, S., Thorburn, D., & Bratkovic, D. (2015). Leigh Syndrome Caused by the MT-ND5 m.13513G>A Mutation: A Case Presenting with WPW-Like Conduction Defect, Cardiomyopathy, Hypertension and Hyponatraemia. *JIMD Rep*, *19*, 95-100. https://doi.org/10.1007/8904_2014_375

Bugiani, M., Invernizzi, F., Alberio, S., Briem, E., Lamantea, E., Carrara, F., Moroni, I., Farina, L., Spada, M., Donati, M. A., Uziel, G., & Zeviani, M. (2004). Clinical and molecular findings in children with complex I deficiency. *Biochim Biophys Acta*, *1659*(2-3), 136-147. https://doi.org/10.1016/j.bbabio.2004.09.006

Calabrese, V., Scapagnini, G., Colombrita, C., Ravagna, A., Pennisi, G., Giuffrida Stella, A. M., Galli, F., & Butterfield, D. A. (2003). Redox regulation of heat shock protein expression in aging and neurodegenerative disorders associated with oxidative stress: a nutritional approach. *Amino Acids*, *25*(3-4), 437-444. https://doi.org/10.1007/s00726-003-0048-2

Clancy, D., & Birdsall, J. (2013). Flies, worms and the Free Radical Theory of ageing. *Ageing Res Rev*, *12*(1), 404-412. https://doi.org/10.1016/j.arr.2012.03.011

Constantinou, J., Sullivan, J., & Mirbahai, L. (2019). Ageing differently: Sex-dependent ageing rates in Daphnia magna. *Exp Gerontol*, *121*, 33-45. https://doi.org/10.1016/j.exger.2019.03.008

Copeland, W. C., & Longley, M. J. (2014). Mitochondrial genome maintenance in health and disease. *DNA Repair (Amst)*, *19*, 190-198. https://doi.org/10.1016/j.dnarep.2014.03.010

Cristescu, M. E., Constantin, A., Bock, D. G., Caceres, C. E., & Crease, T. J. (2012). Speciation with gene flow and the genetics of habitat transitions. *Mol Ecol*, *21*(6), 1411-1422. https://doi.org/10.1111/j.1365-294X.2011.05465.x

Doonan, R., McElwee, J. J., Matthijssens, F., Walker, G. A., Houthoofd, K., Back, P., Matscheski, A., Vanfleteren, J. R., & Gems, D. (2008). Against the oxidative damage theory of aging: superoxide dismutases protect against oxidative stress but have little or no effect on life span in Caenorhabditis elegans. *Genes Dev*, *22*(23), 3236-3241. https://doi.org/10.1101/gad.504808

Dudycha, J. L. (2004). Mortality dynamics of Daphnia in contrasting habitats and their role in ecological divergence. . *Freshwater Biology*, *49*(5), 505-514.

Edman, U., Garcia, A. M., Busuttil, R. A., Sorensen, D., Lundell, M., Kapahi, P., & Vijg, J. (2009). Lifespan extension by dietary restriction is not linked to protection against somatic DNA damage in Drosophila melanogaster. *Aging Cell*, *8*(3), 331-338. https://doi.org/10.1111/j.1474-9726.2009.00480.x

Eleftherianos, I., & Castillo, J. C. (2012). Molecular mechanisms of aging and immune system regulation in Drosophila. *Int J Mol Sci*, *13*(8), 9826-9844. https://doi.org/10.3390/ijms13089826

Enzor, L. A., & Place, S. P. (2014). Is warmer better? Decreased oxidative damage in notothenioid fish after long-term acclimation to multiple stressors. *J Exp Biol*, *217*(Pt 18), 3301-3310. https://doi.org/10.1242/jeb.108431

Fischer, F., Hamann, A., & Osiewacz, H. D. (2012). Mitochondrial quality control: an integrated network of pathways. *Trends Biochem Sci*, *37*(7), 284-292. https://doi.org/10.1016/j.tibs.2012.02.004

Harding, J. J., Blakytny, R., & Ganea, E. (1996). Glutathione in disease. *Biochem Soc Trans*, *24*(3), 881-884. https://doi.org/10.1042/bst0240881

Hashimoto, M., Bacman, S. R., Peralta, S., Falk, M. J., Chomyn, A., Chan, D. C., Williams, S. L., & Moraes, C. T. (2015). MitoTALEN: A General Approach to Reduce Mutant mtDNA Loads and Restore Oxidative Phosphorylation Function in Mitochondrial Diseases. *Mol Ther*, *23*(10), 1592-1599. https://doi.org/10.1038/mt.2015.126

Hekimi, S., Lapointe, J., & Wen, Y. (2011). Taking a "good" look at free radicals in the aging process. *Trends Cell Biol*, *21*(10), 569-576. https://doi.org/10.1016/j.tcb.2011.06.008

Höhn, A., Weber, D., Jung, T., Ott, C., Hugo, M., Kochlik, B., Kehm, R., König, J., Grune, T., & Castro, J. P. (2017). Happily (n)ever after: Aging in the context of oxidative stress, proteostasis loss and cellular senescence. *Redox Biol*, *11*, 482-501. https://doi.org/10.1016/j.redox.2016.12.001

Huoponen, K., Lamminen, T., Juvonen, V., Aula, P., Nikoskelainen, E., & Savontaus, M. L. (1993). The spectrum of mitochondrial DNA mutations in families with Leber hereditary optic neuroretinopathy. *Hum Genet*, *92*(4), 379-384.

Janssen, R. J., Nijtmans, L. G., van den Heuvel, L. P., & Smeitink, J. A. (2006). Mitochondrial complex I: structure, function and pathology. *J Inherit Metab Dis*, *29*(4), 499-515. https://doi.org/10.1007/s10545-006-0362-4

Johnson, F. B., Sinclair, D. A., & Guarente, L. (1999). Molecular biology of aging. *Cell*, *96*(2), 291-302.

Khrapko, K., & Turnbull, D. (2014). Mitochondrial DNA mutations in aging. *Prog Mol Biol Transl Sci*, *127*, 29-62. https://doi.org/10.1016/b978-0-12-394625-6.00002-7

Kukat, A., & Trifunovic, A. (2009). Somatic mtDNA mutations and aging--facts and fancies. *Exp Gerontol*, *44*(1-2), 101-105. https://doi.org/10.1016/j.exger.2008.05.006

Lauri, A., Pompilio, G., & Capogrossi, M. C. (2014). The mitochondrial genome in aging and senescence. *Ageing Res Rev*, *18*, 1-15. https://doi.org/10.1016/j.arr.2014.07.001

Liolitsa, D., Rahman, S., Benton, S., Carr, L. J., & Hanna, M. G. (2003). Is the mitochondrial complex I ND5 gene a hot-spot for MELAS causing mutations? *Ann Neurol*, *53*(1), 128-132. https://doi.org/10.1002/ana.10435

Lopez-Otin, C., Blasco, M. A., Partridge, L., Serrano, M., & Kroemer, G. (2013). The hallmarks of aging. *Cell*, *153*(6), 1194-1217. https://doi.org/10.1016/j.cell.2013.05.039

Luce, K., Weil, A. C., & Osiewacz, H. D. (2010). Mitochondrial protein quality control systems in aging and disease. *Adv Exp Med Biol*, *694*, 108-125.

Ma, Y. Y., Wu, T. F., Liu, Y. P., Wang, Q., Song, J. Q., Li, X. Y., Shi, X. Y., Zhang, W. N., Zhao, M., Hu, L. Y., Yang, Y. L., & Zou, L. P. (2013). Genetic and biochemical findings in Chinese children with Leigh syndrome. *J Clin Neurosci*, *20*(11), 1591-1594. https://doi.org/10.1016/j.jocn.2013.03.034

Marí, M., Morales, A., Colell, A., García-Ruiz, C., & Fernández-Checa, J. C. (2009). Mitochondrial glutathione, a key survival antioxidant. *Antioxid Redox Signal*, *11*(11), 2685-2700. https://doi.org/10.1089/ars.2009.2695

Mayorov, V., Biousse, V., Newman, N. J., & Brown, M. D. (2005). The role of the ND5 gene in LHON: characterization of a new, heteroplasmic LHON mutation. *Ann Neurol*, *58*(5), 807-811. https://doi.org/10.1002/ana.20669

Nathan, C., & Cunningham-Bussel, A. (2013). Beyond oxidative stress: an immunologist's guide to reactive oxygen species. *Nat Rev Immunol*, *13*(5), 349-361. https://doi.org/10.1038/nri3423

Orr, W. C., Mockett, R. J., Benes, J. J., & Sohal, R. S. (2003). Effects of overexpression of copper-zinc and manganese superoxide dismutases, catalase, and thioredoxin reductase genes on longevity in Drosophila melanogaster. *J Biol Chem*, *278*(29), 26418-26422. https://doi.org/10.1074/jbc.M303095200

Orr, W. C., & Sohal, R. S. (1994). Extension of life-span by overexpression of superoxide dismutase and catalase in Drosophila melanogaster. *Science*, *263*(5150), 1128-1130. https://doi.org/10.1126/science.8108730

Page, M. M., Robb, E. L., Salway, K. D., & Stuart, J. A. (2010). Mitochondrial redox metabolism: aging, longevity and dietary effects. *Mech Ageing Dev*, *131*(4), 242-252. https://doi.org/10.1016/j.mad.2010.02.005

Pappolla, M. A., Sos, M., Omar, R. A., & Sambamurti, K. (1996). The heat shock/oxidative stress connection. Relevance to Alzheimer disease. *Mol Chem Neuropathol*, *28*(1-3), 21-34. https://doi.org/10.1007/bf02815201

L., Ma, K. Y., Huang, Y., & Chen, Z. Y. (2014). Biology of ageing and role of dietary antioxidants. *Biomed Res Int*, *2014*, 831841. https://doi.org/10.1155/2014/831841

Pulkes, T., Eunson, L., Patterson, V., Siddiqui, A., Wood, N. W., Nelson, I. P., Morgan-Hughes, J. A., & Hanna, M. G. (1999). The mitochondrial DNA G13513A transition in ND5 is associated with a LHON/MELAS overlap syndrome and may be a frequent cause of MELAS. *Ann Neurol*, *46*(6), 916-919. http://onlinelibrary.wiley.com/store/10.1002/1531-8249(199912)46:6%3C916::AID-ANA16%3E3.0.CO;2-R/asset/16_ftp.pdf?v=1&t=ifmm89r1&s=7f87dad61cd57629fd8f60c79a6b9a4397779ce8

Ray, P. D., Huang, B. W., & Tsuji, Y. (2012). Reactive oxygen species (ROS) homeostasis and redox regulation in cellular signaling. *Cell Signal*, *24*(5), 981-990. https://doi.org/10.1016/j.cellsig.2012.01.008

Reeve, A. K., Krishnan, K. J., & Turnbull, D. (2008). Mitochondrial DNA mutations in disease, aging, and neurodegeneration. *Ann N Y Acad Sci*, *1147*, 21-29. https://doi.org/10.1196/annals.1427.016

Richardson, A. G., & Schadt, E. E. (2014). The role of macromolecular damage in aging and age-related disease. *J Gerontol A Biol Sci Med Sci*, *69 Suppl 1*, S28-32. https://doi.org/10.1093/gerona/glu056

Sazanov, L. A. (2015). A giant molecular proton pump: structure and mechanism of respiratory complex I. *Nat Rev Mol Cell Biol*, *16*(6), 375-388. https://doi.org/10.1038/nrm3997

Schumpert, C., Handy, I., Dudycha, J. L., & Patel, R. C. (2014). Relationship between heat shock protein 70 expression and life span in Daphnia. *Mech Ageing Dev*, *139*, 1-10. https://doi.org/10.1016/j.mad.2014.04.001

St-Pierre, J., Buckingham, J. A., Roebuck, S. J., & Brand, M. D. (2002). Topology of superoxide production from different sites in the mitochondrial electron transport chain. *J Biol Chem*, *277*(47), 44784-44790. https://doi.org/10.1074/jbc.M207217200

Tower, J. (2011). Heat shock proteins and Drosophila aging. *Exp Gerontol*, *46*(5), 355-362. https://doi.org/10.1016/j.exger.2010.09.002

Vartak, R. S., Semwal, M. K., & Bai, Y. (2014). An update on complex I assembly: the assembly of players. *J Bioenerg Biomembr*, *46*(4), 323-328. https://doi.org/10.1007/s10863-014-9564-x

Wang, X., Perez, E., Liu, R., Yan, L. J., Mallet, R. T., & Yang, S. H. (2007). Pyruvate protects mitochondria from oxidative stress in human neuroblastoma SK-N-SH cells. *Brain Res*, *1132*(1), 1-9. https://doi.org/10.1016/j.brainres.2006.11.032

Wittig, I., & Schägger, H. (2009). Native electrophoretic techniques to identify protein-protein interactions. *Proteomics*, *9*(23), 5214-5223. https://doi.org/10.1002/pmic.200900151

Xu, S., Schaack, S., Seyfert, A., Choi, E., Lynch, M., & Cristescu, M. E. (2012). High mutation rates in the mitochondrial genomes of Daphnia pulex. *Mol Biol Evol*, *29*(2), 763-769. https://doi.org/10.1093/molbev/msr243

Zapico, S. C., & Ubelaker, D. H. (2013). mtDNA Mutations and Their Role in Aging, Diseases and Forensic Sciences. *Aging Dis*, *4*(6), 364-380. https://doi.org/10.14336/ad.2013.0400364

Zhang, A. M., Jia, X., Guo, X., Zhang, Q., & Yao, Y. G. (2012). Mitochondrial DNA mutation m.10680G > A is associated with Leber hereditary optic neuropathy in Chinese patients. *J Transl Med*, *10*, 43. https://doi.org/10.1186/1479-5876-10-43

CHAPTER 2 REFERENCES

Balaban, R. S., Nemoto, S., & Finkel, T. (2005). Mitochondria, oxidants, and aging. *Cell*, *120*(4), 483-495. https://doi.org/10.1016/j.cell.2005.02.001

Barata, C., Navarro, J. C., Varo, I., Riva, M. C., Arun, S., & Porte, C. (2005). Changes in antioxidant enzyme activities, fatty acid composition and lipid peroxidation in Daphnia magna during the aging process. *Comp Biochem Physiol B Biochem Mol Biol*, *140*(1), 81-90. https://doi.org/10.1016/j.cbpc.2004.09.025

Beers, R. F., Jr., & Sizer, I. W. (1952). A spectrophotometric method for measuring the breakdown of hydrogen peroxide by catalase. *J Biol Chem*, *195*(1), 133-140.

Blok, M. J., Spruijt, L., de Coo, I. F., Schoonderwoerd, K., Hendrickx, A., & Smeets, H. J. (2007). Mutations in the ND5 subunit of complex I of the mitochondrial DNA are a frequent cause of oxidative phosphorylation disease. *J Med Genet*, *44*(4), e74. https://doi.org/10.1136/jmg.2006.045716

Brandt, U. (2006). Energy converting NADH:quinone oxidoreductase (complex I). *Annu Rev Biochem*, *75*, 69-92. https://doi.org/10.1146/annurev.biochem.75.103004.142539

Brecht, M., Richardson, M., Taranath, A., Grist, S., Thorburn, D., & Bratkovic, D. (2015). Leigh Syndrome Caused by the MT-ND5 m.13513G>A Mutation: A Case Presenting with WPW-Like Conduction Defect, Cardiomyopathy, Hypertension and Hyponatraemia. *JIMD Rep*, *19*, 95-100. https://doi.org/10.1007/8904_2014_375

Bugiani, M., Invernizzi, F., Alberio, S., Briem, E., Lamantea, E., Carrara, F., Moroni, I., Farina, L., Spada, M., Donati, M. A., Uziel, G., & Zeviani, M. (2004). Clinical and molecular findings in children with complex I deficiency. *Biochim Biophys Acta*, *1659*(2-3), 136-147. https://doi.org/10.1016/j.bbabio.2004.09.006

Calabrese, V., Scapagnini, G., Colombrita, C., Ravagna, A., Pennisi, G., Giuffrida Stella, A. M., Galli, F., & Butterfield, D. A. (2003). Redox regulation of heat shock protein expression in aging and neurodegenerative disorders associated with oxidative stress: a nutritional approach. *Amino Acids*, *25*(3-4), 437-444. https://doi.org/10.1007/s00726-003-0048-2

Clancy, D., & Birdsall, J. (2013). Flies, worms and the Free Radical Theory of ageing. *Ageing Res Rev*, *12*(1), 404-412. https://doi.org/10.1016/j.arr.2012.03.011

Constantinou, J., Sullivan, J., & Mirbahai, L. (2019). Ageing differently: Sex-dependent ageing rates in Daphnia magna. *Exp Gerontol*, *121*, 33-45. https://doi.org/10.1016/j.exger.2019.03.008

Copeland, W. C., & Longley, M. J. (2014). Mitochondrial genome maintenance in health and disease. *DNA Repair (Amst)*, *19*, 190-198. https://doi.org/10.1016/j.dnarep.2014.03.010

Cristescu, M. E., Constantin, A., Bock, D. G., Caceres, C. E., & Crease, T. J. (2012). Speciation with gene flow and the genetics of habitat transitions. *Mol Ecol*, *21*(6), 1411-1422. https://doi.org/10.1111/j.1365-294X.2011.05465.x

Doonan, R., McElwee, J. J., Matthijssens, F., Walker, G. A., Houthoofd, K., Back, P., Matscheski, A., Vanfleteren, J. R., & Gems, D. (2008). Against the oxidative damage theory of aging: superoxide dismutases protect against oxidative stress but have little or no effect on life span in Caenorhabditis elegans. *Genes Dev*, *22*(23), 3236-3241. https://doi.org/10.1101/gad.504808

Dudycha, J. L. (2004). Mortality dynamics of Daphnia in contrasting habitats and their role in ecological divergence. . *Freshwater Biology*, *49*(5), 505-514.

Edman, U., Garcia, A. M., Busuttil, R. A., Sorensen, D., Lundell, M., Kapahi, P., & Vijg, J. (2009). Lifespan extension by dietary restriction is not linked to protection against somatic DNA damage in Drosophila melanogaster. *Aging Cell*, *8*(3), 331-338. https://doi.org/10.1111/j.1474-9726.2009.00480.x

Eleftherianos, I., & Castillo, J. C. (2012). Molecular mechanisms of aging and immune system regulation in Drosophila. *Int J Mol Sci*, *13*(8), 9826-9844. https://doi.org/10.3390/ijms13089826

Enzor, L. A., & Place, S. P. (2014). Is warmer better? Decreased oxidative damage in notothenioid fish after long-term acclimation to multiple stressors. *J Exp Biol*, *217*(Pt 18), 3301-3310. https://doi.org/10.1242/jeb.108431

Fischer, F., Hamann, A., & Osiewacz, H. D. (2012). Mitochondrial quality control: an integrated network of pathways. *Trends Biochem Sci*, *37*(7), 284-292. https://doi.org/10.1016/j.tibs.2012.02.004

Harding, J. J., Blakytny, R., & Ganea, E. (1996). Glutathione in disease. *Biochem Soc Trans*, *24*(3), 881-884. https://doi.org/10.1042/bst0240881

Hashimoto, M., Bacman, S. R., Peralta, S., Falk, M. J., Chomyn, A., Chan, D. C., Williams, S. L., & Moraes, C. T. (2015). MitoTALEN: A General Approach to Reduce Mutant mtDNA Loads and Restore Oxidative Phosphorylation Function in Mitochondrial Diseases. *Mol Ther*, *23*(10), 1592-1599. https://doi.org/10.1038/mt.2015.126

Hekimi, S., Lapointe, J., & Wen, Y. (2011). Taking a "good" look at free radicals in the aging process. *Trends Cell Biol*, *21*(10), 569-576. https://doi.org/10.1016/j.tcb.2011.06.008

Höhn, A., Weber, D., Jung, T., Ott, C., Hugo, M., Kochlik, B., Kehm, R., König, J., Grune, T., & Castro, J. P. (2017). Happily (n)ever after: Aging in the context of oxidative stress, proteostasis loss and cellular senescence. *Redox Biol*, *11*, 482-501. https://doi.org/10.1016/j.redox.2016.12.001

Huoponen, K., Lamminen, T., Juvonen, V., Aula, P., Nikoskelainen, E., & Savontaus, M. L. (1993). The spectrum of mitochondrial DNA mutations in families with Leber hereditary optic neuroretinopathy. *Hum Genet*, *92*(4), 379-384.

Janssen, R. J., Nijtmans, L. G., van den Heuvel, L. P., & Smeitink, J. A. (2006). Mitochondrial complex I: structure, function and pathology. *J Inherit Metab Dis*, *29*(4), 499-515. https://doi.org/10.1007/s10545-006-0362-4

Johnson, F. B., Sinclair, D. A., & Guarente, L. (1999). Molecular biology of aging. *Cell*, *96*(2), 291-302.

Khrapko, K., & Turnbull, D. (2014). Mitochondrial DNA mutations in aging. *Prog Mol Biol Transl Sci*, *127*, 29-62. https://doi.org/10.1016/b978-0-12-394625-6.00002-7

Kim, E., Ansell, C.M., & Dudycha, J.L. (2014) Resveratrol and food effects on lifespan and reproduction in the model crustacean Daphnia. *J Exp Zool A Ecol Genet Physiol, 321(1),* 48-56. https://doi.org/10.1002/jez.1836.

Kukat, A., & Trifunovic, A. (2009). Somatic mtDNA mutations and aging--facts and fancies. *Exp Gerontol*, *44*(1-2), 101-105. https://doi.org/10.1016/j.exger.2008.05.006

Lauri, A., Pompilio, G., & Capogrossi, M. C. (2014). The mitochondrial genome in aging and senescence. *Ageing Res Rev*, *18*, 1-15. https://doi.org/10.1016/j.arr.2014.07.001

Liolitsa, D., Rahman, S., Benton, S., Carr, L. J., & Hanna, M. G. (2003). Is the mitochondrial complex I ND5 gene a hot-spot for MELAS causing mutations? *Ann Neurol*, *53*(1), 128-132. https://doi.org/10.1002/ana.10435

Lopez-Otin, C., Blasco, M. A., Partridge, L., Serrano, M., & Kroemer, G. (2013). The hallmarks of aging. *Cell*, *153*(6), 1194-1217. https://doi.org/10.1016/j.cell.2013.05.039

Luce, K., Weil, A. C., & Osiewacz, H. D. (2010). Mitochondrial protein quality control systems in aging and disease. *Adv Exp Med Biol*, *694*, 108-12

Ma, Y. Y., Wu, T. F., Liu, Y. P., Wang, Q., Song, J. Q., Li, X. Y., Shi, X. Y., Zhang, W. N., Zhao, M., Hu, L. Y., Yang, Y. L., & Zou, L. P. (2013). Genetic and biochemical findings in Chinese children with Leigh syndrome. *J Clin Neurosci*, *20*(11), 1591-1594. https://doi.org/10.1016/j.jocn.2013.03.034

Marí, M., Morales, A., Colell, A., García-Ruiz, C., & Fernández-Checa, J. C. (2009). Mitochondrial glutathione, a key survival antioxidant. *Antioxid Redox Signal*, *11*(11), 2685-2700. https://doi.org/10.1089/ars.2009.2695

Mayorov, V., Biousse, V., Newman, N. J., & Brown, M. D. (2005). The role of the ND5 gene in LHON: characterization of a new, heteroplasmic LHON mutation. *Ann Neurol*, *58*(5), 807-811. https://doi.org/10.1002/ana.20669

Nathan, C., & Cunningham-Bussel, A. (2013). Beyond oxidative stress: an immunologist's guide to reactive oxygen species. *Nat Rev Immunol*, *13*(5), 349-361. https://doi.org/10.1038/nri3423

Orr, W. C., Mockett, R. J., Benes, J. J., & Sohal, R. S. (2003). Effects of overexpression of copper-zinc and manganese superoxide dismutases, catalase, and thioredoxin reductase genes on longevity in Drosophila melanogaster. *J Biol Chem*, *278*(29), 26418-26422. https://doi.org/10.1074/jbc.M303095200

Orr, W. C., & Sohal, R. S. (1994). Extension of life-span by overexpression of superoxide dismutase and catalase in Drosophila melanogaster. *Science*, *263*(5150), 1128-1130. https://doi.org/10.1126/science.8108730

Page, M. M., Robb, E. L., Salway, K. D., & Stuart, J. A. (2010). Mitochondrial redox metabolism: aging, longevity and dietary effects. *Mech Ageing Dev*, *131*(4), 242-252. https://doi.org/10.1016/j.mad.2010.02.005

Pappolla, M. A., Sos, M., Omar, R. A., & Sambamurti, K. (1996). The heat shock/oxidative stress connection. Relevance to Alzheimer disease. *Mol Chem Neuropathol*, *28*(1-3), 21-34. https://doi.org/10.1007/bf02815201

Peng, C., Wang, X., Chen, J., Jiao, R., Wang, L., Li, Y. M., Zuo, Y., Liu, Y., Lei, L., Ma, K. Y., Huang, Y., & Chen, Z. Y. (2014). Biology of ageing and role of dietary antioxidants. *Biomed Res Int*, *2014*, 831841. https://doi.org/10.1155/2014/831841

Pulkes, T., Eunson, L., Patterson, V., Siddiqui, A., Wood, N. W., Nelson, I. P., Morgan-Hughes, J. A., & Hanna, M. G. (1999). The mitochondrial DNA G13513A transition in ND5 is associated with a LHON/MELAS overlap syndrome and may be a frequent cause of MELAS. *Ann Neurol*, *46*(6), 916-919. http://onlinelibrary.wiley.com/store/10.1002/1531-8249(199912)46:6%3C916::AID-ANA16%3E3.0.CO;2-R/asset/16_ftp.pdf?v=1&t=ifmm89r1&s=7f87dad61cd57629fd8f60c79a6b9a4397779ce8

Ray, P. D., Huang, B. W., & Tsuji, Y. (2012). Reactive oxygen species (ROS) homeostasis and redox regulation in cellular signaling. *Cell Signal*, *24*(5), 981-990. https://doi.org/10.1016/j.cellsig.2012.01.008

Reeve, A. K., Krishnan, K. J., & Turnbull, D. (2008). Mitochondrial DNA mutations in disease, aging, and neurodegeneration. *Ann N Y Acad Sci*, *1147*, 21-29. https://doi.org/10.1196/annals.1427.016

Richardson, A. G., & Schadt, E. E. (2014). The role of macromolecular damage in aging and age-related disease. *J Gerontol A Biol Sci Med Sci*, *69 Suppl 1*, S28-32. https://doi.org/10.1093/gerona/glu056

Sazanov, L. A. (2015). A giant molecular proton pump: structure and mechanism of respiratory complex I. *Nat Rev Mol Cell Biol*, *16*(6), 375-388. https://doi.org/10.1038/nrm3997

Schumpert, C., Handy, I., Dudycha, J. L., & Patel, R. C. (2014). Relationship between heat shock protein 70 expression and life span in Daphnia. *Mech Ageing Dev*, *139*, 1-10. https://doi.org/10.1016/j.mad.2014.04.001

St-Pierre, J., Buckingham, J. A., Roebuck, S. J., & Brand, M. D. (2002). Topology of superoxide production from different sites in the mitochondrial electron transport chain. *J Biol Chem*, *277*(47), 44784-44790. https://doi.org/10.1074/jbc.M207217200

Tower, J. (2011). Heat shock proteins and Drosophila aging. *Exp Gerontol*, *46*(5), 355-362. https://doi.org/10.1016/j.exger.2010.09.002

Vartak, R. S., Semwal, M. K., & Bai, Y. (2014). An update on complex I assembly: the assembly of players. *J Bioenerg Biomembr*, *46*(4), 323-328. https://doi.org/10.1007/s10863-014-9564-x

Wang, X., Perez, E., Liu, R., Yan, L. J., Mallet, R. T., & Yang, S. H. (2007). Pyruvate protects mitochondria from oxidative stress in human neuroblastoma SK-N-SH cells. *Brain Res*, *1132*(1), 1-9. https://doi.org/10.1016/j.brainres.2006.11.032

Wittig, I., & Schägger, H. (2009). Native electrophoretic techniques to identify protein-protein interactions. *Proteomics*, *9*(23), 5214-5223. https://doi.org/10.1002/pmic.200900151

Xu, S., Schaack, S., Seyfert, A., Choi, E., Lynch, M., & Cristescu, M. E. (2012). High mutation rates in the mitochondrial genomes of Daphnia pulex. *Mol Biol Evol*, *29*(2), 763-769. https://doi.org/10.1093/molbev/msr243

Zapico, S. C., & Ubelaker, D. H. (2013). mtDNA Mutations and Their Role in Aging, Diseases and Forensic Sciences. *Aging Dis*, *4*(6), 364-380. https://doi.org/10.14336/ad.2013.0400364

Zhang, A. M., Jia, X., Guo, X., Zhang, Q., & Yao, Y. G. (2012). Mitochondrial DNA mutation m.10680G > A is associated with Leber hereditary optic neuropathy in Chinese patients. *J Transl Med*, *10*, 43. https://doi.org/10.1186/1479-5876-10-43

CHAPTER 3 REFERENCES

Barber, G. N. (2009). The NFAR's (nuclear factors associated with dsRNA): evolutionarily conserved members of the dsRNA binding protein family. *RNA Biol*, *6*(1), 35-39. https://doi.org/7565 [pii]

Benkirane, M., Neuveut, C., Chun, R. F., Smith, S. M., Samuel, C. E., Gatignol, A., & Jeang, K. T. (1997). Oncogenic potential of TAR RNA binding protein TRBP and its regulatory interaction with RNA-dependent protein kinase PKR. *Embo J*, *16*(3), 611-624. (97186727)

Burugu, S., Daher, A., Meurs, E. F., & Gatignol, A. (2014). HIV-1 translation and its regulation by cellular factors PKR and PACT. *Virus Res*, *193*, 65-77. https://doi.org/10.1016/j.virusres.2014.07.014

Chang, K. Y., & Ramos, A. (2005). The double-stranded RNA-binding motif, a versatile macromolecular docking platform. *Febs J*, *272*(9), 2109-2117.

Chukwurah, E., & Patel, R. C. (2018). Stress-induced TRBP phosphorylation enhances its interaction with PKR to regulate cellular survival. *Sci Rep*, *8*(1), 1020. https://doi.org/10.1038/s41598-018-19360-8

Clerzius, G., Gelinas, J. F., & Gatignol, A. (2011). Multiple levels of PKR inhibition during HIV-1 replication. *Rev Med Virol*, *21*(1), 42-53. https://doi.org/10.1002/rmv.674

Cole, J. L. (2007). Activation of PKR: an open and shut case? *Trends Biochem Sci*, *32*(2), 57-62.

Daher, A., Laraki, G., Singh, M., Melendez-Pena, C. E., Bannwarth, S., Peters, A. H., Meurs, E. F., Braun, R. E., Patel, R. C., & Gatignol, A. (2009). TRBP control of PACT-induced phosphorylation of protein kinase R is reversed by stress [Research Support, N.I.H., Extramural Research Support, Non-U.S. Gov't]. *Molecular and Cellular Biology*, *29*(1), 254-265. https://doi.org/10.1128/MCB.01030-08

Daher, A., Longuet, M., Dorin, D., Bois, F., Segeral, E., Bannwarth, S., Battisti, P. L., Purcell, D. F., Benarous, R., Vaquero, C., Meurs, E. F., & Gatignol, A. (2001). Two dimerization domains in the trans-activation response RNA-binding protein (TRBP) individually reverse the protein kinase R inhibition of HIV-1 long terminal repeat expression. *J Biol Chem*, *276*(36), 33899-33905.

Daniels, S. M., & Gatignol, A. (2012). The multiple functions of TRBP, at the hub of cell responses to viruses, stress, and cancer. *Microbiol Mol Biol Rev*, *76*(3), 652-666. https://doi.org/10.1128/mmbr.00012-12

Daniels, S. M., Melendez-Pena, C. E., Scarborough, R. J., Daher, A., Christensen, H. S., El Far, M., Purcell, D. F., Laine, S., & Gatignol, A. (2009). Characterization of the TRBP domain required for dicer interaction and function in RNA interference. *BMC Mol Biol*, *10*, 38. https://doi.org/1471-2199-10-38 [pii] 10.1186/1471-2199-10-38 [doi]

Feng, G. S., Chong, K., Kumar, A., & Williams, B. R. (1992). Identification of double-stranded RNA-binding domains in the interferon-induced double-stranded RNA-activated p68 kinase. *Proc Natl Acad Sci U S A*, *89*(12), 5447-5451. (92302260)

Fierro-Monti, I., & Mathews, M. B. (2000). Proteins binding to duplexed RNA: one motif, multiple functions. *Trends Biochem Sci*, *25*(5), 241-246.

Garcia, M. A., Gil, J., Ventoso, I., Guerra, S., Domingo, E., Rivas, C., & Esteban, M. (2006). Impact of protein kinase PKR in cell biology: from antiviral to antiproliferative action. *Microbiol Mol Biol Rev*, *70*(4), 1032-1060.

Garcia, M. A., Meurs, E. F., & Esteban, M. (2007). The dsRNA protein kinase PKR: Virus and cell control. *Biochimie*, *89*(6-7), 799-811.

Gil, J., Alcami, J., & Esteban, M. (1999). Induction of apoptosis by double-stranded-RNA-dependent protein kinase (PKR) involves the alpha subunit of eukaryotic translation initiation factor 2 and NF-kappaB. *Mol Cell Biol*, *19*(7), 4653-4663.

Green, S. R., & Mathews, M. B. (1992). Two RNA-binding motifs in the double-stranded RNA-activated protein kinase, DAI. *Genes Dev*, *6*(12B), 2478-2490. (94040712)

Holcik, M., & Sonenberg, N. (2005). Translational control in stress and apoptosis. *Nat Rev Mol Cell Biol*, *6*(4), 318-327.

Katze, M. G. (1995). Regulation of the interferon-induced PKR: can viruses cope? *Trends Microbiol*, *3*(2), 75-78. (95245606)

Katze, M. G., Wambach, M., Wong, M. L., Garfinkel, M., Meurs, E., Chong, K., Williams, B. R., Hovanessian, A. G., & Barber, G. N. (1991). Functional expression and RNA binding analysis of the interferon-induced, double-stranded RNA-activated, 68,000-Mr protein kinase in a cell-free system. *Mol Cell Biol*, *11*(11), 5497-5505. (92017829)

Kazemi, S., Papadopoulou, S., Li, S., Su, Q., Wang, S., Yoshimura, A., Matlashewski, G., Dever, T. E., & Koromilas, A. E. (2004). Control of alpha Subunit of Eukaryotic Translation Initiation Factor 2 (eIF2alpha) Phosphorylation by the Human Papillomavirus Type 18 E6 Oncoprotein: Implications for eIF2alpha-Dependent Gene Expression and Cell Death. *Mol Cell Biol*, *24*(8), 3415-3429.

Kim, Y., Lee, J. H., Park, J. E., Cho, J., Yi, H., & Kim, V. N. (2014). PKR is activated by cellular dsRNAs during mitosis and acts as a mitotic regulator. *Genes Dev*, *28*(12), 1310-1322. https://doi.org/10.1101/gad.242644.114

Kim, Y., Yeo, J., Lee, J. H., Cho, J., Seo, D., Kim, J. S., & Kim, V. N. (2014). Deletion of human tarbp2 reveals cellular microRNA targets and cell-cycle function of TRBP. *Cell Rep*, *9*(3), 1061-1074. https://doi.org/10.1016/j.celrep.2014.09.039

Lancaster, G. I., Kammoun, H. L., Kraakman, M. J., Kowalski, G. M., Bruce, C. R., & Febbraio, M. A. (2016). PKR is not obligatory for high-fat diet-induced obesity and its associated metabolic and inflammatory complications. *Nat Commun*, *7*, 10626. https://doi.org/10.1038/ncomms10626

Laraki, G., Clerzius, G., Daher, A., Melendez-Pena, C., Daniels, S., & Gatignol, A. (2008). Interactions between the double-stranded RNA-binding proteins TRBP and PACT define the Medipal domain that mediates protein-protein interactions. *RNA Biol*, *5*(2), 92-103. https://doi.org/6069 [pii]

Marchal, J. A., Lopez, G. J., Peran, M., Comino, A., Delgado, J. R., Garcia-Garcia, J. A., Conde, V., Aranda, F. M., Rivas, C., Esteban, M., & Garcia, M. A. (2014). The impact of PKR activation: from neurodegeneration to cancer. *Faseb j*, *28*(5), 1965-1974. https://doi.org/10.1096/fj.13-248294

Meurs, E., Chong, K., Galabru, J., Thomas, N. S., Kerr, I. M., Williams, B. R., & Hovanessian, A. G. (1990). Molecular cloning and characterization of the human double-stranded RNA-activated protein kinase induced by interferon. *Cell*, *62*(2), 379-390. (90322433)

Nagata, S., Nagase, H., Kawane, K., Mukae, N., & Fukuyama, H. (2003). Degradation of chromosomal DNA during apoptosis. *Cell Death Differ*, *10*(1), 108-116. https://doi.org/10.1038/sj.cdd.4401161

Nakamura, T., Arduini, A., Baccaro, B., Furuhashi, M., & Hotamisligil, G. S. (2014). Small-molecule inhibitors of PKR improve glucose homeostasis in obese diabetic mice. *Diabetes*, *63*(2), 526-534. https://doi.org/10.2337/db13-1019

Nakamura, T., Kunz, R. C., Zhang, C., Kimura, T., Yuan, C. L., Baccaro, B., Namiki, Y., Gygi, S. P., & Hotamisligil, G. S. (2015). A critical role for PKR complexes with TRBP in Immunometabolic regulation and eIF2alpha phosphorylation in obesity. *Cell Rep*, *11*(2), 295-307. https://doi.org/10.1016/j.celrep.2015.03.021

Nanduri, S., Carpick, B. W., Yang, Y., Williams, B. R., & Qin, J. (1998). Structure of the double-stranded RNA-binding domain of the protein kinase PKR reveals the molecular basis of its dsRNA-mediated activation. *Embo J*, *17*(18), 5458-5465.

Nanduri, S., Rahman, F., Williams, B. R., & Qin, J. (2000). A dynamically tuned double-stranded RNA binding mechanism for the activation of antiviral kinase PKR. *Embo J*, *19*(20), 5567-5574.

Pakos-Zebrucka, K., Koryga, I., Mnich, K., Ljujic, M., Samali, A., & Gorman, A. M. (2016). The integrated stress response. *EMBO Rep*, *17*(10), 1374-1395. https://doi.org/10.15252/embr.201642195

Park, H., Davies, M. V., Langland, J. O., Chang, H. W., Nam, Y. S., Tartaglia, J., Paoletti, E., Jacobs, B. L., Kaufman, R. J., & Venkatesan, S. (1994). TAR RNA-binding protein is an inhibitor of the interferon-induced protein kinase PKR. *Proc Natl Acad Sci U S A*, *91*(11), 4713-4717. (94255397)

Paroo, Z., Ye, X., Chen, S., & Liu, Q. (2009). Phosphorylation of the human microRNA-generating complex mediates MAPK/Erk signaling. *Cell*, *139*(1), 112-122. https://doi.org/S0092-8674(09)00791-0 [pii] 10.1016/j.cell.2009.06.044 [doi]

Patel, C. V., Handy, I., Goldsmith, T., & Patel, R. C. (2000). PACT, a stress-modulated cellular activator of interferon-induced double-stranded RNA-activated protein kinase, PKR. *J Biol Chem*, *275*(48), 37993-37998.

Patel, R. C., & Sen, G. C. (1992). Identification of the double-stranded RNA-binding domain of the human interferon-inducible protein kinase. *J Biol Chem*, *267*(11), 7671-7676. (92218427)

Patel, R. C., & Sen, G. C. (1998). PACT, a protein activator of the interferon-induced protein kinase, PKR. *Embo J*, *17*(15), 4379-4390.

Patel, R. C., Stanton, P., McMillan, N. M., Williams, B. R., & Sen, G. C. (1995). The interferon-inducible double-stranded RNA-activated protein kinase self-associates in vitro and in vivo. *Proc Natl Acad Sci U S A*, *92*(18), 8283-8287. (95396782)

Rojas, M., Vasconcelos, G., & Dever, T. E. (2015). An eIF2alpha-binding motif in protein phosphatase 1 subunit GADD34 and its viral orthologs is required to promote dephosphorylation of eIF2alpha. *Proc Natl Acad Sci U S A*, *112*(27), E3466-3475. https://doi.org/10.1073/pnas.1501557112

Sadler, A. J., & Williams, B. R. (2007). Structure and function of the protein kinase R. *Curr Top Microbiol Immunol*, *316*, 253-292.

Samuel, C. E. (1993). The eIF-2 alpha protein kinases, regulators of translation in eukaryotes from yeasts to humans. *J Biol Chem*, *268*(11), 7603-7606. (93216713)

Saunders, L. R., & Barber, G. N. (2003). The dsRNA binding protein family: critical roles, diverse cellular functions. *Faseb J*, *17*(9), 961-983.

Singh, M., Castillo, D., Patel, C. V., & Patel, R. C. (2011). Stress-induced phosphorylation of PACT reduces its interaction with TRBP and leads to PKR activation [Research Support, Non-U.S. Gov't]. *Biochemistry*, *50*(21), 4550-4560. https://doi.org/10.1021/bi200104h

Singh, M., Fowlkes, V., Handy, I., Patel, C. V., & Patel, R. C. (2009). Essential role of PACT-mediated PKR activation in tunicamycin-induced apoptosis [Research Support, Non-U.S. Gov't]. *Journal of Molecular Biology*, *385*(2), 457-468. https://doi.org/10.1016/j.jmb.2008.10.068

Singh, M., & Patel, R. C. (2012). Increased interaction between PACT molecules in response to stress signals is required for PKR activation. *J Cell Biochem*, *113*(8), 2754-2764. https://doi.org/10.1002/jcb.24152

Smyth, P. G., & Berman, S. A. (2002). Markers of apoptosis: methods for elucidating the mechanism of apoptotic cell death from the nervous system. *Biotechniques*, *32*(3), 648-650, 652, 654 passim.

Tewari, M., Quan, L. T., O'Rourke, K., Desnoyers, S., Zeng, Z., Beidler, D. R., Poirier, G. G., Salvesen, G. S., & Dixit, V. M. (1995). Yama/CPP32 beta, a mammalian homolog of CED-3, is a CrmA-inhibitable protease that cleaves the death substrate poly(ADP-ribose) polymerase. *Cell*, *81*(5), 801-809.

Vaughn, L. S., Bragg, D. C., Sharma, N., Camargos, S., Cardoso, F., & Patel, R. C. (2015). Altered Activation of Protein Kinase PKR and Enhanced Apoptosis in Dystonia Cells Carrying a Mutation in PKR Activator Protein PACT. *J Biol Chem*, *290*(37), 22543-22557. https://doi.org/10.1074/jbc.M115.669408

Williams, B. R. (1999). PKR; a sentinel kinase for cellular stress. *Oncogene*, *18*(45), 6112-6120.

CHAPTER 4 REFERENCES

Bennett, R. L., Blalock, W. L., & May, W. S. (2004). Serine 18 phosphorylation of RAX, the PKR activator, is required for PKR activation and consequent translation inhibition. *Journal of Biological Chemistry*. https://doi.org/10.1074/jbc.M403321200

Bidet, K., Dadlani, D., & Garcia-Blanco, M. A. (2014). G3BP1, G3BP2 and CAPRIN1 Are Required for Translation of Interferon Stimulated mRNAs and Are Targeted by a Dengue Virus Non-coding RNA. *PLoS Pathogens*, *10*(7). https://doi.org/10.1371/journal.ppat.1004242

Cao, X., Jin, X., & Liu, B. (2020). The involvement of stress granules in aging and aging-associated diseases. *Aging Cell*, *19*(4), 1–20. https://doi.org/10.1111/acel.13136

Daher, A., Labbé, R. P., Radetskyy, R., & Gatignol, A. (2017). La protéine kinase R induite par l'interféron: le socle d'un échafaudage riboprotéique de régulation du virus de l'immunodéficience humaine. *Virologie*. https://doi.org/10.1684/vir.2017.0708

De La Cruz-Herrera, C. F., Baz-Martínez, M., Motiam, A. El, Vidal, S., Collado, M., Vidal, A., Rodríguez, M. S., Esteban, M., & Rivas, C. (2017). Phosphorylable tyrosine residue 162 in the double-stranded RNA-dependent kinase PKR modulates its interaction with SUMO. *Scientific Reports*. https://doi.org/10.1038/s41598-017-12777-7

Doherty, J., & Baehrecke, E. H. (2018). Life, death and autophagy. *Nature Cell Biology*, *20*(10), 1110–1117. https://doi.org/10.1038/s41556-018-0201-5

Donnelly, N., Gorman, A. M., Gupta, S., & Samali, A. (2013). The eIF2α kinases: Their structures and functions. *Cellular and Molecular Life Sciences*, *70*(19), 3493–3511. https://doi.org/10.1007/s00018-012-1252-6

Eiermann, N., Haneke, K., Sun, Z., Stoecklin, G., & Ruggieri, A. (2020). Dance with the Devil: Stress Granules and Signaling in Antiviral Responses. *Viruses*, *12*(9), 1–47. https://doi.org/10.3390/v12090984

Fulda, S., Gorman, A. M., Hori, O., & Samali, A. (2010). Cellular stress responses: Cell survival and cell death. *International Journal of Cell Biology*, *2010*. https://doi.org/10.1155/2010/214074

Huang, X., Hutchins, B., & Patel, R. C. (2002). The C-terminal, third conserved motif of the protein activator PACT plays an essential role in the activation of double-stranded-RNA-dependent protein kinase (PKR). *Biochemical Journal*. https://doi.org/10.1042/BJ20020204

Li, S., Peters, G. A., Ding, K., Zhang, X., Qin, J., & Sen, G. C. (2006). Molecular basis for PKR activation by PACT or dsRNA. *Proceedings of the National Academy of Sciences of the United States of America*. https://doi.org/10.1073/pnas.0602317103

Li, S., & Sen, G. C. (2003). PACT-Mediated Enhancement of Reporter Gene Expression at the Translational Level. *Journal of Interferon and Cytokine Research*. https://doi.org/10.1089/107999003772084806

Lloyd, R. E. (2013). Regulation of stress granules and P-bodies during RNA virus infection. *Wiley Interdisciplinary Reviews: RNA*, *4*(3), 317–331. https://doi.org/10.1002/wrna.1162

Marques, J. T., White, C. L., Peters, G. A., Williams, B. R. G., & Sen, G. C. (2008). The role of PACT in mediating gene induction, PKR activation, and apoptosis in response to diverse stimuli. *Journal of Interferon and Cytokine Research*. https://doi.org/10.1089/jir.2007.0006

Meyer, C., Garzia, A., Mazzola, M., Gerstberger, S., Molina, H., & Tuschl, T. (2018). The TIA1 RNA-Binding Protein Family Regulates EIF2AK2-Mediated Stress Response and Cell Cycle Progression. *Molecular Cell*, *69*(4), 622-635.e6. https://doi.org/10.1016/j.molcel.2018.01.011

Mirkes, P. E. (1997). *Cellular Responses to Stress*. 245–275. https://doi.org/10.1007/978-3-642-60445-4_9

Napoletano, F., Baron, O., Vandenabeele, P., Mollereau, B., & Fanto, M. (2019). Intersections between Regulated Cell Death and Autophagy. *Trends in Cell Biology*, *29*(4), 323–338. https://doi.org/10.1016/j.tcb.2018.12.007

Pakos-Zebrucka, K., Koryga, I., Mnich, K., Ljujic, M., Samali, A., & Gorman, A. M. (2016). The integrated stress response. *EMBO Reports*, *17*(10), 1374–1395. https://doi.org/10.15252/embr.201642195

Patel, R. C., & Sen, G. C. (1998). PACT, a protein activator of the interferon-induced protein kinase, PKR. *EMBO Journal*. https://doi.org/10.1093/emboj/17.15.4379

Paul, S., Dansithong, W., Figueroa, K. P., Scoles, D. R., & Pulst, S. M. (2018). Staufen1 links RNA stress granules and autophagy in a model of neurodegeneration. *Nature Communications*, *9*(1). https://doi.org/10.1038/s41467-018-06041-3

Peters, G. A., Dickerman, B., & Sen, G. C. (2009). Biochemical analysis of PKR activation by PACT. *Biochemistry*. https://doi.org/10.1021/bi900433y

Protter, D. S. W., & Parker, R. (2016). Principles and Properties of Stress Granules. *Trends in Cell Biology*, *26*(9), 668–679. https://doi.org/10.1016/j.tcb.2016.05.004

Reineke, L. C., Dougherty, J. D., Pierre, P., & Lloyd, R. E. (2012). Large G3BP-induced granules trigger eIF2α phosphorylation. *Molecular Biology of the Cell*, *23*(18), 3499–3510. https://doi.org/10.1091/mbc.E12-05-0385

Reineke, L. C., Kedersha, N., Langereis, M. A., van Kuppeveld, F. J. M., & Lloyd, R. E. (2015). Stress granules regulate double-stranded RNA-dependent protein kinase activation through a complex containing G3BP1 and Caprin1. *MBio*, *6*(2), 1–12. https://doi.org/10.1128/mBio.02486-14

Reineke, L.C., Tsai, W-C, Jain, A., Kaelber, J.T., Jung, S.Y., & Lloyd R.E. (2017). Casein Kinase 2 Is Linked to Stress Granule Dynamics through Phosphorylation of the Stress Granule Nucleating Protein G3BP1. *Mol Cell Bio*l. 37(4):e00596-16. https://doi.org/10.1128/MCB.00596-16

Reineke, L. C., & Lloyd, R. E. (2015). The Stress Granule Protein G3BP1 Recruits Protein Kinase R To Promote Multiple Innate Immune Antiviral Responses. *Journal of Virology*, *89*(5), 2575–2589. https://doi.org/10.1128/jvi.02791-14

Sadler, A. J., & Williams, B. R. G. (2007). Structure and function of the protein kinase R. In *Current Topics in Microbiology and Immunology*. https://doi.org/10.1007/978-3-540-71329-6-13

Sen, G. C., & Peters, G. A. (2007). Viral Stress-Inducible Genes. In *Advances in Virus Research*. https://doi.org/10.1016/S0065-3527(07)70006-4

Singh, M., Castillo, D., Patel, C. V., & Patel, R. C. (2011). Stress-induced phosphorylation of PACT reduces its interaction with TRBP and leads to PKR activation. *Biochemistry*. https://doi.org/10.1021/bi200104h

Singh, M., Fowlkes, V., Handy, I., Patel, C. V., & Patel, R. C. (2009). Essential Role of PACT-Mediated PKR Activation in Tunicamycin-Induced Apoptosis. *Journal of Molecular Biology*. https://doi.org/10.1016/j.jmb.2008.10.068

Vaughn, L. S. (2015). *Regulation of Stress Response and Innate Immunity by DSRN RNA A-Binding Proteins PACT and TRBP*.

White, J. P., Cardenas, A. M., Marissen, W. E., & Lloyd, R. E. (2007). Inhibition of Cytoplasmic mRNA Stress Granule Formation by a Viral Proteinase. *Cell Host and Microbe*, *2*(5), 295–305. https://doi.org/10.1016/j.chom.2007.08.006

Yang, P., Mathieu, C., Kolaitis, R. M., Zhang, P., Messing, J., Yurtsever, U., Yang, Z., Wu, J., Li, Y., Pan, Q., Yu, J., Martin, E. W., Mittag, T., Kim, H. J., & Taylor, J. P. (2020). G3BP1 Is a Tunable Switch that Triggers Phase Separation to Assemble Stress Granules. *Cell*, *181*(2), 325-345.e28. https://doi.org/10.1016/j.cell.2020.03.046